Molecular and cellular mechanisms of nociception in equine laminitis: purinergic P2X receptors expression and distribution

Thesis submitted in accordance with the requirements of the University of Liverpool for the degree of Doctor of Philosophy

Danae E Zamboulis

September 2013

Molecular and cellular mechanisms of nociception in equine laminitis: purinergic P2X receptors expression and distribution

Thesis submitted in accordance with the requirements of the University of Liverpool for the degree of Doctor of Philosophy

Danae E Zamboulis

September 2013

Acknowledgements

I would like to acknowledge the immeasurable advice and support of my primary supervisors Dr Peter Milner and Dr Mark Senior for their guidance throughout this work and for giving me the opportunity to develop my career in research. Furthermore, I would like to acknowledge my secondary supervisors Professor Peter Clegg and Professor James Gallagher for their expertise and support and the members of the Department of Musculoskeletal Biology I in Leahurst, University of Liverpool.

I am greatly indebted to the Greek State Scolarships Foundation for sponsoring me throughout this PhD degree and to the PetPlan Charitable Trust for generously funding this research.

I would also like to thank my friends, and my coaches and teammates at Birkenhead Park Football club for a warm welcome and their support throughout these 4 years in the UK.

Finally, I would like to thank my parents, Dominique and Dimitri, and my sister, Alexandra, for always being there to support me and helping me achieve my dreams.

Abstract

Equine laminitis manifests as a painful condition of the foot and is characterised by disruption of the dermo-epidermal lamellar bond within the equine hoof. Chronic pain in laminitis leads to debilitation and if unchecked euthanasia of the horse and is therefore a significant welfare issue for horses worlwide. P2X receptors are shown to have a pivotal role in pain pathways as well as other tissue functions making them attractive candidates for research in naturally occurring diseases such as equine laminitis.

In this study, the presence and distribution of P2X receptors in tissues of the equine digit and its associated vasculature and innervation was investigated. The investigation was extended to tissues from horses suffering from naturally occurring chronic active lamintis in an attempt to identify changes in distribution or expression of the receptors in these tissues. Finally, the functionality of the P2X receptors expressed in equine nervous tissue was investigated.

Gene expression (mRNA) for all seven receptors was found in the studied tissues and protein expression for P2X1-3 and 7 receptor subtype proteins in these tissues was confirmed with Western blot analysis. Immunohistochemical analysis of P2X1-3 and 7 receptor subtypes distribution showed differential cellular distribution within normal equine tissue and differential distribution and expression between normal and diseased tissues too. In particular, in a horse with shorter duration of chronic laminitis (1 month), P2X3 receptor subtype immunostaining in DRG neurons presented a marked increase in large neurons which coincided with a decrease in the proportion of these neurons in the DRG. Also, horses suffering from chronic laminitis displayed expression of P2X3 receptor subtype in smooth muscle cells of the palmar digital artery which was absent in normal horses. In chronic laminitic hooves, P2X7 receptor subtype showed particularly strong staining in partially keratinised cells. Finally, intracellular calcium measurements provided evidence for the presence of functional purinergic and P2X receptors in equine spinal cord and DRG cells, respectively.

The expression of P2X receptor subtypes in key equine tissues for laminitis and chronic pain in laminitis and their differential expression in laminitic tissues highlights a potential role in chronic laminitis molecular mechanisms. Further research in this area may provide insights into putative targets for disease modulation and pain management in chronic laminitis and other conditions of the horse associated with chronic pain.

Table of Contents

List of tables

List of figures

Abbreviations

2-MeSATP	2-methylthioadenosine-5'-triphosphate
5-HT	5-hydroxytryptamine
αβ-meATP	*α,β*-Methylene-ATP
ADAMTS	A disintegrin and metalloproteinase with thrombospondin motifs
ADP	adenosine diphosphate
ATF-3	activating transcription factor-3
ATP	adenosine-5'-triphosphate
ATP*γ*S	adenosine-5'-*O*-(3-thiotriphosphate)
βγ-meATP	*β,γ*-Methylene-ATP
BBR	Brilliant Blue G
BSA	bovine serum albumin
BzATP	2'(3')-O-(4-benzoylbenzoyl)adenosine-5'-triphosphate
C2, 4 or 8	second, fourth or eigth cervical
cDNA	complementary DNA
cds	coding sequence
CFRT	cystic fibrosis transmembrane conductance regulator
CNS	central nervous system
DAB	3'3-diaminobenzidine
DEPC	diethylpyrocarbonate
DMEM	Dulbecco's modified Eagle's medium
DMSO	dimethylsulfoxide
DNA	deoxyribonucleic acid
DRG	dorsal root ganglion
DTT	dithiothreitol
EDTA	ethylenediaminetetraacetic acid
EGTA	ethylene glycol tetraacetic acid
ET-1	endothelin-1
F	fungizone (amphotericin B)
FCS	foetal calf serum
HBSS	Hank's balanced salt solution
HRP	horseradish peroxidase

iso-PPADS	*iso*-pyridoxalphosphate-6-azophenyl-2',5'-disulfonic acid tetrasodium salt
MAP kinase	mitogen-activated protein kinase
MMP	matrix metalloproteinase
MOPS	3-(N-morpholino)propanesulfonic acid
mRNA	messenger RNA
MW	molecular weight
NCBI	National Centre for Biotechnology Information
NO	nitric oxide
NPY	neuropeptide Y
o.d.	outside diameter
P3	distal phalanx
PBS	phosphate buffered saline
PBST	0.1% Tween phosphate buffered saline
PCR	polymerase chain reaction
PDL	primary dermal lamellae
PEL	primary epidermal lamellae
PFA	paraformaldehyde
PI3 kinase	phosphatidylinositol kinase
PPADS	pyridoxal 5-phosphate 6-azophenyl-2',4'-disulfonic acid
P/S	penicillin and streptomycin
RNA	ribonucleic acid
rpm	rounds per minute
RT	room temperature
RT-PRC	reverse transcriptase PCR
SADP	suspensory apparatus of the distal phalanx
SD	standard deviation
SDL	secondary dermal lamellae
SEL	secondary epidermal lamellae
T1	first thoracic
TBS	tris buffered saline
TIMP	tissue inhibitor of metalloproteinases
TM	transmembrane segment
TNP-ATP	trinitrophenyl-ATP

UDP	uridine diphosphate
UTP	uridine 5’-triphosphate
WR	working reagent (Pierce BCA protein assay)

Chapter 1

Introduction

1.1 Laminitis

Laminitis is a systemic disease of the horse that manifests as a painful condition of the foot characterized by disruption of the dermo-epidermal lamellar bond within the equine hoof (Hood 1999a, Jones et al. 2007). It is a major problem in the horse, not limited to any specific breed, occupation or geographical region, and is accompanied by severe pain, prolonged chronic course and in its most severe form can culminate in euthanasia (Slater et al. 1995, Hampson et al. 2012).

Laminitis is not a new condition, having been recognised for over 2000 years (Harris 2012), but it continues to be responsible for dysfunction and disruption in the working life of many horses (Hampson et al. 2012). The general prevalence of laminitis is difficult to estimate due to variation in the design of epidemiological studies. Differences in the definition of a "case" and in the population sets included in studies can account for the variability in laminitis prevalence reported in literature. In Australia, a prevalence of laminitis of 23.8% is reported (Buckley et al. 2007), whereas in Great Britain, recent data record a lower prevalence of 0.5-17.1% (Menzies-Gow et al. 2010, Wylie et al. 2013). This is due to a pony club population used by Buckley et al. (2007), which is likely to target more susceptible breeds, and to the inclusion of chronic inactive cases too. On the other hand, in the study by Wylie et al. (2013) the reporting process relied upon veterinary surgeons to report cases, which led to underreporting, and cases included only acute and not recurrent laminitis.

Furthermore, horses affected with laminitis can progress to develop severe or chronic lameness and debilitation. In the UK, Menzies-Gow et al. (2010) report that 33.7% of the animals diagnosed with laminitis presented with repeated episodes. In

addition, annual economical losses associated with the evaluation, treatment and loss of horses after a diagnosis of laminitis are estimated to be at least $13 million (Moore 2009). Thus, the prevalence of laminitis among horses, impacts on the welfare of horses, and the economic and emotional costs have a significant impact on horse owners.

1.1.1 Hoof anatomy

The equine hoof is unique in that a single digit on each limb supports the entire weight of the animal and withstands a considerate biomechanical load (Pollitt 1994). The digit is suspended in the heavily keratinised hoof capsule by an interdigiting lamellar architecture which helps reduce stress and ensures even energy transfer during peak loading of the equine foot. The innermost layer of the hoof wall, *stratum lamellatum*, bears up to 550-600 primary epidermal lamellae which project from its surface in parallel rows facing the outer surface of the distal phalanx. Along the length of each primary epidermal lamellae (PEL) are an extra 150-200 secondary epidermal lamellae (SEL) also orientated towards the distal phalanx. The epidermal lamellae are lined with a layer of epidermal basal cells (Pollitt 1998) (Figure 1.1 and 1.2a).

Beneath the hoof wall is the highly vascular and sensitive corium or dermis which consists of a dense matrix of tough connective tissue containing a network of arteries, veins and capillaries and sensory and vasomotor nerves. The corium provides the hoof with nourishment and bears primary and secondary dermal lamellae (PDL, SDL) which interlock with the epidermal lamellae to form the

suspensory apparatus of the distal phalanx (SADP). On the other end, the deep surface of the corium blends with the periosteum of the distal phalanx to suspend the phalanx in the hoof capsule (Pollitt 1992) (Figure 1.1).

At the interface of the epidermis and the dermis is the basement membrane, a tough, unbroken sheet of extracellular matrix (Figure 1.1 and 1.2b). The basement membrane attaches the basal cells of the lamellar epidermis on one side and the fine connective tissue fibrils emanating from the dorsal surface of the distal phalanx on the other (Pollitt 1998). The epidermal basal cells are firmly attached to the basement membrane with hemidesmosomes and anchoring filaments (French & Pollitt 2004b). Basement membrane changes is one of the earliest pathological events to occur in laminitis and could be the event that initiates the collapse of the lamellar architecture (Visser & Pollitt 2011).

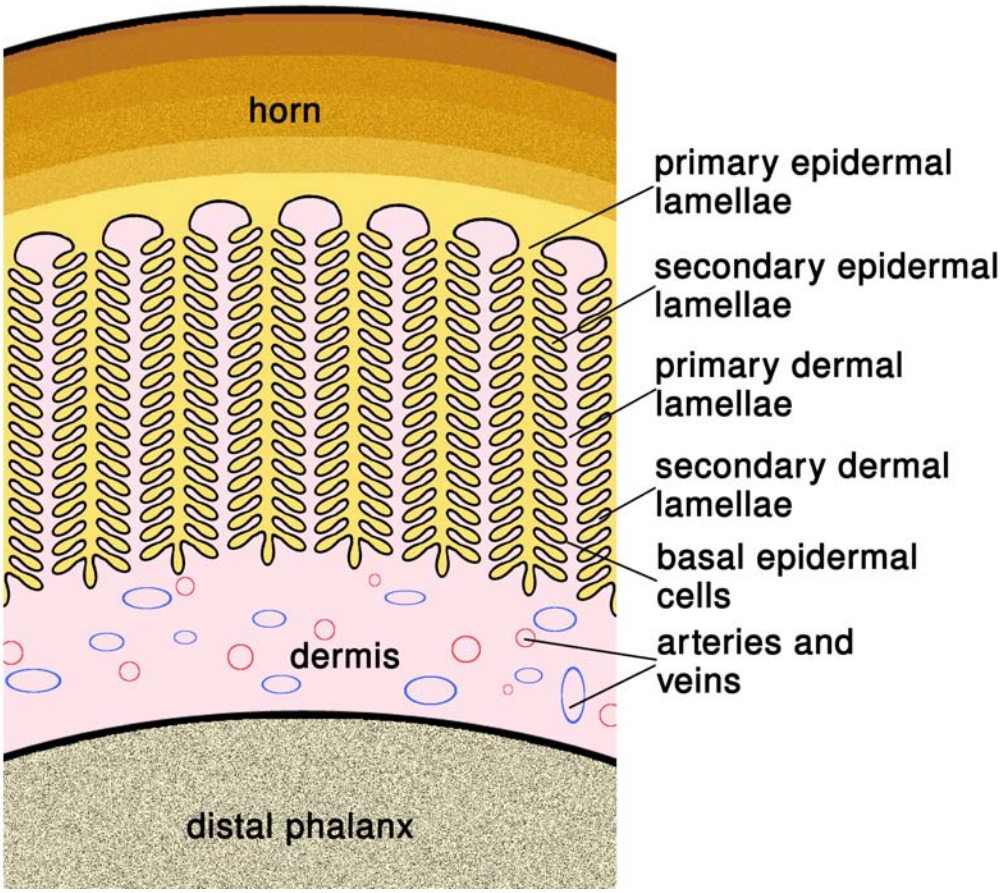

Figure 1.1. Schematic of the suspensory apparatus of the distal phalanx. The primary and secondary epidermal and dermal lamellae interlock to form the SADP. At the interface is the basement membrane and basal epidermal cells. The corium contains a network of arteries, veins and capillaries and at its deep surface blends with the periosteum of the distal phalanx.

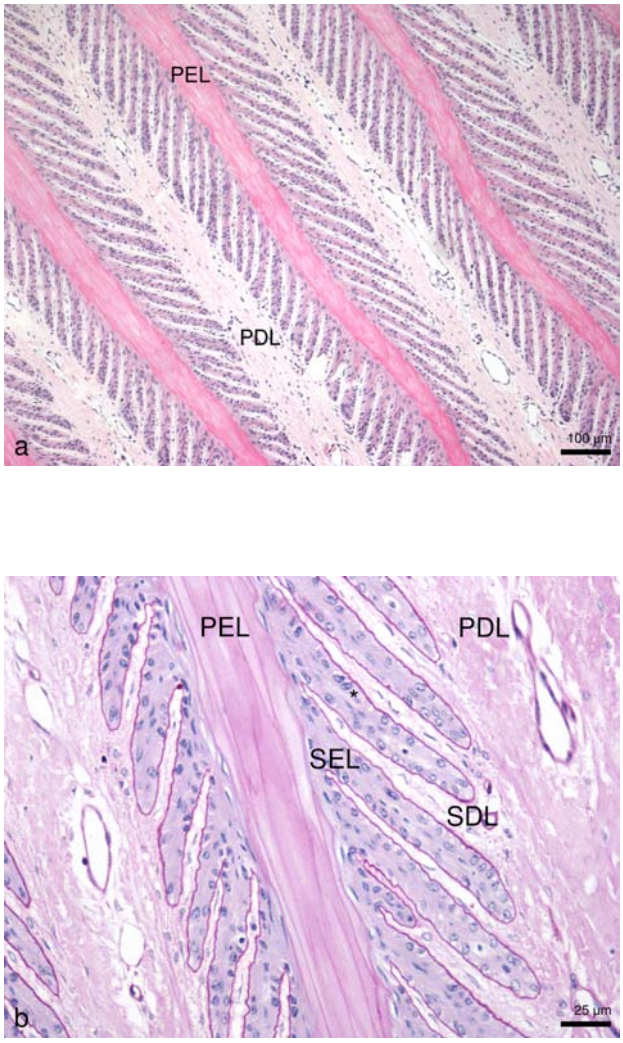

Figure 1.2. Histology of the equine hoof dermo-epidermal junction. (a) PEL and SEL interlocking with the PDL and SDL. The epidermal lamellae are lined with a layer of epidermal cells. Capillaries are present in the SDL, H&E stain. (b) At the interface of the epidermis and the dermis is the basement membrane attached to the basal cells of the epidermis (asterisk), Periodic acid Schiff's stain.

1.1.2 Phases of laminitis

The progression of laminitis can be divided into three phases, the developmental, acute, and chronic phase. The developmental phase is the period between the initial causative insult and the first appearance of clinical signs associated with laminitis. During this period the horse might be showing signs of the inciting event but the actual developmental phase is relatively asymptomatic making it difficult to recognise (Hood 1999b). By the time foot pain is apparent lamellar pathology is underway (Pollitt 2004b). Research around the pathogenesis of laminitis has focused on the developmental phase in an attempt to identify trigger factors of the condition and targets for intervention (Bailey et al. 2009, Budak et al. 2009, de Laat et al. 2013).

The acute phase begins with the onset of clinical foot pain (Hood 1999b). Clinical signs during this phase can include a change in stance and gait with continually shifting weight from one foot to another and lameness, digital pain, bounding digital pulse, and warm feet (Swanson 1999). Treatment strategies in the acute phase focus on analgesia and digital support, as well as resolving any underlying causes triggering the disease (inflammatory diseases, endocrinopathic diseases, etc) (Hood 1999d).

After the acute phase, the horse can make an apparent complete recovery or progress into the chronic phase (Pollitt 2004b). Chronic laminitis has a broad spectrum of clinical presentations, ranging from mild lameness and capable of significant athletic function, to fluctuating episodes of disease, through to severe chronic pain necessitating euthanasia on humane grounds (Morgan et al. 1999). Furthermore, chronic phase laminitis can be further categorised in early chronic

laminitis, where there are no morphological changes to the hoof capsule, chronic stable laminitis, where there are morphological changes to the hoof capsule but the horse is clinically improving, and chronic active laminitis, where the distal phalanx remains unstable and which is usually accompanied by severe pain (Morgan et al. 1999, Stashak 2002, Parks & Mair 2009) (Figure 1.3).

Figure 1.3. Sagittal section of a normal equine hoof (a) and a hoof from a horse suffering from chronic laminitis (b). In the chronic laminitic hoof rotation of the distal phalanx in the hoof capsule is apparent (arrow).

1.1.3 Laminitis aetiopathogenesis

While the precise aetiology of laminitis remains obscure it is clear that its pathogenesis is multifactorial in nature (Robertson et al. 2009) The mechanisms involved in the pathogenesis of laminitis are probably numerous and interrelated, and may represent different events in the complex time course of laminitis rather than individual pathogenetic mechanisms. However, laminitis cases can be categorised based on main aetiology to facilitate their study.

1.1.3.1 Inflammatory laminitis

Inflammatory laminitis includes cases with inflammation as a main cause, such as systemic diseases, especially gastrointestinal disease, but also endometritis, and grain overload. The black walnut- and the carbohydrate overload-induced laminitis models also fall into this category.

The prodromal stages of laminitis are associated with alterations in lamellar vascular function (Peroni et al. 2005) with the presence of warm feet and a bounding digital pulse in the acute phase suggesting a vascular component is active in laminitis (Hood et al. 1993). Vascular events could lead to loss of lamellar tissue function as a result of a complex cascade of events initiated by ischaemia. Primary events in this cascade are necrosis due to anoxia followed by reperfusion injury with peroxidation of cellular and intracellular lipids secondary to the production of superoxide radicals (Hood et al. 1993). Evaluation of digital perfusion in laminitis developmental and acute phases has yielded conflicting data and correlation and interpretation of these

data is difficult because of the different experimental designs used in each study (Pollitt & Davies 1998, Hood et al. 2001). However, several studies, using both the black walnut- and the carbohydrate-induced laminitis model, report an early decrease in lamellar microvascular blood flow detected during the developmental phase of laminitis followed by reperfusion prior to onset of clinical signs (Galey et al. 1990, Hood et al. 1993, Adair et al. 2000, Hood et al. 2001). These observations support an ischaemia/reperfusion mechanism of injury for equine laminitis similar to the one seen in Raynaud's syndrome in human (Hood et al. 1990).

The initial ischaemic insult may be a result of digital vasospasm, which may be locally induced or may be influenced by circulating vasoactive amines released from the gastrointestinal tract (Elliot et al. 2003, Bailey et al. 2004, Elliot & Bailey 2006, Noschka et al. 2009), especially with the equine lamellar dermis showing a predisposition for venoconstriction (Peroni et al. 2006). Ischaemia could also be a result of altered blood flow bypassing lamellar capillaries through arterio-venous anastomoses (Hood et al. 1993, Moore et al. 2004) and may explain equivocal data around hoof wall surface temperature changes (Moore et al. 2004). Other vascular events participating in the development of laminitis include increased postcapillary resistance and possible lamellar oedema (Eaton et al. 1995), damage to the vascular endothelium and endothelial cells dysfunction with increased presence of endothelin-1 (ET-1), activation of leukocytes, haemorrheologic dysfunctions and coagulopathies with platelet activation and subsequent release of vasoactive mediators, such as 5-hydroxytryptamine (5-HT) and thromboxane A_2, which are all consistent with impaired local perfusion (Hood et al. 1993, Weiss et al. 1994, Weiss et al. 1995, Katwa et al. 1999, Elliot et al. 2003, Bailey et al. 2004, Eades et al. 2007, Loftus et al. 2007).

Furthermore, enzymatic events following the haematogenous delivery of 'laminitis trigger factors' to the hoof could also participate in the disruption in lamellar ultrastructure and ultimately dermo-epidermal separation. The enzymatic events include activation of matrix metalloproteinases (MMPs) which causes breakdown of basement membrane collagen and laminin and anchoring filaments (Pollitt 1996, French & Pollitt 2004a). MMPs exist in lamellar hoof where they participate with TIMPs (tissue inhibitors of MMPs) in the cellular reorganisation required for hoof wall growth and wound repair (Pollitt et al. 2003). MMP synthesis may be stimulated by pro-inflammatory cytokines during endotoxaemia (Johnson et al. 1998) or other gut-derived trigger factors such as streptococcal exotoxins and bacterial thermolysin (Mungall et al. 2001).

Studies in tissues from laminitic horses (developmental, acute, and chronic phase) revealed MMP-2 and MMP-9 activity to be substantially greater than in normal horses (Johnson et al. 1998, Pollitt et al. 1998). It was thus suggested that inadvertent and uncontrollable lamellar MMP activation during laminitis developmental phase could be responsible for the dermo-epidermal separation which characterises laminitis (Pollitt et al. 1998, Pollitt et al. 2003). However, a later study found a large variation in the concentrations of lamellar MMPs in laminitic (both experimentally induced and naturally acquired laminitis) and non-laminitic horses and could not confirm a correlation of MMP activity with catalytic activity at the basement membrane (Loftus et al. 2009). Furthermore, in lamellar samples of early developmental laminitis, MMP-9 was found to be largely present in its inactive form while MMP-2 activation occurred more than 12 hours after basement membrane degradation (Visser & Pollitt 2012).

Another protease, ADAMTS-4, has been found upregulated in the developmental phase of carbohydrate overload-induced laminitis and in naturally acquired laminitis (Budak et al. 2009, Coyne et al. 2009). MMP-14, a protease active at the dermal-epidermal interface participating in membrane surface proteolytic events, has also been found upregulated in acute laminitis (Kyaw-Tanner et al. 2008). Activation of MMP-2 and MMP-9 is, therefore, likely to be secondary to the primary event leading to lameness, and the role of other proteases, including MMP-14 and ADAMTSs, needs to be considered (Kyaw-Tanner et al. 2008, Visser & Pollitt 2012).

1.1.3.2 Endocrinopathic laminitis

Endocrinopathic laminitis is defined as laminitis developing from putative hormonal influences rather than pro-inflammatory and intestinal conditions (Johnson et al. 2004). Conditions associated with endocrinopathic laminitis include Equine Cushing's Syndrome, Insulin Resistance (or Equine Metabolic Syndrome or Pasture-Associated Laminitis) and iatrogenic corticosteroid administration. In common to all these conditions are disturbed glucose and insulin regulation, and, most importantly, the development of insulin resistance (McGowan 2008). This category also includes the insulin-induced laminitis model.

Insulin resistance has been identified as a major predisposing condition for laminitis (Treiber et al. 2006b) and prolonged hyperinsulinaemia alone has been shown to induce laminitis in healthy ponies and horses, demonstrating that laminitis can be triggered by insulin (Asplin et al. 2007, de Laat et al. 2010). The mechanisms

linking insulin resistance or hyperinsulinaemia and the development of laminitis include glucose uptake impairment, and vascular and pro-inflammatory effects (Treiber et al. 2006a).

It has been proposed that changes in glucose metabolism and reduced glucose availability to insulin-sensitive cells secondary to insulin resistance could lead to the development of laminitis pathology. The normal equine hoof has been shown to have a high glucose consumption and glucose deprivation induces dermo-epidermal separation in hoof explants *in vitro* by reduction of hemidesmosomes numbers and basal cell cytoskeleton collapse (Pass et al. 1998, French & Pollitt 2004b, Wattle & Pollitt 2004). However, recent data suggest glucose uptake in the hoof is insulin-independent and supporting this, mRNA expression of the insulin-independent glucose transport protein GLUT1 was strong in lamellar tissue whereas mRNA expression of the insulin-dependent glucose transport protein GLUT4 was absent or barely detectable. Laminitis in insulin resistant horses is therefore unlikely to be the result of glucose deprivation (Asplin et al. 2011).

Insulin resistance is also associated with vascular effects, such as vasoconstriction and endothelial damage which are found in laminitis (Treiber et al. 2006a). Under insulin-resistant conditions, impairment of the phosphatidylinositol (PI3) kinase pathway and endothelial production of the vasodilator agent NO, and reduced capillary perfusion are noted (Potenza et al. 2009, Venugopal et al. 2011). Also, increased levels of ET-1 have been found in laminitic lamellar tissue and hyperinsulinemia is known to increase secretion of ET-1 from the endothelium through the mitogen-activated protein (MAP) kinase pathway and enhace ET-1 activity promoting vasoconstriction (Katwa et al. 1999, Potenza et al. 2009, Venugopal et al. 2011).

Furthermore, the presence of insulin resistance is linked to a pro-inflammatory state with circulating cytokines which can contribute to the development laminitis (Dandona et al. 2004, Belknap et al. 2007). Finally, insulin itself, without the presence of an insulin resistance associated pro-inflammatory state, can induce MMP-9 protein levels via the MAP kinase pathway and contribute to the development of endocrinopathic laminitis (Fischoeder et al. 2007, de Laat et al. 2011).

1.1.3.3 Weight-bearing laminitis

Laminitis can also occur as a result of mechanical overload situations and is a relatively common complication in conditions that cause prolonged excessive unilateral weight-bearing in a limb (support limb laminitis) (Redden 2004, Virgin et al. 2011). Support limb laminitis could be a result of direct mechanical overload of the suspensory apparatus of the distal phalanx or reduced digital blood flow caused by a lack of normal cyclic loading and inadequate perfusion of the lamellar tissue followed by potential activation of enzymatic and chemical mediators (van Eps et al. 2010).

1.1.4 Pain in laminitis

Pain is the main clinical feature in laminitis and it is the inability to manage the unrelenting and severe pain associated with the disease that is the most common

cause of euthanasia in laminitic horses (Collins et al. 2010a). Pain first becomes evident at the beginning of the acute phase of laminitis where it manifests as a result of lamellar pathology. In the acute phase of laminitis pain is nociceptive, secondary to actual tissue damage or tissue-damaging stimuli, and inflammatory, with presence of hypersensitivity arising from the interaction of inflammatory mediators with neurons, and can disappear after full resolution of the disease (Kidd & Urban 2001, Nicholson 2006, Collins et al. 2010a). However, in the chronic phase of laminitis, the chronic pain state that can develop has a neuropathic component to it and often persists after resolution of the initiating pathology (Jones et al. 2007, Collins et al. 2010a).

1.1.5 Chronic pain in laminitis

Chronic pain in laminitis is difficult to treat and is the main reason for euthanasia in laminitic horses making pain in laminitis a pathologic entity in itself rather than just a sign.

Pain management in laminitis has traditionally consisted predominantly of anti-inflammatory drug administration (Rietmann et al. 2004). This approach, however, has failed to control pain in chronic laminitic cases and revealed its multifactorial nature (Driessen et al. 2010). The mechanisms responsible for the development of chronic pain in laminitis are not completely clear but they include events occurring secondary to inflammation (inflammatory component) and nerve injury (neuropathic component), both locally in the hoof and centrally in the CNS (Yaksh 2010).

Inflammatory mediators participate in chronic pain by direct stimulation of nociceptors or by producing many and complex changes in afferent nerve fibres ranging from overt activation or sensitisation to other stimuli to alterations in the phenotype and structure of sensory nerves (Dray 1995). In chronic laminitis, plasma concentrations of the pro-inflammatory cytokine TNF-α, a critical factor in neuropathic pain, and lamellar concentrations of inflammatory mediators IL-1 and IL-6 are elevated and are thought to play an important role in chronic laminitic pain (Treiber et al. 2009, Leung & Cahill 2010, Steelman et al. 2013).

Nerve injury has also been reported in laminitis with tearing of the dermo-epidermal lamellar bond resulting in widespread injury to C and A_δ fibres in the dermal layers (Morgan et al. 1999, Driessen et al. 2010). As a consequence of nerve damage, both injured and uninjured axons exhibit abnormal activity including dysregulated gene expression and generation of ectopic discharges leading to the amplification of the response to noxious stimuli as part of peripheral hyperalgesia (Marchand et al. 2005). Peripheral nerve morphology is also altered in digital nerves and reduced numbers of unmyelinated and myelinated fibres are noted compared to normal horses. However, changes are not limited to peripheral nerves, as increased expression of the neuronal injury marker, activating transcription factor-3 (ATF3), and neuropeptide Y (NPY) has been found in C8 dorsal root ganglia (DRG) neurons (innervating the hoof). These changes are similar to those reported in other neuropathic pain states providing evidence for a neuropathic component in the pain state in chronic laminitis (Jones et al. 2007). DRG neurons of chronic laminitic horses have also been shown to strongly express the ionophore protein α2δ, which in rodent pain models is increased in states of hyperalgesia and allodynia (Collins et al. 2010a). Furthermore, in other species, neuropathic pain is also driven by spinal and

supraspinal mechanisms (Ossipov et al. 2000). Ongoing activity in injured nerves triggers central sensitisation with involvement of synaptic modulators and excitatory amino acids, alterations in ion channel kinetics and properties, increased density of ionotropic receptors and activation of kinases pre- and post-synaptically (Constigan et al. 2009).

Finally, other local events are also thought to contribute to the pain state in chronic laminitis. Extensive bone modelling and endosteal oedema have been observed in the distal phalanx of chronic laminitic horses presenting with unrelenting foot pain supporting the presence of increased intraosseous pressure, known to trigger persistent pain (Lemperg & Arnoldi 1978, Morrisset et al. 1999, Collins et al. 2010a). Another important factor for pain may be digital ischaemia following vasoconstriction in response to inflammatory mediators, arterio-venous blood shunting, thrombosis, and compression of the vascular bed (Hood et al. 1994, Grosenbaugh et al. 1999, Morgan et al. 1999). Similarly, increased pressure within the hoof capsule as a result of distal phalanx displacement, oedema that accompanies inflammation or haemorrhage, and dilation of hoof vessels in response to neuropeptides (eg. CGRP) from activated sensory nerve terminals may exacerbate foot pain in chronic laminitis (Hood et al. 1999c, Morgan et al. 1999, Driessen et al. 2010).

Effective pain management in horses with laminitis therefore favours a multi-modal approach that involves a combination of drugs with different pharmacologic mechanisms of action and different target sites within the somatosensory neural conduit (Dutton et al. 2009, Driessen et al. 2010, Guedes et al. 2012).

1.2 Purinergic P2X receptor biology

1.2.1 Adenosine 5'-triphosphate (ATP)

Adenosine 5'-triphosphate (ATP) has a fundamental intracellular role as the universal source of energy in all living cells. In addition to being an intracellular energy source, ATP has now also been recognised as an extracellular signalling molecule (Drury & Szent-Györgyi 1929, Bodin & Burnstock 2001b).

Drury and Szent-Györgyi in 1929 were the first to report extracellular purine actions. They noted extracellular adenosine had a negative chronotropic effect on the heart, a vasodilatory effect on arteries and inhibited intestinal movements (Drury & Szent-Györgyi 1929). Several studies followed showing the extracellular actions of ATP in the nervous system and ATP release from sensory nerves (Feldberg & Hebb 1948, Holton 1959). But it was not until 1972 that a complete purinergic neurotransmission hypothesis was developed (Burnstock 1972). Since then, ATP signalling has been reported in the nervous system, epithelial cells, the immune system and a plethora of other systems where it participates in physiological and pathological processes (Fields & Stevens 2000, Vonend et al. 2002, Schwiebert & Zsembery 2003, Mounkaïla et al. 2005, Bours et al. 2006).

1.2.2 Extracellular ATP release

Following cell membrane damage or necrosis, all cells can potentially release ATP into the extracellular environment, which might be important in triggering

cellular responses to trauma (Fields & Stevens 2000, Cook & McCleskey 2002). In addition, numerous neuronal and non-neuronal cells can release ATP in a controlled manner as part of a physiological mechanism.

In the peripheral and central nervous system, ATP functions as a neurotransmitter and is often co-transmitted with other neurotransmitters. ATP has also a special role in neuronal-glial and glial-glial signalling and is an important gliotransmitter (Abbracchio et al. 2009). In non-neuronal cells, ATP can be released as a result of mechanical stimulation, such as shear stress, cell swelling, or mechanical distension, but also other stimuli such as hypoxia, acidosis, and agonist stimulation (Bodin & Burnstock 2001a, Knight et al. 2002, van der Wijk et al. 2003, Gourine et al. 2005, Orriss et al. 2009, Praetorius & Leipziger 2009, Tu et al. 2010). Finally, spontaneous nucleotide release has been noted in renal epithelia, which appears to provide a tonic signalling input to the cells (Geyti et al. 2008).

ATP release occurs mainly through (i) cytolysis with cell membrane damage or necrosis following physical or biological trauma, (ii) transport via a conductive pore or transporter such as connexins, volume-regulated Cl^- channels, the cystic fibrosis transmembrane conductance regulator (CFTR) and P2X7 receptor itself, and (iii) exocytotic release both by neuronal and non-neuronal cells (Cotrina et al. 1998, Bodin & Burnstock 2001a, Schwiebert & Zsembery 2003, Praetorius & Leipziger 2009, Tu et al. 2010).

1.2.3 Classification of purinergic receptors

Purinergic receptors (also known as purinoceptors) are divided into two classes, P1 or adenosine receptors and P2 purinoceptors recognising primarily ATP, ADP, UTP, and UDP. P2 receptors are further subdivided into two subclasses, P2X receptors which are ligand-gated ion channels and P2Y receptors which are G protein-coupled receptors (Burnstock & Kennedy 1985, Ralevic & Burnstock 1998).

1.2.4 P2X receptor structure and properties

P2X receptors are classical cationic ligand-operated channels that upon ATP binding open the pore permeable to Na^+, K^+ and Ca^{2+} (Ralevic & Burnstock 1998). Each receptor is made of three individual subunits arranged in a "head-to-tail" order (Egan et al. 2006) (Figure 1.4a). P2X subunits are encoded by seven distinct genes, P2X1-P2X7 (North 2002). Individual subunits have intracellular amino- and carboxy-termini, a large extracellular loop, and two hydrophobic transmembrane segments, TM1 and TM2 (Egan et al. 2006) (Figure 1.4b). The extracellular loop contains the ATP binding pocket, binding sites for agonists, antagonists and modulators, and additional structure elements that influence the receptor's deactivation and desensitisation rates (Vial et al. 2004, Li et al. 2008). Gating properties of the ion channel by agonist vary dramatically with receptor subtype, with P2X2, P2X4, and P2X7 homomeric channels showing slow desensitisation and P2X1 and P2X3 channels exhibiting rapid activation and desensitisation (North 2002). The extracellular loop also contains cysteine residues, some of which

participate in disulfide bond formation and likely define the tertiary structure of the protein (Vial et al. 2004). The P2X receptor TM regions are thought to form the central ion conduction pore and participate in the conformational changes during receptor activation (North 2002, Egan et al. 2006). P2X subunits can assemble to form either homomeric or heteromeric receptors. Diversity of the P2X receptors phenotypes is yielded by different subunit combinations and the receptors' functional and pharmacological properties are directly determined by their subunit composition (Torres et al. 1999).

Activation of P2X receptors by ATP results in a momentary increase in the free concentration of intracellular calcium and thus, initiation of cell functions (Egan et al. 2006, Li et al. 2008). The intracellular calcium accumulation is achieved in two distinct ways. First, P2X mediate a membrane depolarization that opens voltage-dependent Ca^{2+} channels. Second, the receptor itself is permeable to Ca^{2+} and cations travel through the channel into the cell (Egan et al. 2006). Also, during prolonged agonist application, P2X2, P2X4 and P2X7 receptor channel is reported to progressively dilate to provide a permeation pathway to molecules with a molecular weight of up to ~900 Da; a process termed cell permeabilisation (Virginio et al. 1999, Dunn et al. 2001, North 2002, Yan et al. 2008).

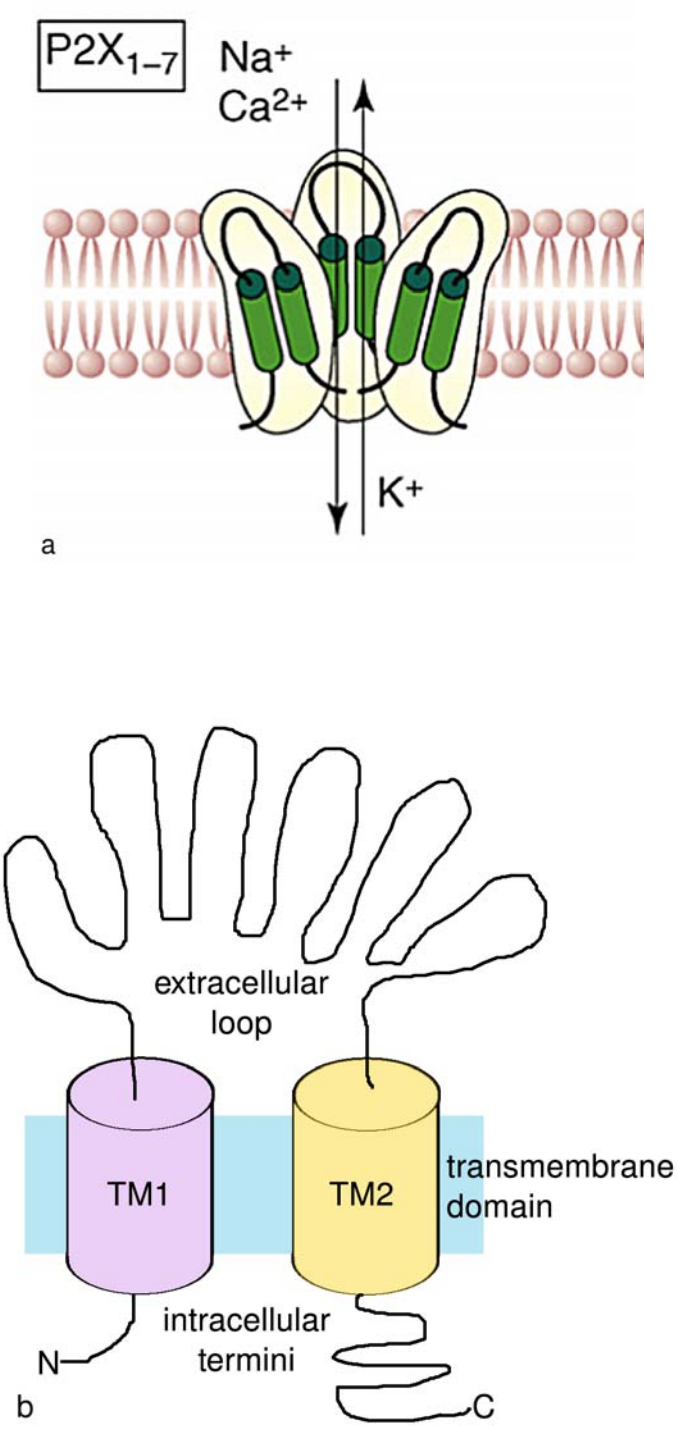

Figure 1.4. (a) P2X receptor structure (Abbracchio et al. 2009, reproduced with permission). (b) P2X protein domains.

1.2.5 P2X receptors agonists and antagonists

The development of subtype-specific agonists for P2X receptors is difficult and therefore not many are available. In Table 1.1 are summarised some widely used P2X agonists and antagonists and their specificity.

Table 1.1. Widely used P2X receptors agonists and antagonists and their specificity.

	Specificity	**References**
P2X agonists		
$\alpha\beta$-meATP and	P2X receptors, higher potency for	Dunn et al. 2001,
$\beta\gamma$-meATP	P2X1 and P2X3 receptors	Coddou et al. 2011
ATPγS	P2X receptors except P2X7	Watano et al. 2004
	receptors and several P2Y receptors	
2-meSATP	P2X and P2Y receptors	Coddou et al. 2011
BzATP	potent for P2X7 receptors	Baraldi et al. 2004
P2X antagonists		
Suramin	P2X and other purinergic receptors	Dunn & Blakeley 1988
PPADS	P2X1, P2X2, P2X3, P2X5, and	Connolly 1995
	$P2Y_1$ receptors	Jacques-Silva et al. 2004
	weak or ineffective against P2X4,	
	P2X6, and P2X7 receptors	
Iso-PPADS	P2X receptors, potency may be	Connolly 1995,
	species-dependent	North 2002
TNP-ATP	P2X1, P2X3, and P2X2/3 receptors	Thomas et al. 1998,
		Virginio et al. 1998
Oxidised ATP	potent for P2X7 receptors	Wiley et al. 1994
KN-62, KN-04	potent for P2X7 receptors	Gargett & Wiley 1997
BBR	P2X7 receptors	Jiang et al. 2000
A-317491	P2X3-containing receptors	Jarvis et al. 2002

1.2.6 P2X1-7 receptor subtypes distribution

Since 1994, when the first P2X receptor was cloned from rat cDNA (Valera et al. 1994), P2X receptors have been identified in many vertebrates, in virtually all mammalian tissues, mediating a large variety of responses, from fast transmission at central synapses, contraction of smooth muscle cells, and macrophage activation to proliferation and cell death (reviews Burnstock & Knight 2004, Burnstock & Verkhratsky 2009).

Although, P2X receptors have been found to be widely distributed, they are also specifically distributed among different tissues in the vertebrate body (North 2002).

P2X1 receptor subtype was originally cloned from rat *vas deferans* smooth muscle and although it has been found in other cells (e.g. neurons and platelets) it is most highly expressed in smooth muscle cells of various organs, such as vessels, and urinary bladder, where it participates in smooth muscle contraction (Valera et al. 1994, Clifford et al. 1998, Nori et al. 1998, Petruska et al. 2000, Vial & Evans 2000).

P2X2 receptor subtype is found in sensory neurons in homomeric receptors or co-localised with P2X3 subunits where they contribute to nociceptive responses and chemosensory and mechanosensory transduction (Prasad et al. 2001, Zhong et al. 2001, Wang & Neuhuber 2003, Cockayne et al. 2005). P2X2 channel is also expressed in epithelial cells where it may affect functions such as vesicle trafficking, protein secretion and signal-transduction pathways (Taylor et al. 1999, Glass et al. 2000).

P2X3 receptor subtype was originally cloned from rat DRG cDNA (Chen et al. 1995) and is consistently located in neuronal cells (Bradbury et al. 1998) with

functional studies using P2X3 knockout mouse lines confirming an important role of the P2X3 channel in nociceptive signalling (Cockayne et al. 2000, Souslova et al. 2000).

P2X4 receptor subtype, on the contrary, appears to have a very wide distribution pattern which includes the central and peripheral nervous systems, skeletal and smooth muscle, epithelial and endothelial cells, to only name a few (Bo et al. 2003, Kaczmarek-Hajek et al. 2012). Attention, however, has been drawn to its expression in microglia and implication in the pathogenesis of neuropathic pain (Tsuda et al. 2003).

P2X5 receptor subtype has been predominently found in the central nervous system and the immune system, but is also associated with cell differentiation of epithelial and other cells (Lê et al. 1997, Gröschel-Stewart et al. 1999a, Gröschel-Stewart et al. 1999b, Hoebertz et al. 2003).

P2X6 receptor subtype is predominant in skeletal muscle, widespread in the central and peripheral nervous systems where it overlaps to a large extent the expression pattern of P2X4 and P2X2 subtypes and can also be found in epithelial cells often together with the P2X4 subtype (Collo et al. 1996, Nawa et al. 1998, Glass et al. 2000, Turner et al. 2003).

Finally, P2X7 receptor subtype is expressed in most cell types, including haematopoietic cells, different types of glial cells in the central and peripheral nervous system, epithelial cells, bone cells, and others (Collo et al. 1997, Gröschel-Stewart et al. 1999a, Gartland et al. 2001, Zhang et al. 2005). P2X7 channel contributes to inflammatory responses and the development of chronic inflammatory and neuropathic pain but also mediates apoptosis in various cells types (Schulze-Lohoff et al. 1998, Gröschel-Stewart et al. 1999a, Solle et al. 2001, Labasi et al.

2002, Chessell et al. 2005, Kong et al. 2005). Differences in P2X receptor subtype expression within and between tissue types appear to therefore allow for tissue- and zonal-specific response to extracellular ATP release.

1.2.7 P2X receptors in pain pathways

Since ATP was first found to induce pain, research focused on identifying P2X receptor subtypes involved in pain pathways, their localization in the nervous system and their potential role and regulation in physiological and pathological pain states. P2X3 and P2X2/3 receptors, in particular, have a major role in pain mechanisms (Jarvis 2003). P2X3 and P2X2/3 receptors are upregulated in sensory neurons in different chronic pain models and functional studies confirm an important role for these receptors in nociception (Cockayne et al. 2000, Souslova et al. 2000, Jarvis et al. 2002, Ueno et al. 2003, Pan et al. 2009). At peripheral and spinal sites, P2X3 and P2X2/3 receptors have been shown to play a crucial role facilitating pain transmission whereas at supraspinal sites they are thought to have an inhibitory role (Jarvis 2003, Fukui et al. 2006) (Figure 1.5).

P2X4 receptors are normally expressed in small amounts in the microglia of the central nervous system (CNS) and are not involved in acute pain behaviour in physiological pain states. However, in cases of nerve injury an upregulation of P2X4 receptor subtype is noted in activated microglia of the spinal cord and activation of the receptors has been indicated to be not only necessary but also sufficient for causing allodynia (Tsuda et al. 2003). Like P2X4 receptor subtype, P2X7 receptors are modulating pain transmission through indirect mechanisms and not direct

neuronal activation (Donnelly-Roberts & Jarvis 2007). P2X7 receptors have been identified in microglia, astrocytes, satellite and Schwann cells and are thought to be involved in abnormal pain sensation and development and maintenance of neuropathic pain (North 2002, Chessell et al. 2005, Donnelly-Roberts & Jarvis 2007). Other receptors, such as P2X4/6 or P2X1/5 or P2X2, P2X4, and P2X6 subtypes identified centrally have also been suggested to participate in pain pathways (Chizh & Illes 2001, Nakatsuka & Gu 2006) (Figure 1.5). Finally, the existence of a natively expressed heteromeric P2X4/7 receptor subtype has been reported in bone marrow-derived macrophages and a potential integrative mechanism of the nociceptive roles of both P2X4 and P2X7 receptors in chronic pain states has been suggested (Guo et al. 2007).

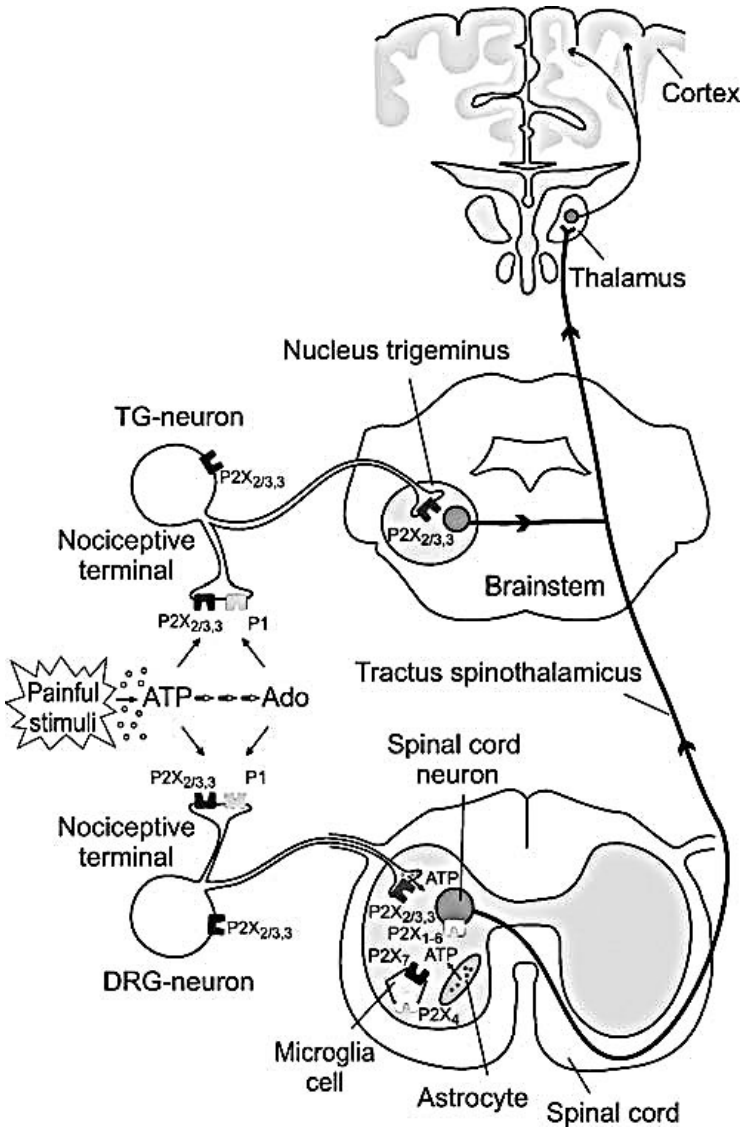

Figure 1.5. Ascending control of pain and localization of pain relevant P2X receptors in both neuronal and non-neuronal cells along the neuraxis (Wirkner et al. 2007, reproduced with permission).

1.3 P2X receptors in equine laminitis - Hypothesis

Purinergic signalling has been demonstrated to have an important role in across tissue systems and P2X and P2Y receptors participate in the regulation of many functions. Here, the investigation of P2X receptor expression in equine tissue was chosen as they have key roles in functions such as neurotransmission and chronic pain but also autocrine loops of endothelial and epithelial cells making them an interest target for study in a multifactorial condition such as laminitis. Also, more data and tools are available for P2X receptors compared to P2Y receptors making their study in a species like Equids more accessible. However, P2Y receptor expression in Equids may also present an interest and future work should include the study of their expression too.

In nociception, P2X2 and P2X3 receptors have an important role (Jarvis 2003) with P2X3 and P2X2/3 knockout mice exhibiting a reduction in pain sensation (Cockayne et al. 2000, Cockayne et al. 2005). P2X4 and P2X7 receptors expressed in glia are also involved in abnormal pain sensation (Tsuda et al. 2003, Chessell et al. 2005) (see 1.2.7 P2X receptors in pain pathways). Therefore, their study in horses could reveal important targets for pain therapeutics in chronic laminitic pain for which no effective treatments are available.

Also, vasoconstriction and its role in the development of laminitis and chronic laminitis is an important part of laminitis research (Hood et al. 1993, Moore et al. 2004) and purinergic regulation of vascular tone, with a particular role for P2X1 receptors expressed in smooth muscle (Burnstock 2009) may advance research in this area. Hypoxia and glucose deprivation, which may develop in lamellar tissues

during laminitis vascular events, are also known to trigger purinergic signalling (Cavaliere et al. 2001). Moreover, cycles of hypoxia and reoxygenation have been suggested as a pathogenetic mechanism behing vascular events in laminitis (Hood et al. 1993) and recent work has revealed altered purinergic signalling with increased $P2X_1$ receptor expression to occur following cycles of hypoxia-glucopenia and reoxygenation (Elliott et al. 2013).

Additionally, P2X5 and P2X7 receptors have been shown to participate in the early differentiation, terminal differentiation, and death of human keratinocytes (Greig et al. 2003), and therefore present an interest in the study of the events leading to dyskeratosis in laminitis. Moreover, the observed dyskeratosis in laminitic hooves has been suggested to occur secondary to aberrant insulin signalling via the MAP kinase pathway (Asplin et al. 2010). This may further implicate P2X receptors as MAP kinase signalling is one of the known downstream pathways following activation of the receptors (Donelly-Roberts et al. 2004, Seino et al. 2006). Furthermore, P2X7 receptor has a pivotal role in apoptosis (Schulze-Lohoff et al. 1998, Kong et al. 2005) and investigation of P2X7 receptor expression in epidermal basal cells may give an insight in the increased apoptosis rates in epidermal basal cells present in laminitic hooves (Faleiros et al. 2004, Asplin et al. 2010). P2X7 receptor is also involved in purinergic signalling in response to mechanical stimuli and in mechanically stimulated bone remodelling (Li et al. 2005, Panupithu et al. 2008) and may participate in the pathogenesis of mechanical overload lamintis but also in the events occurring in the hoof following increased pressure in the hoof capsule after the development of laminitis and bone remodelling in chronic laminitis.

Finally, P2X receptors may be implicated in the enzymatic events occurring in laminitis. P2X7 receptor has been found to mediate the release of proteases, such

as ADAMTSs and MMP-9 (Gu & Wiley 2006, Arandjelovic et al. 2012), which are elevated in lamellar tissue in inflammatory laminitis (Kyaw-Tanner et al. 2008, Visser & Pollitt 2012), supporting a role for P2X receptors in the enzymatic events occuring in inflammatory laminitis. In endocrinopathic laminitis, insulin itself can induce MMP-9 protein levels (de Laat et al. 2011) via insulin receptor activation and altered MAP kinase signalling (Fischoeder et al. 2007) possibly involving P2X receptor signalling (Donelly-Roberts et al. 2004, Seino et al. 2006).

Since purinergic signalling may have an important role in laminitis pathogenesis and development, investigation of P2X receptors expression in equine tissues related to laminitis could provide a better understanding of ongoing changes occurring during laminitis and P2X antagonists may be a useful tool for disease modulation.

1.4 Aims

The aims of this study are:

1. To identify the presence of P2X receptors in equine tissue
2. To characterise the distribution of P2X receptors in the equine hoof and its associated vasculature and innervation
3. To identify changes in expression and distribution of P2X receptors in the equine hoof and associated vasculature and innervation in horses suffering from chronic laminitis

4. To investigate the functionality of the P2X receptors expressed in equine nervous tissue and characterise them pharmacologically

Chapter 2

Materials and Methods

2.1 Samples

Equine tissue samples were collected with owner consent immediately post mortem from euthanized horses in accordance with institutional ethical approval. Animals included horses that had no previous history or evidence of fore limb or neurological disease and horses in a chronic active stage of laminitis (in accordance with Pollitt & Collins 2011). Sampled tissues included palmar digital artery (*a. digitalis lateralis/medialis*), palmar digital vein (*v. digitalis lateralis/medialis)*, palmar digital nerve (*n. digitalis palmaris lateralis/medialis)*, hoof, ipsilateral C8 DRG and spinal cord (forming median nerve (*n. medianus)* which innervates the hoof), ipsilateral C4 DRG and spinal cord (not innervating the hoof).

Palmar digital artery, vein, and nerve

The palmar digital neurovascular bundle was located on the side of the pastern, the palmar digital artery, vein and nerve were identified and a ~3 cm long segment was dissected from each (Figure 2.1a).

Hoof

The hoof was removed and samples, comprising of hoof wall and corium, were taken from the middle aspect of the dorsal hoof (adapted from Pollitt 1996). Briefly, hooves were cleaned, and with the sole on the base plate of the band saw, the first cut was in a lateral to medial direction palmar to the *processus extensorius* of P3. Subsequentally, cuts were made sagittally on either side of the hoof midline, 1 cm apart. With the newly cut surface on the base plate the remaining tissue block was trimmed to remove the bulk of the outer hoof wall and all but the dorsal cortex

of the distal phalanx. Finally, four transverse cuts, ~0.5 cm apart, were made starting below the coronary band and ending before the tip of P3 to obtain the samples, and a scalpel was used to excise excess hoof wall and the dorsal cortex of the distal phalanx from the samples (Figure 2.1b and c, and 2.2).

C4 and C8 DRG and spinal cord segments

The vertebral column from C2 to the T1 was dissected out and the spinal cord was exposed with a longitudinal cut on the contralateral side of the side of interest just abaxial to the spinal processes effectuated with the help of a band saw. Once the spinal cord was exposed, C4 and C8 spinal segments were located and transected with a scalpel. The respective DRGs were then located in the intraspinal space and a cut to the spinal nerve distal to the DRG was made to dissect out the spinal cord segment with the attached DRG. Finally, the DRG and spinal cord segments were separated and excess tissue was removed with a scalpel (Figure 2.1d, e, and f).

Figure 2.1. Equine sampled tissues. (a) Skin incision on the side of the pastern revealing the palmar digital neurovascular bundle (arrow). (b) Sagittal section of a normal hoof. The insert shows a hoof sample before trimming excess hoof wall and the distal phalanx bone. (c) Sagittal section of a hoof from a chronic laminitic horse with obvious rotation and sinking of P3 (arrow). (d) Use of the band saw for a longitudinal cut of the vertebral column to expose the spinal cord. (e) Longitudinal section of the vertebral column exposing the spinal cord. (f) C4 spinal cord with respective DRG (arrow) before separation.

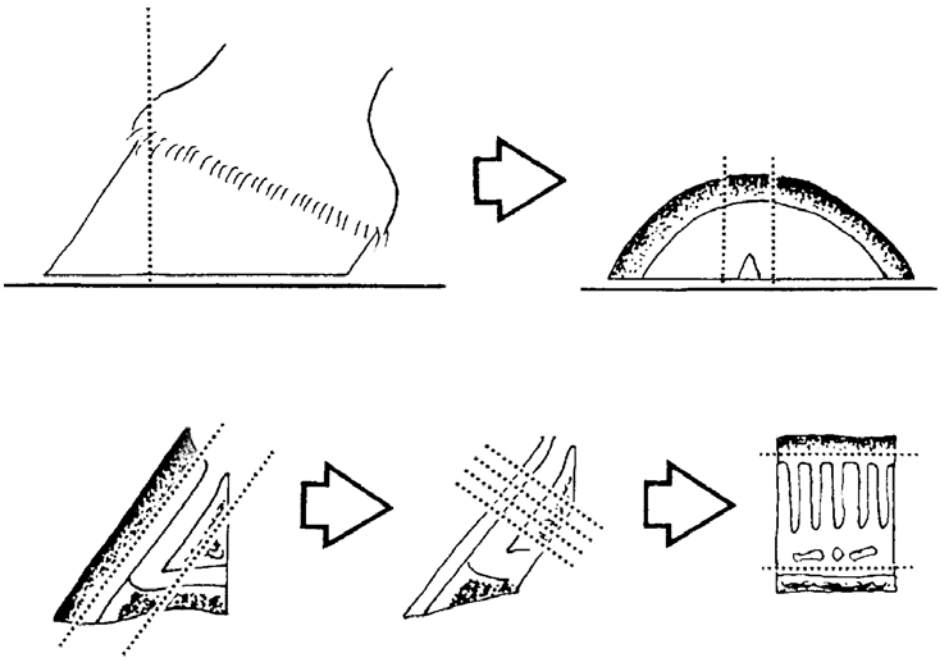

Figure 2.2. Band saw protocol carried out for the collection of hoof samples (adapted from Pollitt 1996).

2.2 Molecular biology experiments

2.2.1 RNA extraction

Samples for mRNA signal detection were collected in RNA*later* (Applied Biosystems) and stored at -80 ^{o}C until they were processed for RNA extraction. For RNA extraction, tissue samples were weighed and homogenised in TRI Reagent (Applied Biosystems) (150 mg tissue/1 mL TRI Reagent). Briefly, the weighed tissue was diced and placed in liquid nitrogen along with a dismembrator chamber and ball. Once frozen, the diced tissue was placed in the chamber with the ball and homogenised at 2000 rpm for 45 seconds (Mikro-Dismembrator U, B.Braun Biotech International). In case the homogenisation was incomplete, the chamber and its content were placed back in liquid nitrogen and the dismembration cycle was repeated until the tissue was fully homogenised. The homogenised tissue was then placed in TRI Reagent.

TRI Reagent suspensions were vortexed and left at room temperature (RT) for 30 minutes before centrifugation at 12,000 g at 2-8 ^{o}C for 10 minutes. The supernatant was collected in a new eppendorf tube and chloroform (200 µL/1 mL TRI Reagent) was added to the suspension. The tube was then shaken vigorously by hand for 15 seconds and left at RT for 2-3 minutes before centrifugation at 12,000 g at 2-8 ^{o}C for 15 minutes. The colourless aqueous upper phase containing RNA (400 µL/1 mL TRI Reagent) was transferred to a new eppendorf tube. Total RNA was isolated with the RNeasy® Mini Kit (Qiagen) according to the manufacturer's instructions. Briefly, an equal volume of 70% ethanol in DEPC treated water was added to the collected aqueous phase and mixed by pipetting. 700 µL of the sample

was transferred to an RNeasy spin column and centrifuged at 10,000 rpm (RT) for 15 seconds. The flow-through was discarded and the step was repeated with the remaining sample. Buffer RW1 (350 μL) was added to the RNeasy spin column, the column was centrifuged at 10,000 rpm for 15 seconds and the flow-through discarded. At this stage, a DNase digestion step (RNase-free DNase set, Qiagen) was performed to remove possible traces of genomic DNA from the samples. In a new eppendorf tube DNase I stock solution (10 μL/sample) was added to Buffer RDD (70 μL/sample) and the solution was mixed by gently inverting the tube. The DNase incubation mix (80 μL) was added directly to the RNeasy spin column membrane and the column was left at RT for 15 minutes. Buffer RW1 (350 μL) was then added to the RNeasy spin column, the column was centrifuged at 10,000 rpm for 15 seconds and the flow-through discarded. The RNA isolation protocol was continued with Buffer RPE wash steps. More specifically, Buffer RPE (500 μL) was added to the RNeasy spin column and centrifuged at 10,000 rpm for 15 seconds. The flow-through was discarded and the step was repeated with a 2 minutes centrifugation. The RNeasy spin column was placed in a new collection tube, centrifuged at full speed for 1 minute, and then placed in a new 1.5 mL eppendorf tube. RNase-free water (30 μL) was added directly to the column membrane and the column was centrifuged at 10,000 rpm for 1 minute to elute the RNA. The RNA yield of the samples was determined with a NanoDrop 1000 Spectrophotometer (ThermoScientific) and the samples were stored at -80 ^{o}C.

2.2.2 RNA and DNA measurements

RNA and DNA concentration measurements were carried out with a NanoDrop 1000 Spectrophotometer (Thermoscientific). Purity of DNA and RNA samples was assessed using the ratio of absorbance at 260 and 280 nm with a ratio of ~1.8 for "pure" DNA and ~2.0 for "pure" RNA.

2.2.3 cDNA synthesis

Reverse Transcriptase polymerase chain reaction (RT-PCR) was used to synthetise complementary DNA (cDNA) from RNA samples. For this purpose, 1-2 µg of extracted RNA, 1 µL/µg RNA of Random Primers (0.5 µg/µL, Promega) and RNase-free water to a volume of 13 µL were mixed in a 0.5 mL Eppendorf tube, heated at 70 ^{o}C for 5 minutes (Px2 Thermal Cycler, Thermo Electron Corporation) and quickly chilled on ice. Following this, 12 µL of mastermix, containing 5 µL of M-MLV 5x Reaction buffer (Promega), 1 µL each of dATP, dCTP, dGTP and dTTP (10 mM, Bioline), 1 µL M-MLV Reverse Transcriptase (200 U/µL, Promega), 0.625 µL of RNasin® Plus RNase Inhibitor (40 U/µL, Promega) and RNase-free water to 12 µL, were added to the mixture and the tube incubated at 37 ^{o}C for 60 minutes followed by 10 minutes at 95 ^{o}C to inactivate the reverse transcriptase. Finally, the DNA concentration of the obtained cDNA samples was measured with a NanoDrop 1000 Spectrophotometer and the samples were stored at -20 ^{o}C.

2.2.4 PCR amplification

Primers for equine P2X1-7 receptors amplification were designed with the primer design software PrimerExpress v3.3 or manually (P2X3), based on the predicted equine P2X1-7 mRNA sequences in NCBI (National Centre for Biotechnology Information) and Ensembl databases (Table 2.1).

Primers were designed with at least one primer from a pair spanning an exon junction and with the forward and reverse primers located on different exons (thereby spanning an intron). The amplicon length was set to 150-1000 base pairs and where possible, the amplicon was selected to be closer to the 3' end of the mRNA sequence (nucleotide sequence at the 3' end generally more fully elucidated). The following primer design parameters were also set for a successful amplification. Primer length was set to 16-24 base pairs and the primer melting temperature was set between 58 and 60 ^{o}C (within 2 ^{o}C of each other). The primers' GC content was set to 30-60% with not more than 3 Gs or Cs in the last 5 bases at the 3' end of the primer. Furthermore, the number of maximum consecutive complementary primer base pairs was set to 4 and the number of maximum total complementary primer base pairs was set to 8. Finally, the primer pair candidates were screened for specificity against the equine transcriptome (NCBI Transcript Reference Sequences) with the online tool Primer-BLAST (NCBI). Table 2.2 summarises equine P2X1-7 primers and their properties.

Table 2.1. Equine predicted P2X1-7 transcripts accession numbers, NCBI and Ensembl databases.

P2X receptor	**Accession number**	
	NCBI	Ensembl
P2X1	XM_001504730.1	ENSECAT00000010642
P2X2	-	ENSECAT00000017460
P2X3	XM_001504914.1	ENSECAT00000018031
P2X4	XM_001492153.2	ENSECAT00000025636
P2X5	XM_001918102.1	ENSECAT00000026624
		ENSECAT00000026645
P2X6 or	XM_001488204.2	ENSECAT00000009106
P2X-like 1 orphan		(ENSECAT00000000120)
receptor		(ENSECAT00000019561)
P2X7	XM_001495572.1	ENSECAT00000010815

Table 2.2. Equine primers used in PCR reactions.

Primer pair		Sequence	Amplicon length	Annealing temperature
eqP2X1	forward	TGAGTACGACACGCCTCGAA	569 bp	59^{o}C
	reverse	TGCGCCTTTTGACCTTGAA		
eqP2X2	forward	AATTCCAGTTCTCTAAGGGCAACA	186 bp	59^{o}C
	reverse	CCCAGTTGATAATGACCCCAAT		
eqP2X3	forward	CAGTGGAAATGCCTGTCATGA	281 bp	59^{o}C
	reverse	GGCCTTGTCCAAGTCGCA		
eqP2X4	forward	CGGCTACAACTTCAGGTTTGC	272 bp	59^{o}C
	reverse	CCTGATCGTAATCTGCCACATATT		
eqP2X5	forward	ACCCCAGGGAGAGAACGTCTT	527 bp	60^{o}C
	reverse	TGCATTCGGAGGGAGCTTTAT		
eqP2X6	forward	CAACTTCAGGACAGCCACTCACT	216 bp	59^{o}C
	reverse	GCTTCTCCATCCACGTACAACA		
eqP2X7	forward	TTCCTACGTTATCTTTGCCTTGGT	169 bp	59^{o}C
	reverse	GGTGTAGTCTGCGGTGTCGAA		

PCR was used to amplify equine P2X1-7 cDNA from cDNA samples. PCR reactions were performed in 50 μL final volumes containing 5 μL of 10x PCR Buffer (with $MgCl_2$, Sigma-Aldrich), 1 μL of dNTP mix (10 mM, Bioline), 15 pmol each of the appropriate forward and reverse primers (Applied Biosystems) (Table 2.2), 0.5 μL *Taq* DNA Polymerase (5 U/μL, Sigma) and 1 μL of cDNA sample in distilled water. Cycling conditions consisted of a step of denaturation at 94 ^{o}C for 10 minutes, 35 cycles of denaturation at 94 ^{o}C for 30 seconds, annealing at primer-specific temperature (Table 2.2) for 30 seconds, and elongation at 72 ^{o}C for 1 minute, followed by a final elongation step at 72 ^{o}C for 10 minutes (Px2 Thermal Cycler, Thermo Electron Corporation). In all experiments, negative controls were included which substituted distilled water for template.

2.2.5 PCR products DNA agarose gel electrophoresis

PCR amplified products were analysed by agarose gel electrophoresis. Agarose gels were composed of 1% (w/v) agarose (Promega) in 1x TAE buffer (50x TAE buffer, Bio-Rad) containing 5 μL per 100 mL ethidium bromide (10 mg/mL, Bio-Rad). After the gel had polymerised, it was transferred to a gel electrophoresis tank and submerged in 1x TAE buffer. 10 μL of PCR product were mixed with 2 μL of GelPilot DNA loading dye 5x (Qiagen) prior to loading into the wells of the gel. TrackIt™ 1 Kb Plus DNA ladder (Invitrogen) (10 μL) was used alongside PCR products. Electrophoresis was performed at a constant voltage of 140 V for 50-60 minutes or 80 V for 40-50 minutes, depending on the size of the gel. DNA products were visualised under a UV transilluminator (GeneGenius BioImaging System) and a

photograph was taken (GeneSnap). Acquired images were processed using Adobe Photoshop CS3 extended v10.0 image processing programme. PCR amplified products' identity was confirmed by size comparison with the predicted equine sequences and by subsequent DNA sequencing.

2.2.6 PCR products clean up and gel extraction

PCR amplified products' identity was confirmed by size comparison of the generated amplicon to the predicted sequences and by subsequent DNA sequencing. For that purpose, PCR products to be used in subsequent DNA sequencing reactions were purified.

PCR products generating a single band after agarose gel electrophoresis were purified with a QIAquick PCR purification kit (Qiagen) according to the manufacturer's instructions. Briefly, Buffer PB was added to PCR samples (5:1) and the mixture was applied to a QIAquick column to bind DNA. The column was centrifuged at 13,000 rpm for 30-60 seconds and the flow-through discarded. 750 μL of Buffer PE was applied to the column and the centrifugation step was repeated. The flow-through was discarded and the column was centrifuged at 13,000 rpm for an additional 1 minute. The column was then placed in a clean eppendorf tube and 30 μL of Buffer EB were added to the column membrane. The column was left to stand for 1 minute and then centrifuged at 13,000 rpm for 1 minute to elute DNA.

PCR products generating multiple bands were purified with a MinElute gel extraction kit (Qiagen). Briefly, the right sized band was excised of the agarose gel with a scalpel and weighed in an eppendorf tube. Buffer QG was added to the gel

slice (3:1) (100 μg ≈ 100 μL) and the tube was incubated at 50 ^{o}C for 10 minutes or until the gel slice had completely dissolved. 1 gel slice volume of isopropanol was added to the epperdorf tube and mixed by inverting the tube. The mixture was applied to a MinElute spin column, to bind DNA, and centrifuged at 10,000 rpm for 1 minute. The flow-through was discarded and 500 μL of Buffer QG was added to the column. The centrifugation step was repeated and the flow-through discarded. 750 μL of Buffer PE was added to the column and the column was left to stand 5 minutes before repeating the centrifugation. The flow-through was discarded and the QIAquick column was centrifuged for an additional 1 minute. The column was then placed in a clean eppendorf tube and 10 μL of Buffer EB were added to the column membrane. The column was left to stand for 1 minute and then centrifuged at 10,000 rpm for 1 minute to elute DNA. The concentration of the eluted DNA was measured with a NanoDrop 1000 Spectrophotometer and the samples were stored at -20 ^{o}C.

2.2.7 PCR products sequencing and analysis

PCR product identity was confirmed by band size and subsequent DNA sequencing. For this purpose, purified PCR products (1 ng DNA/μL per 100 bp) were sent along with the corresponding primer pair for sequencing at Source BioScience LifeSciences (Nottingham). The DNA sequencing results, forward and reverse nucleotide sequences, were read and analysed with 4Peaks software and Microsoft Office Word 2008. Reverse nucleotide sequences were converted to forward (Complementor tool, justbio.com) and forward and reverse nucleotide sequences were aligned (Aligner tool, justbio.com) to get eqP2X1-7 amplicon sequences.

eqP2X1-7 amplicon sequences were then compared with the respective predicted sequences by NCBI and Ensembl databases (Aligner tool, justbio.com). Where changes in nucleotide sequence were noted (compared to the predicted ones), alterations of the reading frame and changes in the resulting amino acid sequence were investigated (Translator tool, Aligner tool, justbio.com).

2.3 Western blot analysis

2.3.1 Protein extraction

Samples collected for Western blot experiments were snap frozen in liquid nitrogen and stored at -80 ^{o}C until processed for protein extraction. For this purpose, tissue samples were weighed and homogenised (for tissue homogenisation see tissue homogenisation step in 2.2.1 RNA extraction). The homogenised tissue was then placed in ice cold RIPA buffer (Sigma) supplemented with cOmplete Mini protease inhibitor cocktail tablets (1 tablet/10 mL of extraction buffer, Roche) (3 mL supplemented RIPA buffer/g of tissue), vortexed and incubated on ice for 30 minutes before centrifugation at 10,000 g at 4 ^{o}C for 10 minutes. The supernatant was collected and centrifuged again until the obtained lysate was clear.

2.3.2 Protein concentration measurements

The protein concentration of the samples lysates was measured with the Pierce BCA protein assay (Pierce BCA protein assay kit, Thermo Scientific). Briefly, 9 bovine serum albumin (BSA) diluted standards of known protein concentrations, ranging from 2000 μg/mL to 0 μg/mL, and the sample lysates to be measured (1:25 dilution) were prepared in protease inhibitor cocktail complemented RIPA buffer. Working reagent (WR) solution (200 μL/replicate of protein standard and unknown sample) was then prepared by mixing 50 parts of BCA Reagent A with 1 part of BCA Reagent B. 25 μL of protein standards and unknown protein samples were loaded in duplicate into a 96-well plate and 200 μL of WR was added to each well. The 96-well plate was mixed thoroughly by hand for 30 seconds and incubated at 37 ^{o}C for 30 minutes. After incubation, the plate was allowed to cool to room temperature, and was then placed into a photometric microplate absorbance reader (Multiskan FC, Thermo Scientific). A colorimetric quantitative analysis was obtained at a wavelength of 570 nm with the SkanIt Software 2.5.1 (Thermo Scientific) package and quantitative readings were saved in a Microsoft Office Excel 2008 file. The average values of protein standards' and samples' replicates readings were calculated and the average value of the blank standard was subtracted from all other averages. A standard curve was then created using the protein standards corrected values against their known protein concentrations (μg/ml) and the equation it yielded was used for the calculation of protein concentrations of unknown samples. The obtained protein concentrations for unknown samples were then multiplied by 25 to account for the initial samples' dilution. Negative control samples substituting water for sample were used.

2.3.3 Antibody selection

Antibodies raised against equine P2X1-7 receptor proteins are not commercially available. Therefore, antibodies raised against other species P2X receptor proteins were selected based on the homology of their immunogen peptide amino acid sequence to the respective equine predicted amino acid sequence (Table 2.3). Additionally, P2X1-7 equine proteins are predicted to share similar post translational modifications with the human and rat P2X1-7 proteins (http://prosite.expasy.org/).

Table 2.3. Details of homology of the selected P2X1-7 receptor antibodies immunogen peptides amino acid sequences to the respective equine predicted amino acid sequences.

P2X antibody	Manufacturer	Immunogen peptide	Species	Location	Equine sequence (predicted)	Similarity	
P2X1	APR-001 Alomone, Jerusalem	DPVATSSTLGLQENMRTS	rat	382-399 (C-terminus)	DPTTTSSTLG LQENMKTS	15/18	83.33%
P2X2	ab48864 Abcam, Cambridge	YPKFHFSKGNIADRTDGY LKRCTFHEASDLYCPIFK LGFIVEKAGESFTE	human	205-254 (extracellular)	YPKFQFSKGNIENRKDGYL KRCTFHEVSDLYCPIFKLGFI VEQAGENFTE	43/50	86%
P2X3	RA10109 Neuromics, Edina	VEKQSTDSGAYSIGH	rat/mouse	383-397 (C-terminus)	EEKQSTDSGAYSIGH	14/15	93.33%
P2X4	ab82329 Abcam, Cambridge	GHSFQDMAVEGGIMGIQVNW DCNLDRAASLCLPRYSFRRLD TRDVEHNVSPGYNFRFAKYY RDLAGNEQRTLIKAYGIRFDII VFGKAGKFDIIPTMINIGSGLA LLGMATVLCDIIVLYC	human	240-360	GHSFQDMAVEGGIMGIQIK WNCNLDRAASLCLPKYSFR RLDTRDVDHNVSPGYNFRF AKYYNDLTGTEHRTLIKAY GIRFDIIVFGKAGKFDIIPTMI NIGSGLALLGVATVLCDVIV LYC	110/121	90.91%
P2X4	APR-002 Alomone, Jerusalem	KKYKYVEDYEQGLSGEMNQ	rat	370-388 (C-terminus)	KKYKYVADYDQGLGSESD Q	13/19	68.42%
P2X5	APR-005 Alomone, Jerusalem	RENAIVNVKQSQILHPVKT	rat	437-455 (C-terminus)	LGNGKVNVEQPQNLQTVEA	8/19	42.11%
P2X6	ab80979 Abcam, Cambridge	LYVDREAHFYWRTKYEEAK APKATANSVWRELALASQAR LAECLRRSSAPA	human	350-400	LYVDGEAHFYWSTKYEEAK APKRTAPAP - incomplete	22/28	78.57%
P2X7	APR-008 Alomone, Jerusalem	KKGWMDPQSKGIQTGRC	mouse	136-152 (extracellular)	KKGWMDPQSKGIQTGRC	17/17	100%

2.3.4 Western blot

Western blot experiments were carried out to validate the use of the selected P2X1-7 antibodies in equine tissue. Sample size was set to 25 μg protein following preliminary Western blot analysis experiments with sample serial dilutions. Protein samples (25 μg) were mixed with lane marker non-reducing sample buffer (Thermo Scientific) and DTT (0.1 M) (Sigma) and denatured in a Unitek HBS-130 heated rack at 70 ^{o}C for 10 minutes. Samples used in Western blots for P2X2, P2X4, and P2X6 proteins did not undergo the denaturation step since P2X2, P2X4, and P2X6 antibodies showed better results with non-denatured samples. A NuPAGE 4-12% Bis-Tris gel cassette (Invitrogen) was inserted into an XCell Surelock Mini-Cell gel tank (Invitrogen) and submerged with 1x NuPAGE MES SDS Running Buffer (20x NuPAGE MES SDS Running Buffer, Invitrogen). Samples and 10 μL of Novex Sharp pre-stained protein standard (Invitrogen) were loaded on the gel and separated with a Bio-Rad PowerPac 300 at 200 V for 35 minutes. In the meantime, a Protran nitrocellulose membrane (Whatman), 2 filter papers and 6 sponge blotting pads were pre-soaked in transfer buffer (50 mL of 20x NuPAGE Transfer Buffer (Invitrogen) and 200 mL of methanol in 750 mL of ultrapure water) for 15 minutes. After sufficient separation of the samples, the gel was taken out of the cassette and a gel/blot sandwich was created by placing the pre-soaked nitrocellulose membrane on one side of the gel, one piece of pre-soaked filter paper on top of the nitrocellulose membrane, and the second piece of pre-soaked filter paper on the other side of the gel. All air bubbles were smoothed out and the gel/blot sandwich was placed in the Xcell II blot module (Invitrogen) in between the six pre-soaked sponge blotting pads with the nitrocellulose membrane on the side facing the anode. The blot module was

placed in the gel tank and transfer buffer was added to it before subjecting it to a constant power supply of 30 V for 1 hour 40 minutes.

After sufficient voltage exposure, the nitrocellulose membrane was removed from the gel/blot sandwich and placed into a PBS filled plastic tray and agitated on a Stuart Scientific Gyro Rocker SSL3 for 5 minutes. PBS was discarded and 1% skimmed dry milk PBS (Western blot blocking solution) was added to the membrane and agitated at RT for 1 hour to block non-specific binding. The blocking solution was then replaced with primary antibody solution, primary antibody (Table 2.4) in 5% skimmed dry milk PBS 0.1% Tween (PBST), and incubated at 4 ^{o}C overnight under gentle agitation.

After sufficient incubation, the primary antibody solution was removed and the membrane was washed 3 times in PBST for 5 minutes before adding the secondary antibody solution, 1:1000 goat anti-rabbit HRP-conjugated IgG (Sigma) in 5% skimmed dry milk PBST. The membrane was incubated with the secondary antibody solution at RT for 1 hour under gentle agitation. After incubation, the secondary antibody solution was discarded and the membrane washed, 3 times in PBST for 5 minutes, before adding 6 mL Oxidising Reagent Plus and Enhanced Luminal Reagent Plus (1:1) (Western Lightning-Plus ECL detection kit, PerkinElmer) and shaking in hand for 1 minute. Excess solution was drained off the nitrocellulose membrane and the membrane was placed in a clear plastic cover and in a luminescence cabinet (UVP ChemiDoc-it imaging system). The membrane was exposed to UV light for 20 to 30 minutes and images were created using VisionWorksLS image acquisition and analysis software package and processed using Adobe Photoshop CS3 extended v10.0 image processing programme. Equine P2X1-7 proteins molecular weight (MW) was calculated based on the predicted

amino acid sequences (NCBI, Ensembl) (MW tool, http://web.expasy.org/compute_pi/) and protein identification was based on the MW of the detected bands.

Control experiments were carried out with omission of the primary antibody. Additionally, for P2X1 and P2X7 receptor proteins, control experiments with pre-incubation of the primary antibody with its immunogen peptide were carried out. Briefly, P2X1 and P2X7 primary antibodies were pre-incubated with their respective immunogen peptides (2 µg peptide/µg antibody) (Alomone, Jerusalem) for 1 hour under gentle agitation before adding the primary antibody solution to the membrane for overnight incubation.

2.3.5 Coomassie stain/Mass spectrometry

To validate antibody specificity, the identity of the western blot bands was also checked by mass spectrometry. For this purpose, the samples lysates were separated electrophoretically on a NuPAGE 4-12% Bis-Tris gel (see 2.3.4 Western blot experiments) and stained with a 0.02% Coomassie Brilliant Blue stain solution. To prepare 500 mL of 0.02% w/v Coomassie Brilliant Blue stain solution 100 mg of Brilliant Blue R (BBR) (Sigma) was dissolved in 20 mL of ultrapure water and mixed to 30 mL of methanol. Once BBR was dissolved, 135 mL of methanol, 45 mL of acetic acid, and 270 mL of ultrapure water were added to the solution and mixed.

Once the gel was run, it was placed in a glass container, submerged in Coomassie stain solution and left for 2.5 hours under gentle agitation. The Coomassie stain solution was then replaced with a Coomassie destain solution (25

mL of acetic acid and 25 mL of methanol in 200 mL of ultrapure water) in order to visualise the protein bands. The destain solution was left for 30 minutes (under gentle agitation) and replaced with some fresh one until the gel matrix was clear. The bands corresponding to the bands seen on P2X Western blots were cut out, placed in an eppendorf tube and sent to the University of Manchester Protein Mass Spectrometry Core Facility for mass spectrometry analysis.

2.4 Histology and immunohistochemistry experiments

2.4.1 Samples preparation

Samples for histology or immunohistochemistry were fixed in 4% neutral buffered paraformaldehyde (PFA) for 24 hours and sent to the University of Liverpool Pathology department where they were embedded in paraffin, cut in 6 μm sections and mounted on polylysine slides.

2.4.2 Histology

Sections for histologic analysis were sent to the University of Liverpool Pathology department where H&E stain was carried out. H&E sections were visualised using Nikon eclipse 80i microscope and pictures were acquired with Nikon DS-L2 standalone control unit and analysed using Adobe Photoshop CS3 extended V10.0 image processing programme. H&E stained tissue samples were

assessed and descriptive analysis performed. For palmar digital artery and vein, the *tunica media* layer, containing the smooth muscle cells, was measured and expressed as a ratio of overall vessel thickness.

For hoof sections, changes in hoof histology in chronic laminitic horses were described as mild, moderate or severe (Hampson et al. 2012). The criteria used for the classification of changes in hoof histology included lengthening of the primary epidermal lamellae (PEL), attenuation and tapering of the tips of secondary epidermal lamellae (SEL) and the presence of abnormal columns of partially keratinised cells on either side of the keratinised axis of the PEL for mild changes, marked straightening and elongation of the SEL for moderate changes, and loss of lamellar architecture and organised recognisable SEL rows.

Finally, for C4 and C8 DRG sections, neuronal cell body size, small (<30 μm), medium (30-60 μm), and large (>60 μm) (adapted from Holford et al. 1994), and distribution were defined.

2.4.3 Immunohistochemistry

Antibody specificity was validated for P2X1-3, 7 antibodies (based on Western Blot results) and these were subsequently used in immunohistochemical analysis.

Sections for immunohistochemistry were deparaffinised and rehydrated in two washes of xylene, 100%, and 95% ethanol solution for 10 minutes and in two washes of ultrapure water for 5 minutes. Once rehydrated, the slides were submitted to antigen retrieval treatment.

The appropriate antigen retrieval method for each antigen/antibody was determined experimentally. The slides were submitted to two heat-induced antigen retrieval methods, citrate buffer and ethylenediaminetetraacetic acid (EDTA) buffer, two enzymatic antigen retrieval methods, proteinase and trypsin, or no antigen retrieval treatment at all, to find the treatment that gave optimal staining for each antibody.

The heat-induced antigen retrieval treatments consisted of incubation of the slides in 10 mM citrate buffer pH6 (sodium citrate trisodium salt dihydrate) or 1 mM EDTA buffer ph9 at sub-boiling temperature of ~96 ^{o}C for 25 minutes. The slides were subsequently left in the buffer until it cooled down to RT and washed twice in ultrapure water for 5 minutes for citrate buffer or put straight in ultrapure water for two washes of 5 minutes for EDTA buffer. The proteinase antigen retrieval treatment consisted of incubation of the slides in PBS at 37 ^{o}C for 5 minutes, followed by an additional 5 minutes in a 0.05% w/v proteinase solution (bacterial proteinase type XXIV, Sigma) at 37 ^{o}C and finally of two washes in ice-cold Tris Buffered Saline (TBS) (2.42 g of Trizma base and 8 g of sodium chloride in 1 L of ultrapure water) for 5 minutes. The trypsin antigen retrieval treatment consisted of incubation of the slides with 0.25% w/v trypsin (Gibco) at RT for 10 minutes and two subsequent washes in TBS for 5 minutes.

Assession of the obtained staining to determine the antigen retrieval treatment that gave the best results for each antibody was based on the presence of staining, the location of the staining, the staining intensity, and the presence of background staining. Antibodies for P2X1 and P2X2 receptor protein showed optimal staining with the proteinase antigen retrieval treatment, whereas P2X3 receptor protein

antibody showed optimal staining with the citrate pH6 buffer and P2X7 receptor protein antibody with the EDTA pH9 buffer antigen retrieval treatment.

Following antigen retrieval treatment, the slides were washed in ultrapure water for 5 minutes and incubated in a 3% hydrogen peroxide solution for 10 minutes to block endogenous peroxidase activity. After the endogenous peroxidase block, the slides were washed twice in ultrapure water for 5 minutes and then in TBS for an additional 5 minutes.

Each section was subsequently blocked with 400 µL of 10% normal goat serum (Vector Laboratories) in TBS (blocking solution) at 25 ^{o}C (Roller-Blot Hybridiser HB-3D, Techne) for 1 hour to prevent non-specific antibody binding. The blocking solution was replaced with 100 µL primary antibody solution, primary antibody in blocking solution (Table 2.4), and the slides were incubated at 25 ^{o}C for 1 hour 10 minutes. After sufficient incubation with the primary antibody, the slides were washed in TBS three times for 5 minutes, and 95 µL of Zytochem Plus HRP Polymer anti-rabbit (Zytomed Systems) was added to each section at 25 ^{o}C for 40 minutes. The slides were washed in TBS three times for 5 minutes before adding 300 µL of 3'3-diaminobenzidine (DAB) solution (SigmaFast DAB with metal enhancer, Sigma) for 30 seconds or 1 minute for P2X3 antibody. Once staining had developed, the slides were immersed in ultrapure water for 5 minutes and counterstained in Delafield's hematoxylin (Fluka) for 10 seconds before being washed in tap water. Finally, the sections were dehydrated in two washes of 95% ethanol solution, 100% ethanol, and xylene for 10 seconds in the first wash and 5 minutes in the second. Once dehydrated, the slides were coverslipped with Clarion mounting medium (Santa Cruz Biotechnology).

The sections were visualised under a Nikon eclipse 80i microscope. Pictures were taken with a Nikon DS-L2 standalone control unit and processed with Adobe Photoshop CS3 extended V10.0 image processing programme.

Control experiments were carried out with omission of the primary antibody and substitution of the primary antibody with non-immune rabbit polyclonal IgG (isotope control) (Abcam).

Table 2.4. P2X1-7 antibodies used in Western blot and immunohistochemistry experiments with their respective concentrations. Antibody specificity was validated for P2X1-3, 7 antibodies and these were subsequently used in immunohistochemical analysis.

Antibody	**Manufacturer**	**WB antibody concentration**	**IHC antibody concentration**
P2X1	APR-001 Alomone, Jerusalem	1:200	1:200
P2X2	ab48864 Abcam, Cambridge	0.6 μg/mL	1:125
P2X3	RA10109 Neuromics, Edina	1:1000	1:1000
P2X4	ab82329 Abcam, Cambridge	1:300	-
	APR-002 Alomone, Jerusalem	1:200	-
P2X5	APR-005 Alomone, Jerusalem	1:200	-
P2X6	ab80979 Abcam, Cambridge	10 μg/mL	-
P2X7	APR-008 Alomone, Jerusalem	1:200	1:200

2.4.4 Semi-quantitative immunohistochemistry

Semi-quantitative immunohistochemistry was carried out for immunostained sections of normal horses and horses suffering from chronic laminitis for P2X receptor subtypes and tissues that presented with a special interest (eg. P2X3 receptor subunit in DRG).

Acquired pictures of immunostained sections were analysed for staining intensity using Adobe Photoshop CS3 extended V10.0 image processing programme. Pictures of all representative fields of the immunostained sections were taken and three or five of them were randomly selected for analysis for P2X7 and P2X3 staining, respectively. The selected pictures were corrected for white balance on Adobe Photoshop before proceeding to staining intensity measurements.

P2X3 receptor subtype staining intensity measurements

For quantification of P2X3 receptor subtype staining intensity in C4 and C8 DRG neurons, staining intensity was measured in individual cells. Each cell was selected and the cell area and mean gray scale intensity for the cell (with exclusion of the nucleus) were obtained. All measurements were exported in a text file and analysed in Microsoft Office Excel 2008. The diameter of the cells was calculated based on the measured cell area ($d = 2\sqrt{(A/\pi)}$), and the calculated pixels were converted to μm using the scale bar (104 pixels = 100 μm). The cell measurements (diameter and gray scale measurements) were sorted in cell diameter ascending order for each picture and the cells were split into three categories based on diameter; small-sized with $d<30$ μm, medium-sized with d 30-60 μm, and large-sized with $d>60$ μm. Subsequently, the average and standard deviation of the gray scale

measurements were calculated for each cell category in each horse (5 fields) and staining intensity in C8 DRG for each horse was normalised against C4 DRG staining of the same horse. Finally, normalised C8 DRG staining intensity for chronic laminitic horses was expressed as a ratio to normalised staining intensity of C8 DRG in non-laminitic horses and plotted against the duration of chronic laminitis. For this purpose, 3 variables surface plots were carried out in SigmaPlot for Windows 12.5.

P2X7 receptor subtype staining intensity measurements

For quantification of P2X7 receptor staining intensity in C4 and C8 DRG sections, staining intensity was measured by selecting an immunostained structure (immunostained myelin sheath) and then expanding the selection to all immunostained structures on the picture (Select similar command). The mean gray scale intensity of the selection was then recorded and the same process was repeated selecting a counterstained nuclei to measure counterstain intensity. All measurements were input in an Excel file and the average values were calculated for each horse. Finally, P2X7 staining intensity was normalised for respective counterstain intensity and corrected values for normal and chronic laminitic horses were tested for significance (see 2.8 Statistical analysis).

2.5 Electrophysiology experiments

2.5.1 Tissue digestion and neurons extraction

C4 and C8 DRGs were dissected out of normal and chronic laminitic horses within 1-2 hours of death, placed in ice-cold growth medium (Dulbecco's modified Eagle's medium, low glucose, pyruvate (DMEM), 31885-023, Gibco) supplemented with 10% foetal calf serum (FCS) (Lonza), 100 U/mL penicillin, 100 mg/mL streptomycin (P/S) (Gibco) and 500 ng/mL amphotericin B (F) (Gibco), and enzymatically digested for the extraction of DRG neurons.

The following steps for the extraction of DRG cells were executed in a class I laminar flow hood under aseptic conditions with the use of sterile tools and sterile filtered solutions (0.2 μm filters, Whatman). The dissected DRGs were washed twice in Hank's balanced salt solution (HBSS) (Gibco), placed in a petri dish in ice-cold growth medium, and diced with a scalpel. The diced DRGs were added to the digestion solution, 2 mg/mL of collagenase I (Worthington) and 5 mg/mL of dispase II (Sigma) in growth medium, and the mixture was incubated in a shaking incubator (SI500, Stuart) at 37 ^{o}C at 180-200 rpm for 5 hours or overnight until the samples were fully digested.

Once digested, the samples were strained with 40 μm Falcon cell strainers (BD) to remove gross tissue debris, centrifuged at 400 g for 5 minutes to spin the cells down, and resuspended in HBSS in order to wash the cells. The cells were washed a second time in HBSS and a fire-polished Pasteur pipette (Volac, Poulten & Graf) was used to triturate the cell suspension and dissociate cell clumps. The cell suspension was subsequently gently overlaid onto a 22% isotonic Percoll solution

(Sigma) and centrifuged at 950 g for 20 min to remove myelin and cell debris. The supernatant containing the myelin and cell debris was discarded and the cells were washed twice in HBSS, resuspended in growth medium, plated in 75 cm^2 flasks and placed in a humidified incubator at 37 ^oC with an atmosphere of 5% CO_2 until use the next day.

2.5.2 Cell preparation

Whole-cell and perforated whole-cell patch-clamping experiments were performed on freshly isolated C4 and C8 DRG neurons for 1 to 4 days after extraction.

For this purpose, plated cells were lifted from the 75 cm^2 flasks using trypsin. Briefly, growth medium was removed and the cell layer was washed twice with HBSS, before 2.5 mL of 0.25% Trypsin-EDTA (Gibco) was added to the cells. The cells were incubated at 37 ^oC for 5 minutes and and a volume of growth medium equal to the volume of trypsin was used to halt digestion. The cells were then transferred to a 15 mL falcon tube, spun down, and washed twice in HBSS, before resuspending in serum free growth medium (supplemented DMEM without FCS) and plating at high density (empirical) on poly-L-lysine coated glass-bottom Petri dishes (35 mm with 14 mm hole). Plated Petri dishes were left for a minimum of 30 minutes in a humidified incubator (37 ^oC, 5% CO_2) for neurons to adhere.

2.5.3 Set up

Microscope

For patch-clamping, an inverted compound microscope with fixed stage set up on an anti-vibration table was used. An electrode holder was positioned on a manual micromanipulator and connected to a remote hydraulic micromanipulator for the fine movement of the electrode. The electrode was connected to an Axopatch 200a amplifier (Axon Instruments, USA) and a DigiData 1200B interface (Axon Instruments, USA) attached to a PC running the WinEDR software (Dr. John Dempster, University of Strathclyde) for data acquisition. Finally, a ground electrode, connected to the amplifier's circuit ground terminal, was placed in the dish water bath to set the zero level.

Water bath and agonist and antagonist delivery

A constant perfusion system was set up with one tip providing fresh extracellular solution (Table 2.5) and the other one draining the overflowing solution in a waste container. P2X agonists were applied locally onto the patched neuron with a U-tube drug delivery system and P2X antagonists were perfused into the bath (for 10 min) before agonist application.

Micropipettes

Patch micropipettes were pulled from fire-polished 1.5mm o.d. borosilicate capillary tubes (Sutter Instrument, Novato CA, USA, supplied by INTRACEL, UK) with a vertical two-step electrode puller (PC-10 Puller, Narishige). When filled, the

fabricated micropipettes had a resistance in the range of 5-9 MΩ for whole-cell patch-clamping and 1.6-4 MΩ for perforated whole-cell patch-clamping.

Cell selection

Neurons were identified amongst other DRG cells based on their size (larger than all other DRG cells). A suitable neuron for patch-clamping was selected, and moved to the centre of the microscope field. Suitable cells included single, phase-bright cells isolated from neighbouring cells and potential debris (Figure 2.4a).

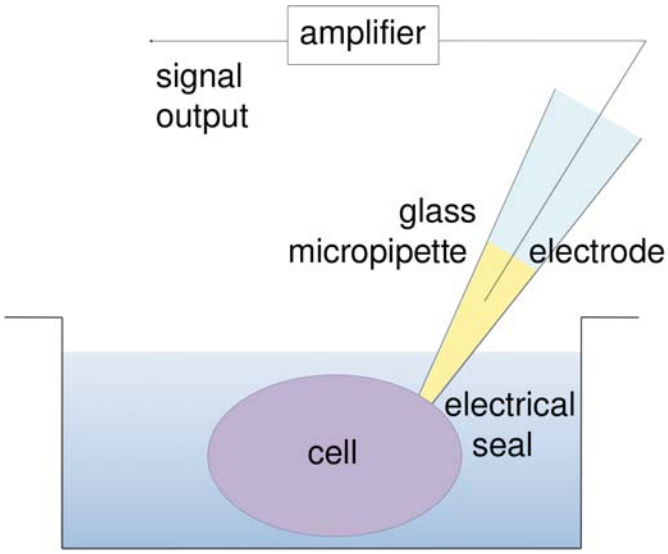

Figure 2.3 Schematic of the patch clamp technique. A glass micropipette is pressed against a cell to form a high resistance electrical seal and the electrode contained in the micropipette converts ion currents generated by the cell into electrical currents which are read by the amplifier (patch clamp).

2.5.4 Whole-cell patch-clamp

The bottom half of a glass micropipette was filled with internal pipette solution (filtered, 0.2 μm filter) (Table 2.5) and trapped air bubbles were removed by gentle tapping of the pipette shaft. The micropipette was then attached to the electrode holder and its tip was dipped into the bath. The Seal test was selected in the WinEDR software and the Seal test protocol was run. The micropipette was manoeuvred near the centre of view and gradually brought down over the cell. The fine controls of the manipulator were then used to bring the pipette down onto the surface of the cell. Once contact was made with the cell, the electrode resistance, monitored on the computer screen, spontaneously increased. At this stage, gentle suction was applied to the micropipette to help the formation of a seal. As the seal started forming, the micropipette resistance gradually increased and the trace on the computer screen took the shape of a flat line.

Once a stable seal of a resistance higher than 1 GΩ (gigaseal) was achieved, attempts were made to break the cell membrane patch under the pipette to achieve a whole-cell patch-clamp. Rupture of the cell membrane and electrical access to the intracellular space was indicated on the computer screen by the sudden appearance of large capacity transients at the leading and trailing edges of the pulse. If a gigaseal or a whole-cell configuration could not be achieved the cell was dropped, the micropipette discarded, and a new cell was located to repeat the procedure.

Table 2.5. Composition of electrophysiology extracellular and intracellular solutions.

Extracellular solution		
NaCl	150 mM	8.77 g/L
$MgCl_2$	1 mM	0.20 g/L
$CaCl_2$	1 mM	0.11 g/L
D-glucose	10 mM	1.80 g/L
HEPES mM	10 mM	2.38 g/L
pH adjusted at 7.4		

Intracellular solution		
$C_6H_{11}KO_7$	140 mM	32.80 g/L
NaCl	5 mM	0.29 g/L
EGTA	10 mM	3.80 g/L
HEPES	10 mM	2.38 g/L
pH adjusted at 7.3		

2.5.5 Perforated whole-cell patch-clamp

For the perforated whole-cell patch-clamp technique, an amphotericin B solution (210 µg/mL) was used for the internal pipette solution. The amphotericin B stock solution was made up in dry dimethylsulfoxide (DMSO) (30 µg/µL) and kept away from light at -20 ^{o}C (for up to one week). The amphotericing B working solution was prepared by mixing 7 µL of stock solution in 993 µL of pipette solution. During the experiments, the working solution was kept on ice in the dark and renewed every 2-3 hours. The bottom half of the micropipette was filled with the amphotericin B solution and the micropipette's tip was backfilled with the internal pipette solution by dipping the tip in the internal pipette solution for 3 to 5 seconds. A neuron to clamp was then selected and a stable gigaseal was formed following the same procedure as for the whole-cell patch-clamp technique. Once a gigaseal was formed, the amphotericin B solution contained in the micropipette was left to work until access to the intracellular space was gained or for a maximum of 40 minutes. Perforation of the cellular membrane was identified on the computer screen by the appearance of large capacity transients at the leading and trailing edges of the pulse.

If no change was observed after 40 minutes, the cell was dropped, and a new pipette with fresh amphotericin B solution was used on a new cell.

2.5.6 Patch-clamp recordings

Recordings were made with the cells held at -60 mV and data were acquired with a DigiData 1200B interface (Axon Instruments, USA) attached to a PC running the WinEDR software (Dr. John Dempster, University of Strathclyde).

2.6 Intracellular calcium measurements

2.6.1 Cells

Calcium measuring experiments were carried out in C8 DRG cells cultured to confluence and freshly isolated C8 spinal cord segment cells. For this purpose, C4 and C8 DRGs and spinal cord segments were dissected out of normal horses, placed in ice-cold medium (P/S, F, and 10% FCS DMEM) and processed for cell extraction (see 2.5.1 Tissue digestion and neurons extraction). The extracted cells were used directly (spinal cord) or plated in 75 cm^2 flasks and cultured to confluence (C8 DRG). After culture, the DRG cell population was mainly consisting of supportive cells, ie. satellite glial cells, Schwann cells, and fibroblasts, and few or no neurons (Figure 2.4b).

The viability of the extracted or cultured cells was determined with the trypan blue exclusion method. Briefly, 10 μL of 0.4% trypan blue solution (Sigma Aldrich) was mixed with 40 μL of cell suspension (1:5) and left at room temperature for 2-3 minutes. The cell suspension (20 μL) was then pipetted into a haemocytometer chamber and the live and dead cells contained in 5 squares were counted under the microscope. The calculated percentage of unstained cells (vs total number of cells) represented the percentage of viable cells.

Furthermore, in order to be used in calcium measuring experiments, the cell density of the cell suspensions was determined. For this purpose, approximately 20 μL of cell suspension was pipetted into a haemocytometer chamber and the number of cells in 5 squares was counted under the microscope. The average count of cells per square was then calculated and the total number of cells per mL was calculated (cells per mL = average count of cells per square x 10^4).

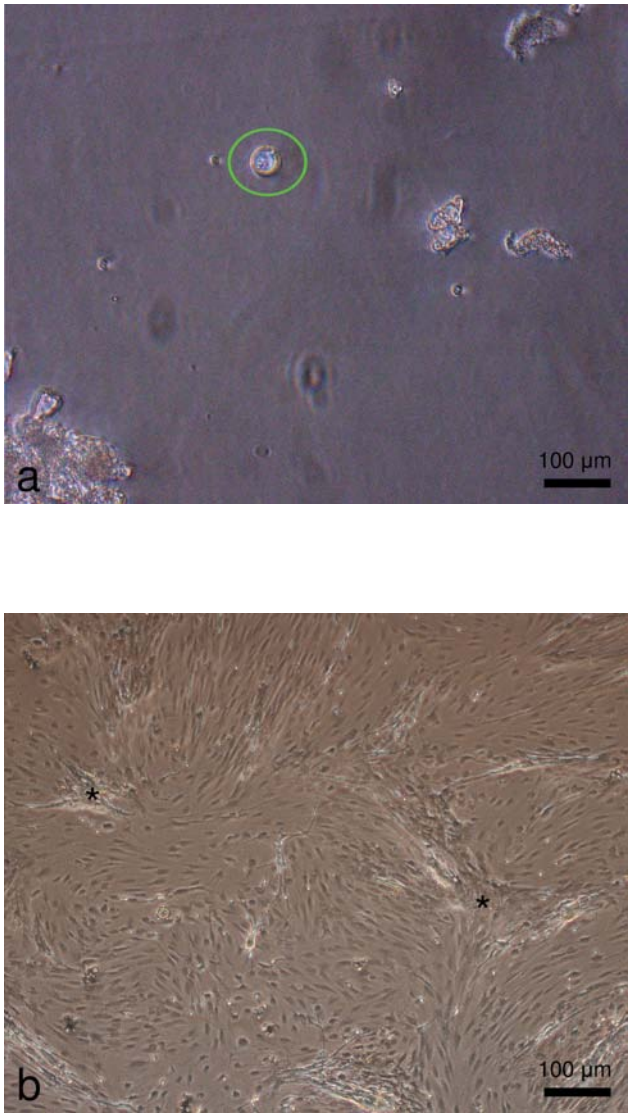

Figure 2.4. (a) DRG neuron for patch-clamping (circled); single, phase-bright, and isolated from neighbouring cells and potential debris. (b) DRG cells after culture. The population is mainly consisting of supportive cells and few neurons (asterisk).

2.6.2 Dye, cell preparation, and equipment

For calcium measuring experiments, Fura-2 AM (Ca^{2+}) indicator (Life Technologies) was used, a UV excitable ratiometric fluorescent dye with excitation peaks of 340 nm (Ca^{2+}-bound dye) and 380 nm (Ca^{2+}-free dye) and an emission peak of 510 nm (Paredes et al. 2008).

In order to load Fura-2 AM into the cells, the plated cells were trypsinised (see 2.5.2 Cell preparation) and resuspended in phenol red-free DMEM (11880-028, Gibco) (supplemented with L-glutamine, Gibco) or bicarbonate-free MOPS-buffered isotonic saline (Table 2.6). The cell suspension was then incubated with 6 μM of Fura-2 AM at 37 ^{o}C for 30 minutes in the dark. After incubation, the cells were washed twice and resuspended in phenol red-free DMEM or bicarbonate-free MOPS-buffered isotonic saline at a density of 250,000 cells/mL or 500,000 cells/mL, for fluorescence plate reader or spectrofluorimeter recordings, respectively.

Recordings were made in a fluorescence plate reader (FLX800 Microplate Fluorescence Reader, Bio-Tek Instruments Inc) or a spectrofluorimeter (F-2000 Fluorescence spectrophotometer, Hitachi), both regulated at 37 ^{o}C. The dye was alternately excited at 380 nm and 340 nm, with fluorescence emission measured at 510 nm.

Table 2.6. Bicarbonate-free MOPS-buffered isotonic saline composition.

Bicarbonate-free MOPS-buffered isotonic saline		
NaCl	145 mM	8.47 g/L
KCl	5 mM	0.37 g/L
$MgSO_46H_2O$	1 mM	0.20 g/L
$CaCl_2$	2 mM	2 mL of 1 M solution (110.99 g/L)
MOPS	10 mM	2.09 g/L
D-glucose	10 mM	1.80 g/L
pH adjusted at 7.4 at 37 ^oC		

2.6.3 Fluorescence plate reader recordings

Recordings in the fluorescence plate reader were carried out in C8 DRG cells from one normal horse (cultured to confluence). For this purpose, 200 µL of Fura-loaded cell suspension (250,000 cells/mL) was loaded in the wells of a black 96 well-plate and the potent P2X7 agonist, 2′(3′)-O-(4-benzoylbenzoyl)adenosine 5′-triphosphate triethylammonium salt (BzATP) (Sigma), and the non-selective P2X antagonist, iso-pyridoxalphosphate-6-azophenyl-2',5'--disulfonic acid tetrasodium salt (*iso*-PPADS) (Tocris Bioscience), were used to challenge the cells. BzATP was used at concentrations of 10, 50, 100, 500 µM and 1 mM and *iso*-PPADS was used at a concentration of 20 µM (Table 2.7).

Fluorescence was, initially, measured in resting cells to establish a signal baseline and then in agonist and antagonist challenged cells to record changes in intracellular calcium ($[Ca^{2+}]_i$) levels. For this purpose, single F_{340} and F_{380} fluorescence measurements were taken from the wells before and straight after the addition of BzATP (10, 50, 100, 500 µM and 1 mM) (n = 1). Subsequently, 20 µM

iso-PPADS was added to fresh cells, the plate was incubated at 37 ^{o}C for 30 minutes in the dark, and single F_{340} and F_{380} fluorescence measurements were taken from the *iso*-PPADS-incubated cells before and straight after the addition of BzATP (10, 50, 100, 500 μM and 1 mM) (n = 1).

2.6.4 Spectrofluorimeter recordings

Calcium measuring experiments with the spectrofluorimeter were carried out in C8 DRG cells from two normal horses cultured to confluence and freshly isolated C8 spinal cord cells from one normal horse. For this purpose, 750 μL of cell suspension (500,000 cells/mL) was placed in a polystyrene semi-micro cuvette (Sarstedt) for each series of measurements while the stock of loaded cells was maintained on ice in the dark.

Background measurements were performed to correct for buffer fluorescence and cell autofluorescence. For this purpose, 5 F_{340} and F_{380} fluorescence measurements were made in the used cell suspensions in absence of Fura-2AM dye and these were used to correct subsequent F_{340} and F_{380} measurements.

Selective and non-selective P2X agonists and antagonists were used to challenge the cells and the cells' intracellular calcium responses were recorded. Specifically, the non-selective P2X agonist ATP (Sigma) was used at concentrations of 5, 10, 50, 100, 200 and 500 μM (C8 spinal cord cells, n = 1), the potent P2X7 agonist BzATP was used at concentrations of 0.5 , 5 and 50 μM in preliminary experiments (C8 DRG cells, n = 1) and 10, 50, 100, 200 μM (C8 DRG cells, n = 3), the non-selective P2X antagonist *iso*-PPADS at a concentration of 20 μM (C8 DRG

cells, n = 3), and the P2X7 selective antagonist BBG (BDH) at a concentration of 1 mM (C8 DRG cells, n = 3). The use of P2X antagonists was combined with stimulation of the cells with 100 μM BzATP.

For stimulation experiments, 5 fluorescence measurements were initially made to establish the signal baseline in resting cells (before the addition of the agonist). The agonist was then added to the cell suspension and signal recordings were made for periods of 300 seconds, with intervals of 2-3 seconds for the first 30 seconds (0-30 seconds), 10 seconds for the next 150 seconds (30-180 seconds), and 30 seconds for the last 120 seconds (180-300 seconds). For P2X antagonists, the cell suspension was preincubated with the antagonist for 10 minutes at 37 ^{o}C in the dark before being placed in the spectrofluorimeter. Once in the spectrofluorimeter, fluorescence measurements were made as mentioned above. Measurements were also carried out in calcium free buffer, bicarbonate-free MOPS-buffered isotonic saline lacking $CaCl_2$ and supplemented with ethylene glycol tetraacetic acid (EGTA) (1 mM) (Sigma) to chelate Ca^{2+}, after stimulation with 5 μM of BzATP (C8 DRG cells, n = 1). Measuresements were carried out as mentioned above for 120 seconds.

2.6.5 Data analysis

Data were acquired and transferred to an Excel spreadsheet for analysis. Average values for background measurements at each wavelength were calculated and subtracted from respective subsequent measurements to correct for background and autofluorescence. F_{340}/F_{380} ($F_{\text{Ca-bound}}/F_{\text{Ca-free}}$) fluorescence ratios, reflecting $[Ca^{2+}]_i$ concentrations, were then calculated for all measurements using the corrected

values. For the signal baseline in resting cells where multiple measurements were taken, the average value of these measurements was calculated and used. F_{340}/F_{380} fluorescence ratios following agonist addition were expressed in graphs in relation to baseline signal by subtracting baseline F_{340}/F_{380}. Also, maximum fold or percent changes in Fura-2 fluorescence were calculated for all used P2X agonists and antagonists by dividing the maximal F_{340}/F_{380} by the baseline F_{340}/F_{380}. For P2X antagonists, the percent of inhibition was also calculated. For this purpose, the difference in maximal F_{340}/F_{380} with and without the antagonist was divided by the maximal F_{340}/F_{380} without the antagonist. Finally, where replicates were used the mean was calculated and expressed as mean ± stardard deviation (SD).

2.7 Intracellular calcium imaging

For calcium imaging experiments, Fluo-4 AM (Ca^{2+}) indicator (Life Technologies) was used; a single wavelength dye with an excitation peak of 494 nm and an emission peak of 506 nm. Fluorescence was monitored with a Olympus CK40 microscope (equipped with a CX-DMG-2 mirror cube) and recorded with ProgRes® Mac CapturePro 2.7 software (Jenoptik).

Cells used in calcium imaging experiments were freshly isolated from C8 DRG from three normal horses (see 2.5.1 Tissue digestion and neurons extraction). Extracted DRG cells were resuspended in phenol red-free DMEM at low density (empirical) and plated in poly-L-lysine coated 24-well plates (0.01% poly-L-lysine solution, Sigma). The cells were left to adhere overnight in a humidified incubator (37 ^{o}C, 5% CO_2). Once the cells were attached to the wells, the growth medium was

discarded and the cell layer was washed with sterile PBS before loading the Fluo-4 AM dye. For this purpose, the cells were incubated with 5-10 μM of Fluo-4 AM at 37 ^{o}C for 30 minutes in the dark. One well was loaded with dye at each time so the used cells were always freshly loaded. After incubation, the cells were washed twice and phenol red-free DMEM was added to the well. The cells were left for 10 additional minutes in the dark in a humidified incubator before use.

The 24-well plate was placed under the microscope and neuron cells were identified based on size. A photo of the cells in a resting state was acquired with ProgRes® Mac CapturePro 2.7 software before addition of the agonist. After addition of the agonist, photos of the stimulated cells were taken every 2 seconds for 60 seconds. The agonist used in this experiment was ATP at a concentration of 1 mM.

The photos acquired with ProgRes® Mac CapturePro 2.7 software were analysed with Adobe Photoshop CS3 to measure fluorescence intensity. The fluorescence intensity of the background was measured using mean gray value measurements to correct cell fluorescence for background fluorescence. The cell of interest was then selected and the mean gray value of the cell was obtained. The process was repeated for all photos with the same selection and the acquired values were input in an Excel sheet. Background fluorescence intensity values were subtracted from the respective cell fluorescence intensity values to correct for background fluorescence and the changes to fluorescence 30 seconds after agonist application were calculated by dividing the fluorescence at 30 seconds after agonist application by the baseline fluorescence in resting cells (F/F_{rest}).

Table 2.7. Summary of cells, materials and P2X agonists and antagonists used in intracellular calcium measuring and imaging experiments.

	Calcium measuring experiments		**Calcium imaging experiments**
	Fluorescence plate reader	**Spectrofluorimeter**	
Tissue	C8 DRG	C8 DRG and spinal cord	C8 DRG
Dye	Fura-2 AM	Fura-2 AM	Fluo-4 AM
Cell preparation	cell suspension 250,000 cells/mL	cell suspension 500,000 cells/mL	plated in 24-well plates (low density)
Equipment	fluorescence plate reader (FLX800 Microplate Fluorescence Reader, Bio-Tek Instruments Inc)	spectrofluorimeter (F-2000 Fluorescence spectrophotometer, Hitachi)	Olympus CK40 microscope, CX-DMG-2 mirror cube
P2X agonists	BzATP (10, 50, 100, 500, 1000 μM)	ATP (5, 10, 50, 100, 200, 500 μM) BzATP (10, 50, 100, 200 μM)	ATP (1 mM)
P2X antagonists	*iso*-PPADS (20 μM)	*iso*-PPADS (20 μM) BBG (1 mM)	

2.8 Statistical analysis

Data were tested for Normality using the Shapiro-Wilk test (SPSS Statistics 21 and web version http://sdittami.altervista.org/shapirotest/ShapiroTest.html) significant differences in data sets were determined with Student's *t* test (independent, two tailed) (Microsoft Office Excel 2008). The level of significance was set at $P < 0.05$ and data were presented as mean ± SD. For correlation analysis of hoof changes vs. time, the Pearson correlation coefficient (r) was calculated.

Chapter 3

Distribution of purinergic P2X receptors in the equine digit, cervical spinal cord and dorsal root ganglia

(published work under the title «Distribution of purinergic P2X receptors in the equine digit, cervical spinal cord and dorsal root ganglia» Zamboulis et al. (2013) *Purinergic Signalling* PMID: 23381684) (see Appendix for full text)

3.1 Introduction

The recognition of ATP as an extracellular signalling molecule was noted in the 1920s (Drury & Szent-Györgyi 1929), but it was the late 1970s when ATP was reported to induce pain sensation (Burnstock 2006). Since this time, ATP activation of purinergic signalling pathways has been described in neurons and related cells in both the peripheral and central nervous systems (North 2004, Abbracchio et al. 2009). In addition to functions in the nervous tissues, the role of P2X receptor activation by ATP in non-excitable cells (such as leukocytes and epithelial cells) is being increasingly recognised (Burnstock & Verkhratsky 2010). Endogenous ATP release by endothelial and epithelial cells in response to alterations in the local tissue environment (for example, hypoxia/acidosis) can result in responses such as cell proliferation, differentiation and survival (Ray et al. 2002, Schwiebert et al. 2002). Differences in P2X receptor subtype expression within and between tissue types may therefore allow for tissue- and zonal-specific response to extracellular ATP release and help to elucidate the potential role of P2X receptors in a number of physiological and pathological processes.

Purinergic signalling in the horse has received little attention. Ko et al. (1994) first investigated purinergic signalling in horses in cultured sweat gland epithelial cells with the existence of P2Y receptors in equine sweat gland later confirmed (Wilson et al. 1998, Bovell et al. 2013). Also, Zerpa et al. (2013) report the presence of P2X1-3 and 7 receptor subtypes in equine digital vessels and their implication in regulation of vascular tone. Evidence for the presence of purinergic signalling in the horse therefore exists. P2X receptor subtype distribution in equine tissues, however, has not been extensively studied and is of interest for its participation in the

regulation of physiological processes in the horse.

The aim of this chapter was to identify and characterise the distribution of P2X receptor subtypes in tissues in the equine digit and associated nervous tissue, including the peripheral nerves, dorsal root ganglia and cervical spinal cord with a view to understanding their role in these tissues. For this purpose, primers for equine P2X1-7 receptor transcripts were designed and the existence of P2X1-7 mRNA expression in these tissues was investigated. Subsequently, Western blot experiments were run to validate the specificity of the selected P2X receptor antibodies in equine tissue and investigate P2X receptor subtype protein expression. Finally, immunohistochemistry experiments were carried out to determine the cellular distribution of P2X1-3, 7 receptor subtypes in sampled tissues.

3.2 Study design

- **Sample collection** – Tissue samples were collected from euthanased horses (n = 5) with no previous history or evidence of forelimb or neurological diesease. Sampled tissues included the palmar digital artery, vein, and nerve, hoof, ipsilateral C8 DRG and spinal cord (innervating the hoof) and ipsilateral C4 DRG and spinal cord (not innervating the hoof) (see 2.1 Samples p.35).

- **Identification of P2X1-7 receptor subtype mRNA signal in equine tissue** – mRNA was extracted from sampled tissues and reverse transcription was carried out to synthesize cDNA. Primers for equine P2X1-7 mRNA were

designed (based on predicted sequences from NCBI and Ensembl databases) and used in PCR reactions for amplification of P2X1-7 cDNA. PCR products identity was confirmed by size comparison with the predicted equine sequences and by subsequent DNA sequencing (see 2.2 Molecular biology experiments p.39).

- **Validation of P2X1-7 antibodies in equine tissue** – Proteins were extracted from sampled tissues and used in western blot analyses carried out to validate P2X1-7 antibodies in equine tissue. Western blot bands' identity was confirmed by size comparison with (the MW of) predicted amino acids sequences, preincubation of the antibodies with their respective immunogen peptides, and mass spectrometry analysis (see 2.3 Western blot analysis p.48).

- **Characterisation of P2X1-3, 7 receptor subtype proteins distribution in equine tissue** – P2X1-3. 7 antibodies validated in equine tissue were used for immunohistochemical characterisation of their respective proteins' distribution in equine sampled tissues. P2X1-3, 7 antibodies staining specificity was confirmed with immunohistochemistry control experiments with omission of the primary antibody and with substitution of the primary antibody with non-immune rabbit IgG (see 2.4.3 Immunohistochemistry p.56).

3.3 Results

3.3.1 Molecular biology experiments

All designed primers produced PCR products of the expected size and P2X1-7 transcripts were expressed in all sampled equine tissues (Figure 3.1).

The identification of P2X1-7 amplified products as P2X1-7 amplicons was based on their size and subsequent DNA sequencing and genome-wide similarity searches (Blast, NCBI). Comparison of the produced nucleotide sequences with the predicted ones gave a perfect match for all but the P2X5 transcript which was found to combine parts of sequences matching the NCBI predicted P2X5 transcript (XM_001918102.1), the Ensembl predicted P2X5 transcripts (ENSECAT00000026624, ENSECAT00000026645) or neither NCBI/Ensembl predicted P2X5 transcripts (Table 3.1 and 3.2). The mismatches in P2X5 nucleotide sequence did not result in interruption or overall alteration of the transcript's reading frame but the resulting amino acid sequence was altered for the codons containing the mismatches (Table 3.3). P2X1-7 amplicons from all tissues were sequenced and tissue-related differences in the nucleotide sequences were not detected.

P2X1, 3-6 receptor subtype partial coding sequences (cds) were deposited in NCBI database (accession KC790392 to KC790396, respectively).

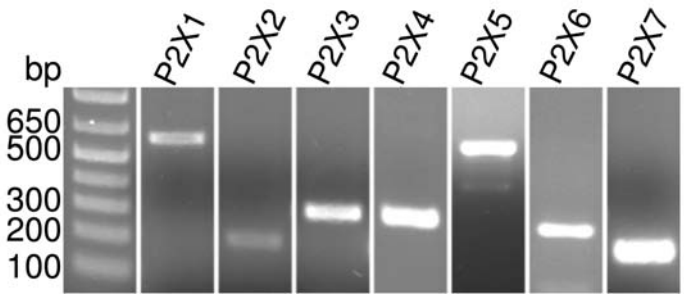

Figure 3.1. Representative bands from agarose gel electrophoresis of eqP2X1-7 PCR products from sampled equine tissues cDNA (P2X1- P2X4 and P2X7 C8 DRG, P2X5 and P2X6 C4 DRG) showing products of the expected size. bp = base pairs

Table 3.1. Nucleotide sequences of sequenced equine P2X1-4, 6 & 7 PCR products. Highlighted in grey are the nucleotide sequences for the forward and reverse primers.

P2X amplicon	Nucleotide sequence
P2X1 amplicon	TGAGTACGAC ACGCCTCGAA TGGTGCTGGT TCGCAACAAG AAGGTGGGCG TCGTCTTCCG CCTGATCCAG CTCGTGGTTC TGGTCTACGT CATTGGGTGG
	GTGTTTGTCT ACGAGAAGGG TTACCAGACC TCCAGCAGCC TCATCAGCAG CGTGTCTGTG AAACTCAAGG GCCTGGCAGT GACGCAGCTC CCAGGCCTGG
	GCCCCCAGGT CTGGGACGTG GCTGACTACG TCTTCCCAGC TCAGGGCGAC AACTCCTTTG TGGTCATGAC CAATTTCATC GCGACCCCAA AGCAGGCTCA
	AGGCTACTGT GCAGAGCACC CGGAAGGCGG CACGTGCGCG GATGATAGCG GCTGCATCCC TGGGAAGGCA GAGAGGAAGG CCCAAGGCAT CCGCACGGGC
	AAGTGTGTGG CCTTCAATGA CACCGTGCAA ACGTGTGAGA TCTTTGGCTG GTGCCCCGTG GAGGTGGACG ATGACATCCC ACGCCCTGCC CTTCTCCGAG
	AGGCCGAGAA CTTCACTCTC TTCATCAAGA ACAGCATCAG CTTTCCACGC TTCAAGGTCA AAAGGCGCA
P2X2 amplicon	AATTCCAGTT CTCTAAGGGC AACATTGAGA ACCGGAAGGA TGGCTACCTG AAACGCTGCA CATTCCATGA GGTCTCGGAT CTCTACTGCC CCATTTTCAA
	GCTGGGCTTC ATAGTGGAGC AGGCAGGGGA AAACTTCACG GAGCTGGCAC ACACGGGTGG CGTCATTGGG GTCATTATCA ACTGGG
P2X3 amplicon	CAGTGGAAAT GCCTGTCATG ATGGAAGCTG AGAATTTCAC TATTTTCATC AAGAACAGCA TCCGTTTCCC TCTCTTCAAC TTTGAAAAGG GTAACCTGCT
	TCCCAACCTG ACGGCCGCCG ACATAAAGAC ATGCCGCTTC CACCCTGACA AGTCCCCTTT CTGCCCCATC TTGCGGGTGG GGGATGTGGT CAAGTTTGCG
	GGGCAGGATT TTGCCAAACT GGCCAGCACG GGTGGAGTTC TGGGCATTAA GATTGGCTGG GTGTGCGACT TGGACAAGGC C
P2X4 amplicon	CGGCTACAAC TTCAGGTTTG CCAAGTACTA CAATGACCTG ACAGGCACAG AGCACCGCAC ACTCATCAAG GCCTACGGCA TCCGCTTCGA CATCATCGTG
	TTTGGAAAGG CTGGGAAGTT TGACATCATC CCTACCATGA TCAACATTGG CTCTGGCTTG GCGCTCTTAG GGGTGGCAAC AGTGCTGTGT GACGTCATAG
	TCCTCTACTG CATGAAGAAA AAATACTACT ATCGGGAGAA GAAATATAAA TATGTGGCAG ATTACGATCA GG
P2X6 amplicon	CAACTTCAGG ACAGCCACTC ACTGGAGGGA GGCCTCAGGC TTGGAGGCCC GGAGTCTGCT CAAACTCTAC GGGATCCGCT TCGACATCCT CGTCACTGGG
	CGGGCAGGGA AGTTCGGGCT CATCCCCACA ACCATCACTC TGGGCACTGG AGCGGCCTGG CTGGGTGTGA TCACCTTCTG CTGTGACCTG CTGCTGTTGT
	ACGTGGATGG AGAAGC
P2X7 amplicon	TTCCTACGTT ATCTTTGCCT TGGTGAGTGA CAAGCGGTAC CAGCGGAAAG AGCCTCTAAT CAGCTCTGTG CACACCAAGG TGAAAGGAAT AGCAGAGGTG
	AGAGAGGAGA TTATAGAGAG CGGAGCGAAG AAGGTGGTGC AGAGCGTCTT CGACACCGCA GACTACACC

Table 3.2. Nucleotide sequence alignement of P2X5 PCR amplicon to NCBI and Ensembl predicted equine P2X5 transcripts (XM_001918102.1, ENSECAT00000026624, ENSECAT00000026645, respectively). In areas of mismatches, matching sequences are noted in green and mismatching in red.

eqP2X5 transcript	Nucleotide sequence
Ensembl26624	ACCCCAGGGAGAGAACGTCTTCTTCATTGTCACCAACCTGATTGTGACCCCTAACCAGCGGCAGGGAACCTGTGCTGAGAGTGAAAACATCCCTGACGGCCTGTGCTATAAG
Ensembl26645	ACCCCAGGGAGAGAACGTCTTCTTCATTGTCACCAACCTGATTGTGACCCCTAACCAGCGGCAGGGAACCTGTGCTGAGAGTGAAAACATCCCTGACGGCCTGTGCTATAAG
NCBI	ACCCCAGGGAGAGAACGTCTTCTTCATTGTCACCAACCTGATTGTGACCCCTAACCAGCGGCAGGGAACCTGTGCTGAGAGTGAAAACATCCCTGACGGCCTGTGCTATAAG
P2X5 amplicon	----------TAACCAGCGGCAGGGAACCTGTGCTGAGAGTGAAAACATCCCTGACGGCCTGTGCTATAAG
	**********
Ensembl26624	GACAGCGACTGCCCTCCTGGGGAGCCTGTTGTGGCTGGAAATGGAGTGAAGACTGGCCGCTGCCTGCGGGCTGGGAAAATGCAAAGGG-CACCTGTGAGATCTTCG-----T
Ensembl26645	GACAGCGACTGCCCTCCTGGGGAGCCTGTTGTGGCTGGAAATG---TGAAGACTGGCCGCTGCCTGCGGGCTGGGAAAATGCAAAGGG-CACCTGTGAGATCTTCG-----T
NCBI	GACAGCGACTGCCCTCCTGGGGAGCCTGTTGTGGCTGGAAATGGAGTGAAGACTGGCCGCTGCCTGCGGGCTG--AAAATGCAAAGGG-CACCTGTGAGATCTTCGCCTGAT
P2X5 amplicon	GACAGCGACTGCCCTCCTGGGGAGCCTGTTGTGGCTGGAAATGGAGTGAAGACTGGCCGCTGCCTGCGGGCTGGGAAAATGCAAAGGGGCACCTGTGAGATCTTCGCCTGGT
	********** ********** ********** ********** *
Ensembl26624	GCCCAGTGGAGACAAAGTCCAGGCCATCGAAGCCACTCCTGGGCAAGGCTGAAGACTTCACTGTTTACATAAAGAACTTCATTCGCTTCCCCAAATTCAACTTCTCCAAGAC
Ensembl26645	GCCCAGTGGAGACAAAGTCCAGGCCATCGAAGCCACTCCTGGGCAAGGCTGAAGACTTCACTGTTTACATAAAGAACTTCATTCGCTTCCCCAAATTCAACTTCTCCAAGAC
NCBI	GCCCAGTGGAGACAAAGTCCAGGCCATCGAAGCCACTCCTGGGCAAGGCTGAAGACTTCACTGTTTACATAAAGAACTTCATTCGCTTCCCCAAATTCAACTTCTCCAAGAC
P2X5 amplicon	GCCCAGTGGAGACAAAGTCCAGGCCATCGAAGCCACTCCTGGGCAAGGCTGAAGACTTCACTGTTTACATAAAGAACTTCATTCGCTTCCCCAAATTCAACTTCTCCAAGAC
	**********
Ensembl26624	CAATGTGCTGGACACCGAAGACAGATCTTACCTGAAGTTCTGTCAATTTGACCCCAAGAACCTCTACTGCCCCATCTTCCGAGTGGGGTCCTTGGTCAGCTGGGCGGGGAGC
Ensembl26645	CAATGTGCTGGACACCGAAGACAGATCTTACCTGAAGTTCTGTCAATTTGACCCCAAGAACCTCTACTGCCCCATCTTCCGAGTGGGGTCCTTGGTCAGCTGGGCGGGGAGC
NCBI	CAATGTGCTGGACACCGAAGACAGATCTTACCTGAAGTTCTGTCAATTTGACCCCAAGAACCTCTACTGCCCCATCTTCCGAGTGGGGTCCTTGGTCAGCTGGGCGGGGAGC
P2X5 amplicon	CAATGTGCTGGACACCGAAGACAGATCTTACCTGAAGTTCTGTCAATTTGACCCCAAGAACCTCTACTGCCCCATCTTCCGAGTGGGGTCCTTGGTCAGCTGGGCGGGGAGC
	**********
Ensembl26624	AACTTCCAGGACATAGCCCTGCAGGGTGGTGTGATAGGAATTCAGATTGAATGGGACTGTGATCTTGATAAAGCTCCCTCCGAATGCA
Ensembl26645	AACTTCCAGGACATAGCCCTGCAGGGTGGTGTGATAGGAATTCAGATTGAATGGGACTGTGATCTTGATAAAGCTCCCTCCGAATGCA
NCBI	AACTTCCAGGACATAGCCCTGCAGGGTGGTGTGATAGGAATTCAGATTGAATGGGACTGTGATCTTGATAAAGCTCCCTCCGAATGCA
P2X5 amplicon	AACTTCCAGGACATAGCCCTGCAGGGTGGTGTGATAGGAATTCAGATTGAATGGGACTGTGATCTTGATAAAGCTCCCTCCGAATGCA
	**********

Table 3.3. Alignment of equine P2X5 translated amplicon amino acid sequence against the NCBI and Ensembl predicted P2X5 amino acid sequences (XP_001918137, ENSECAP00000022228 (transcript ENSECAT00000026624), ENSECAP00000022248 (transcript ENSECAT00000026645), respectively) for the transcript region containing the mismatches. In areas of mismatches, matching sequences are highlighted in green and mismatching in red.

Equine P2X5 protein		Location	Amino acid sequence
translated amplicon sequence			CPPGEPVVAGNGVKTGRCLRAGKMQRGTCEIFAWCPVET
NCBI	XP_001918137	112-149	CPPGEPVVAGNGVKTGRCLRA-ENAKGTCEIFA-CPVET
Ensembl	ENSECAP00000022228	89-126	CPPGEPVVAGNGVKTGRCLRAGKMQR--APVRSSCPVET
Ensembl	ENSECAP00000022248	89-125	CPPGEPVVAGN-VKTGRCLRAGKMQR--APVRSSCPVET
			********** ********* *****

3.3.2 P2X1-7 protein Western blot analysis

Western blot analysis revealed protein bands around the expected size for P2X1-3, 7 proteins (55, 42, 50, and 79 kDa, respectively) in all sampled tissues (Figure 3.2a, Table 3.4). P2X1 and P2X7 protein Western blots also showed secondary protein bands at higher molecular weights (110 kDa and ~170 kDa, and 110 kDa and 140 kDa, respectively) (Figure 3.2a). Expression of higher molecular weight bands is recognised in P2X receptor expression analysis where dimer and trimer formation occurs (Jiang et al. 2005). Control experiments with pre-incubation of P2X1 and P2X7 receptor antibodies with their immunogen peptide resulted in a reduction in the intensity of the protein bands confirming P2X1 and P2X7 receptor antibody specificity to the peptide (Figure 3.2b).

Antibody specificity for P2X4, P2X5, and P2X6 receptor antibodies could not be confirmed as their Western Blots showed multiple bands at molecular weights other than the expected for each protein. The Western blots with P2X4 receptor antibodies (Abcam, Alomone) revealed a multitude of bands at different molecular

weights other than the expected band (43 and 50 kDa, respectively). P2X5 receptor Western blot showed a band around the expected size (50 kDa) along with a strong band at a smaller molecular weight which was not attenuated after preincubation of P2X5 receptor antibody with its immunogen peptide. The Western blot with P2X6 receptor antibody revealed a band around the expected size (48 kDa) in nervous tissue but bands at higher molecular weights that did not follow the same pattern were also present.

Mass spectrometry was used as an additional tool to confirm the identity of the P2X protein bands. However, the results of the mass spectrometry analysis of the excised bands did not show the presence of P2X receptor proteins but other proteins present in the sampled tissues (Table 3.5). So, with mass spectrometry not being able to confirm the presence of P2X receptor subtype proteins, the identification of P2X protein bands in Western Blots was based on their size and control experiments.

Table 3.4. Predicted MW for equine P2X1-3, 7 receptor subtype proteins, antibody manufacturer documented MW for P2X1-3, 7 proteins, and observed MW for equine P2X1-3, 7 receptor subtype proteins in analysed samples (along with the accession number of equine predicted P2X1-3, 7 receptor proteins).

P2X receptor subtype	Predicted MW (kDa)	Antibody datasheet MW (kDa)	WB protein band MW (kDa)	Accesion number (NCBI, Ensembl)
P2X1	45	50 and 52 (human)	55	XP_001504780
P2X2	39	40 (human)	42	ENSECAP00000014190
P2X3	44	50 (and 75) (rat)	50	XP_001504964
P2X7	69	70 (and 120) (human)	79	XP_001495622

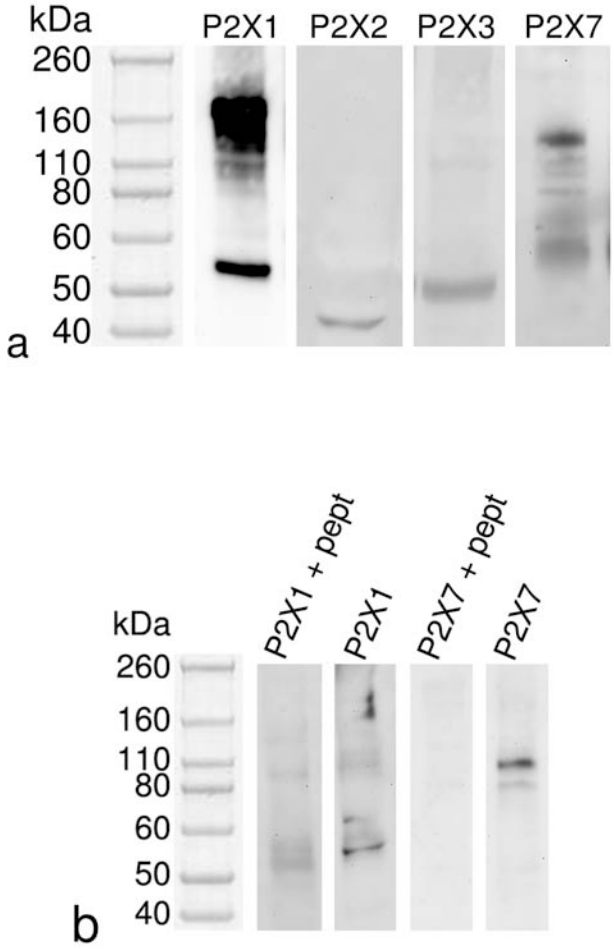

Figure 3.2. (a) Western blot analysis for P2X1-3, 7 proteins showing validation of P2X1-3, 7 antibodies against equine homologues. Shown are representative bands of Western blots for P2X1-3, 7 proteins in equine tissue samples lysates (P2X1 palmar digital artery lysate, P2X2 and P2X3 C8 DRG lysate, P2X7 hoof lysate). The bands observed at 55, 42, 50 and 79 kDa represent P2X1-3, 7 proteins, respectively, whereas the bands observed at higher molecular weights correspond to the protein's glycosylated form or multimer. (b) Western blot analysis for P2X1 and P2X7 antibodies (palmar digital vein lysate) with and without preincubation with the immunogen peptide. Note the significant reduction in band intensities for P2X1 (55kDa) and P2X7 (79 kDa) receptor subtype proteins following pre-incubation with the immunogen peptide.

Table 3.5. Mass spectrometry results, top hits.

	Top hits	Function	Sample
Band 1	actin, aortic smooth muscle isoform 1	major constituent of contractile apparatus	p. d. artery
	filamin-A like	crosslinks actin filaments in orthogonal networks in cortical cytoplasm and links actin filaments to membrane glycoproteins	
	thymidine phosphorylase-like	catalyzes the reversible phosphorolysis of thymidine, promotes angiogenesis	
Band 2	glial fibrillary acidic protein	intermediate filament protein (type III)	hoof
	septin-7	filament-forming cytoskeletal GTPase, involved in cytokinesis	
	calreticulin-like	associated with the endoplasmic reticulm	
Band 3	serum albumin	blood plasma protein	spinal cord
	fructose-biphosphate aldolase	key role in glycolysis and gluconeogenesis	
	vimentin	intermediate filamen protein (type III), major cytoskeletal component of mesenchymal cells	

3.3.3 P2X1-3, 7 receptor subtype immunohistochemical analysis

Palmar digital artery and vein

Figure 3.3 shows the distribution of P2X1-3, 7 receptor subtype proteins in palmar digital artery and vein. P2X1, 2, 7 receptor subtype proteins were demonstrated in the smooth muscle cells in the *tunica media* of the palmar digital artery and vein whereas P2X3 receptor subtype positive staining was identified in smooth muscle cells of the vein but not the artery. P2X7 receptor subtype staining in smooth muscle cells exhibited characteristic patterning, being localised in a thin line adjacent to the nucleus. Palmar digital artery and vein endothelial cells were immunopositive for P2X2 receptor subtype whereas only palmar digital vein endothelial cells were immunopositive for P2X3 receptor subtype.

Hoof

In the equine hoof, P2X1-3 receptor subtype staining predominately occurred in epidermal basal cells. Additionally, P2X1 and P2X2 receptor subtype staining was seen in the dermis capillaries and small vessels. P2X7 receptor subtype staining was present in the epidermal basal cells and in corium fibroblasts (Figure 3.4).

Palmar digital nerve

In the palmar digital nerve, P2X1 and P2X2 receptor subtype staining was mostly present in nerve fibres and to a lesser extent in Schwann cells (Figure 3.5). P2X3 receptor subtype staining was present only in nerve fibres and P2X7 receptor subtype staining was seen exclusively in Schwann cells.

Dorsal root ganglia and spinal cord

In C4 and C8 DRG, P2X1 receptor subtype staining was seen mainly in neurons and faintly in satellite glial cells. P2X2 receptor subtype staining, in comparison, was present in both DRG neurons and satellite glial cells. P2X3 receptor subtype staining was present in DRG neurons only whereas P2X7 receptor subtype staining was strong in DRG Schwann cells (Figure 3.6).

In C4 and C8 spinal cord segments, P2X1-3, 7 receptor subtype staining was present in dorsal horn neurons and ependymal cells with P2X3 receptor subtype staining strongest in neuronal cell body and projections. P2X1, 2, 7 receptor subtype staining was also present in dorsal horn glial cells (Figure 3.7).

No staining was observed in control experiments with omission of the primary antibody and substitution of the primary antibody with non-immune rabbit polyclonal IgG (Figure 3.8 and 3.9).

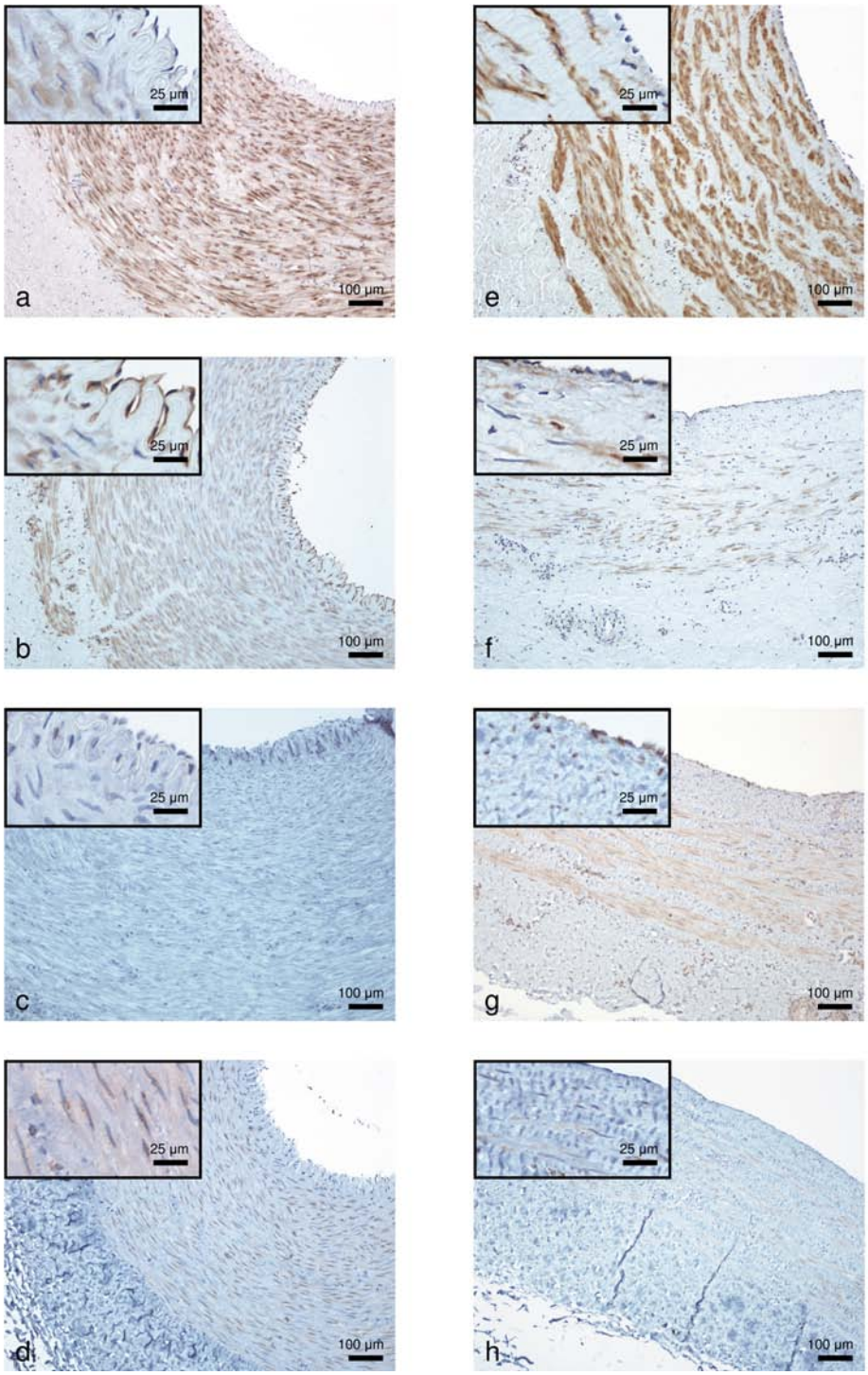

Figure 3.3. Immunostaining for P2X1 (a, e), P2X2 (b, f), P2X3 (c, g) and P2X7 (d, h) receptor subtypes in equine palmar digital artery (a-d) and vein (e-h). (a, e) P2X1 receptor subtype was present in the smooth muscle cells in the *tunica media* of the palmar digital artery (a) and vein (e). Insert shows representative image of positive smooth muscle cells. (b, f) P2X2 receptor subtype was present in the smooth muscle cells in the *tunica media* and the endothelial cells of the palmar digital artery (b) and vein (f). Insert shows representative image of positive endothelial and smooth muscle cells. (c, g) P2X3 receptor subtype was not found in the palmar digital artery (c) but was present in the smooth muscle cells in the *tunica media* and the endothelial cells of the palmar digital vein (g). Insert shows representative image of endothelial and smooth muscle cells. (d, h) P2X7 receptor subtype was present in the smooth muscle cells in the *tunica media* of the palmar digital artery (d) and vein (h). Insert shows representative image of P2X7 receptor subtype staining in smooth muscle cells.

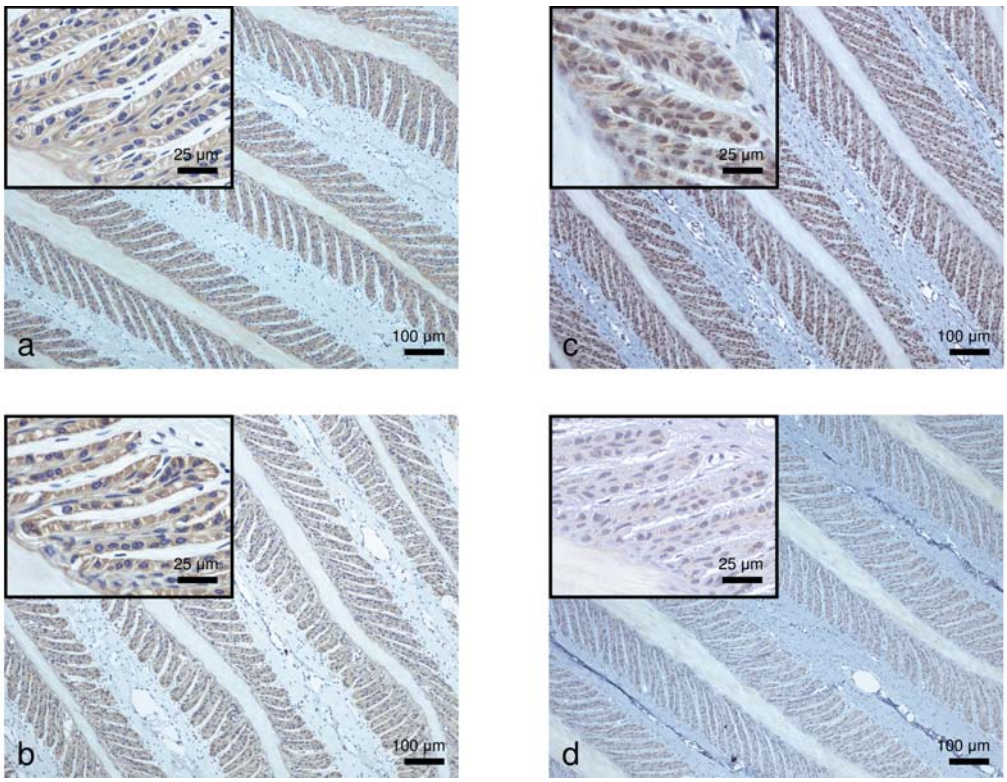

Figure 3.4. Immunostaining for P2X1 (a), P2X2 (b), P2X3 (c) and P2X7 (d) receptor subtypes in equine hoof. P2X1-3, 7 receptor subtypes staining predominately occurred in epidermal basal cells. Inserts show representative images of positive epidermal basal cells.

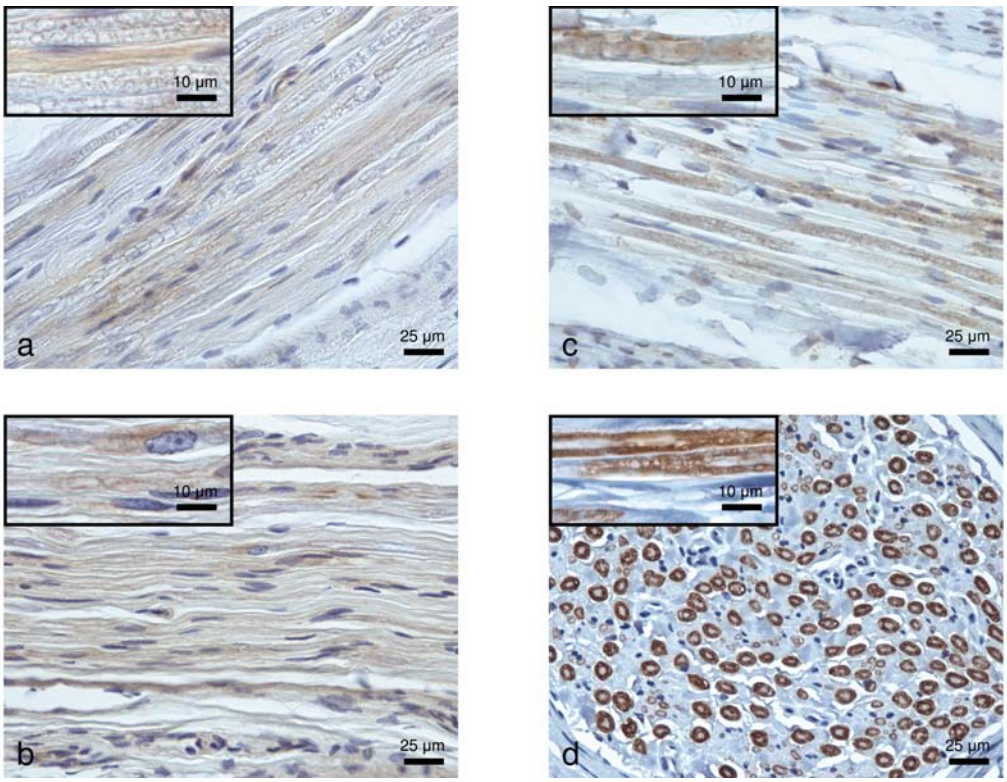

Figure 3.5. Immunostaining for P2X1 (a), P2X2 (b), P2X3 (c) and P2X7 (d) receptor subtypes in equine palmar digital nerve. (a, b) P2X1 (a) and P2X2 (b) receptor subtype staining was strong in nerve fibres but faint in Schwann cells. Inserts show representative images of positive Schwann cells and nerve fibre. (c) P2X3 receptor subtype staining was present only in nerve fibres. Insert shows representative image of a positive nerve fibre. (d) P2X7 receptor subtype staining was seen exclusively in Schwann cells. Insert shows representative image of longitudinal section of positive Schwann cells myelin sheath.

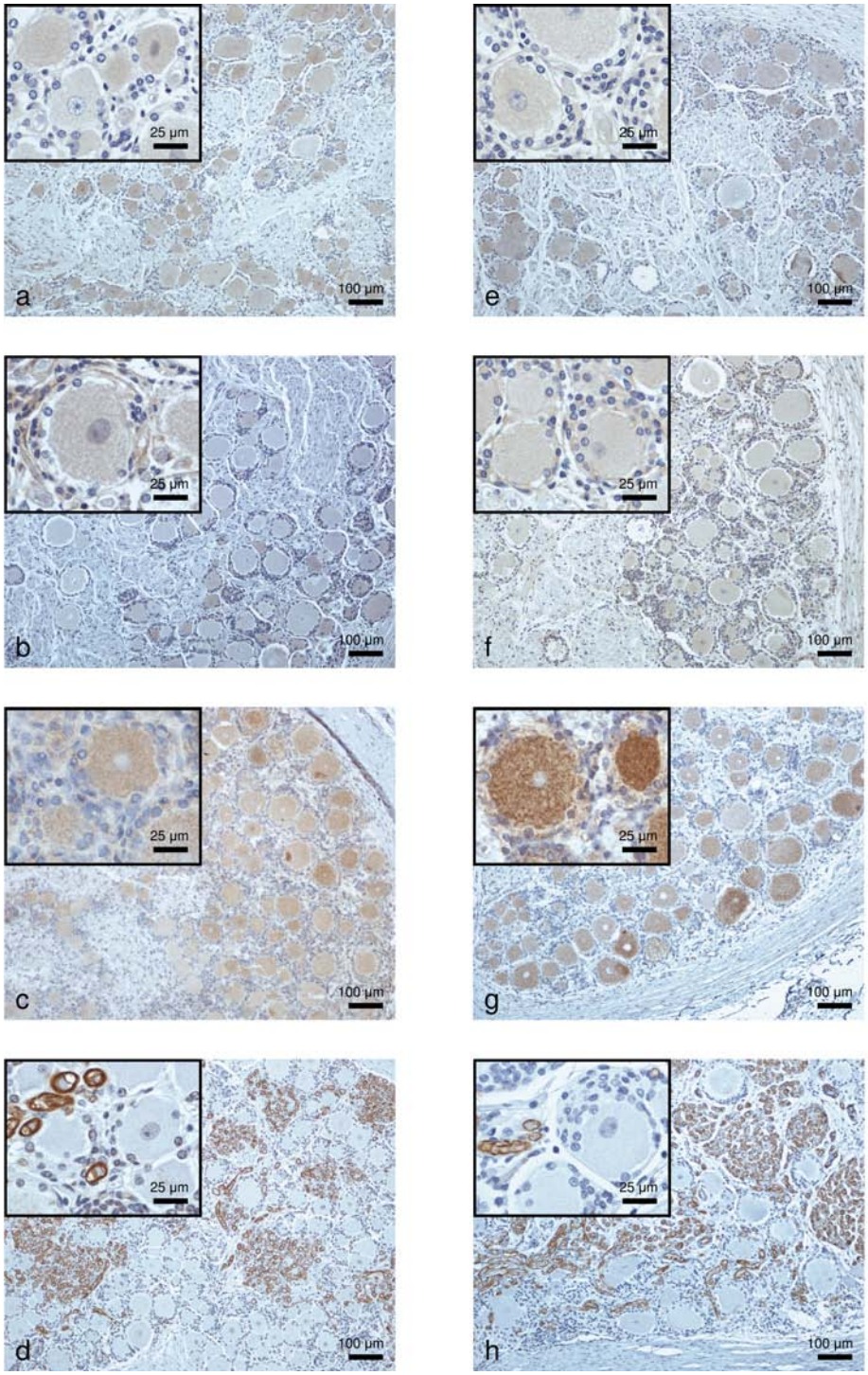

Figure 3.6. Immunostaining for P2X1 (a, e), P2X2 (b, f), P2X3 (c, g) and P2X7 (d, h) receptor subtypes in equine C4 (a-d) and C8 (e-h) DRG. (a, e) P2X1 receptor subtype staining was strong in DRG neuronal cells but faint in satellite glial cells in C4 (a) and C8 (e) DRG. Insert shows representative image of positive neurons and satellite glial cells. (b, f) P2X2 receptor subtype staining was present in both DRG neurons and satellite glial cells in C4 (b) and C8 (f) DRG. Insert shows representative image of positive neurons and satellite glial cells. (c, g) P2X3 receptor subtype staining was present only in DRG neurons in C4 (c) and C8 (g) DRG. Insert shows representative image of positive neurons. (d, h) P2X7 receptor subtype staining was strong in Schwann cells in C4 (d) and C8 (h) DRG. Insert shows representative image of positive Schwann cells myelin sheaths.

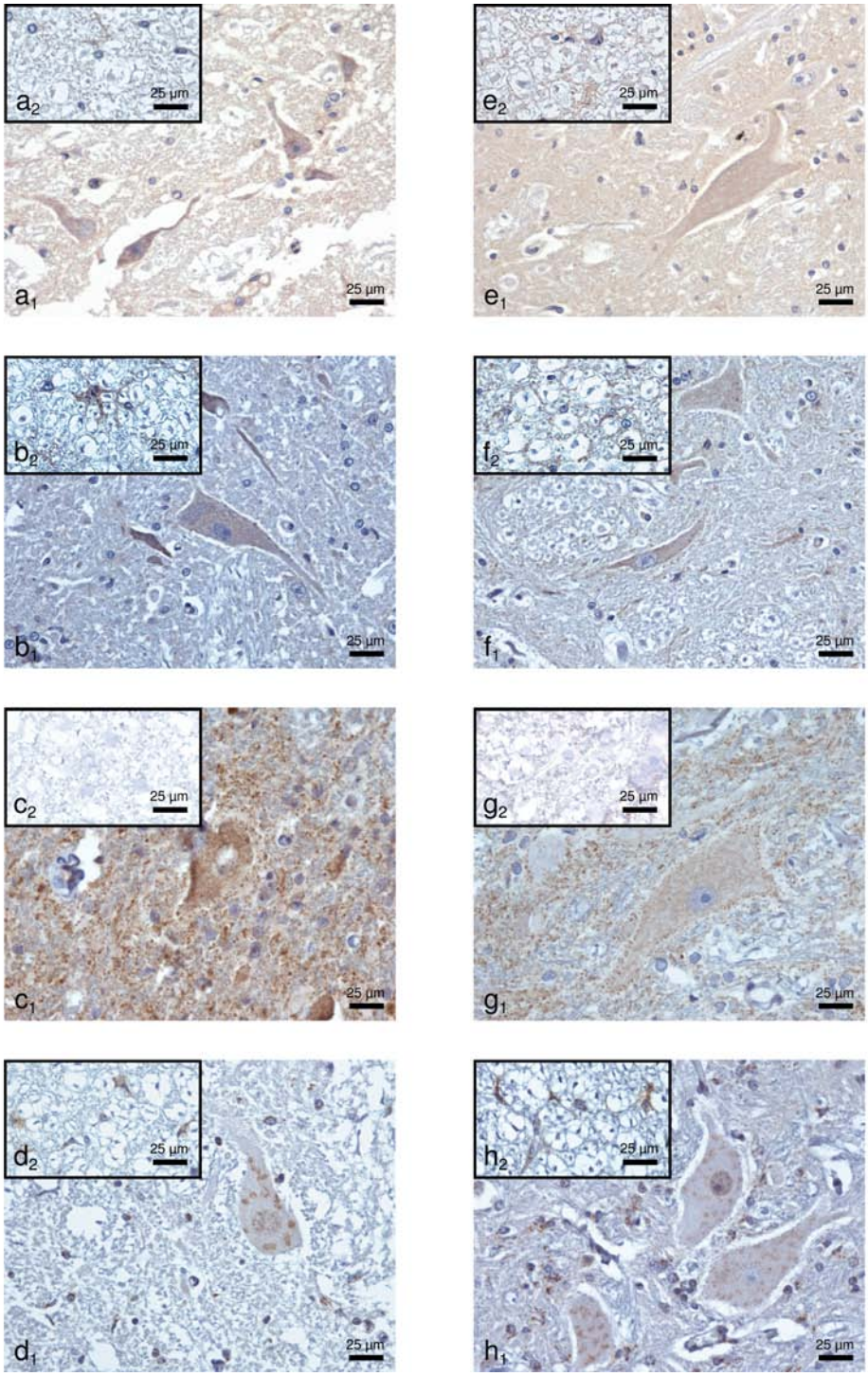

Figure 3.7. Immunostaining for P2X1 (a, e), P2X2 (b, f), P2X3 (c, g) and P2X7 (d, h) receptor subtypes in equine C4 (a-d) and C8 (e-h) spinal cord segments. (a, e) P2X1 receptor subtype was present in dorsal horn neurons (a_1 and e_1) and glial cells (inserts a_2 and e_2) in C4 and C8 spinal cord segments. (b, f) P2X2 receptor subtype was present in dorsal horn neurons (b_1 and f_1) and glial cells (inserts b_2 and f_2) in C4 and C8 spinal cord segments. (c, g) P2X3 receptor subtype staining was strong in dorsal horn neurons cell body and projections (c_1 and g_1) but absent in glial cells (inserts c_2 and g_2) in C4 and C8 spinal cord segments. (d, h) P2X7 receptor subtype was present in dorsal horn neurons (d_1 and h_1) and glial cells (inserts d_2 and h_2) in C4 and C8 spinal cord segments.

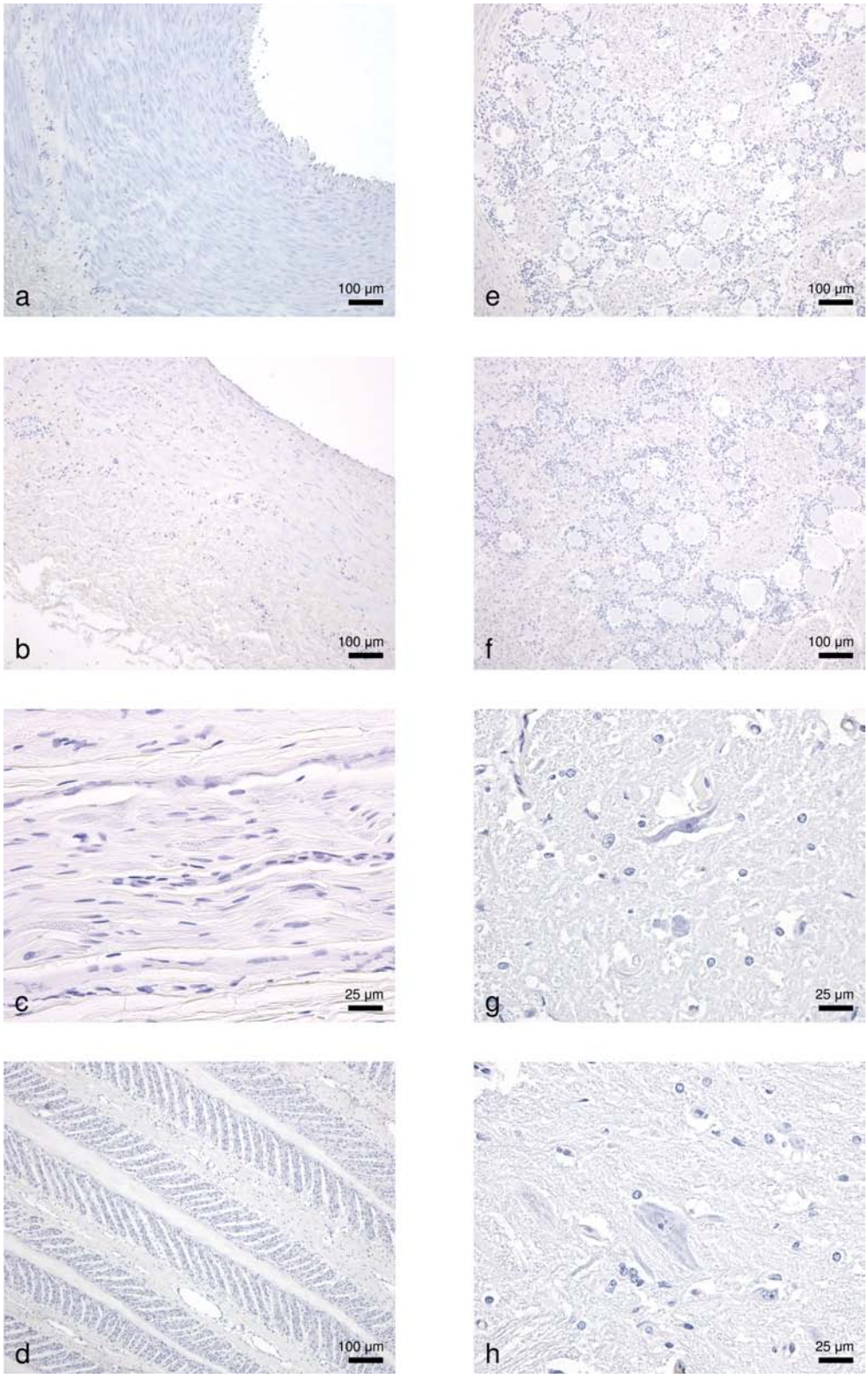

Figure 3.8. Immunohistochemistry control with the omission of primary antibody for palmar digital artery (a), palmar digital vein (b), palmar digital nerve (c), hoof (d), C4 dorsal root ganglion (e), C8 dorsal root ganglion (f), C4 spinal cord segment (g) and C8 spinal cord segment (h). No immunostaining was observed in each of the tissue types.

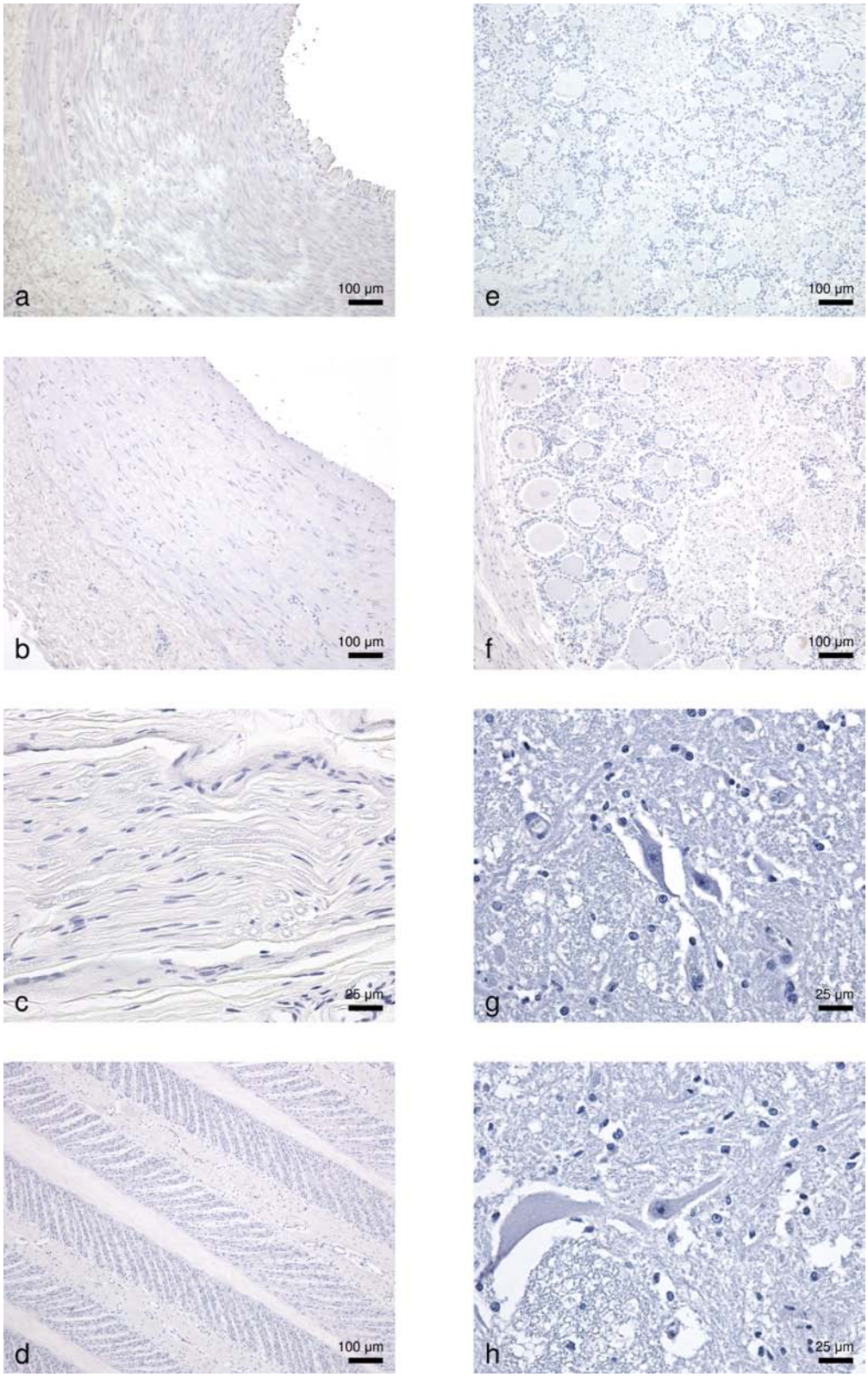

Figure 3.9. Immunohistochemistry control with substitution of primary antibody with non-immune rabbit IgG for palmar digital artery (a), palmar digital vein (b), palmar digital nerve (c), hoof (d), C4 dorsal root ganglion (e), C8 dorsal root ganglion (f), C4 spinal cord segment (g) and C8 spinal cord segment (h). No immunostaining was observed in each of the tissue types.

3.4 Discussion

Purinergic P2X receptors have been identified in both excitable and non-excitable cells and have important roles in neuronal transmission and regulation as well as cell growth, differentiation and survival (Neary & Burnstock 1996, Abbrachio et al. 2009, Burnstock & Verkhratsky 2010). In this chapter, the presence of P2X1-7 receptor subtypes was identified in equine tissue, specifically the hoof and its vasculature and innervation. Also, the location and distribution of four key receptor subtypes (P2X1-3, 7) was demonstrated in these tissues, showing important differences in cellular location and suggesting that heterogeneity in receptor expression may be important in normal cellular and tissue function.

PCR experiments identified gene expression (mRNA) for all seven P2X receptor subtypes in equine tissues. mRNA signal of P2X1-7 receptor subtypes was found in all sampled tissues supporting previous findings of widespread P2X gene expression throughout mammalian tissues (review Burnstock & Knight 2004).

The PCR amplicons were sequenced and the nucleotide sequences matched the predicted ones for P2X1-4, 6-7 receptor mRNA (NCBI and Ensembl). The P2X5 amplicon was found to combine parts of sequences matching the NCBI predicted transcript, the Ensembl predicted transcripts or neither NCBI/Ensembl predicted transcripts. The mismatches between P2X5 amplicon nucleotide sequence and NCBI and Ensembl predicted nucleotide sequences did not result in interruption or alteration of the transcript's reading frame. However, translation of the codons containing the mismatches and alignment against the predicted amino acid sequences revealed differences in the amino acid sequences, either due to predicted sequences

inaccuracy or the existence of equine P2X5 protein splice variants. Future work including the amplification and sequencing of the full equine P2X5 transcript length from several animals and different tissues may help elucidate the existence of equine P2X5 protein splice variants.

DNA sequencing did not reveal any tissue-related differences in P2X1-7 amplicons' nucleotide sequences in the samples. Expression of splice variants in tissues though has been documented for P2X receptors and they may account for the heterogeneity of P2X responses in tissues in health and disease (Carpenter et al. 1999, Lynch et al. 1999, Mankus et al. 2011). The absence of P2X splice variants in the samples in the present study (despite the wide range of tissues examined) could be attributed to the analysis of a small part of the P2X receptor transcripts as opposed to the full transcript length. This is the first report of eqP2X1-7 cDNA sequencing and P2X1, 3-6 receptor subtype partial cds have been deposited in NCBI database for future reference (accession KC790392 to KC790396, respectively).

After mRNA signal was detected in equine tissue, Western blot analysis was used to investigate protein expression in the same tissues and validate the use of P2X receptor antibodies in equine tissue. Antibodies raised against equine P2X1-7 receptor subtype proteins are not commercially available and therefore antibodies raised against other species were selected based on the homology of their immunogen peptide amino acid sequence to the respective equine predicted amino acid sequence. P2X receptor proteins show high inter-species similarity, reaching up to 99% (Volonté et al. 2006). Here, the amino acid sequences of the selected antibodies (immunogen peptides) and the predicted equine P2X receptor proteins showed high similarity (83.33-100%) for the antibodies whose specificity in equine

tissue was validated (P2X1-3, 7) and lower (42.11-78.57%) for the other antibodies (P2X4-6) (see Table 2.4).

Antibody specificity was validated for P2X1-3, 7 receptor antibodies and P2X1-3, 7 receptor subtype proteins presence was observed in all sampled tissues. P2X4-6 receptor antibodies' specificity could not be confirmed with the Western Blot experiments and they were not used in subsequent experiments. However, P2X4-6 receptor subtypes protein presence and distribution in equine tissue presents some interest with regards to laminitis and chronic laminitic pain. P2X4 receptor subtype has been suggested to participate in chronic pain states by instigating pain hypersensitivity through its activity on spinal microglia and peripheral macrophages (review Trang & Salter 2012). Similarly, P2X6 receptor subtype is widespread in the nervous system (Collo et al. 1996) and could participate in the modulation of neurotransmission contributing to the pain state present in equine laminitis. Finally, P2X5 receptor subtype participation in keratinocyte differentiation (Greig et al. 2003) could help understand the events occuring in the equine hoof in laminitis. Therefore, additional P2X4-6 receptor antibodies targeting different protein epitopes with higher inter-species similarity should be tested in the future to achieve validation of their use in equine tissue.

Some discrepancy between actual and predicted molecular weights for bands was present in P2X1-3, 7 blots (Table 3.4) and is most likely explained by glycosylation and other post-translational modifications occurring in P2X proteins (North 2002, Jiang et al. 2005), prediction errors (see P2X5 mRNA), and/or inter-species differences (antibody datasheet MW). Also, some Western blots (P2X1 and P2X7) revealed bands of higher molecular weight in addition to the main band at the expected size. P2X receptor protein expression analysis has demonstrated dimer and

trimer formation resulting in Western blot bands of higher molecular weight (Jiang et al. 2005). Where results showed bands of molecular weight higher than expected (P2X1 and P2X7), control experiments with immunogen peptide pre-incubation confirmed the bands' identity. Mass spectrometry analysis was undertaken to attempt to determine the identity of the bands seen in Western blot experiments. The results, however, showed the presence of other proteins and did not confirm the presence of P2X receptor subtype proteins in the analysed bands. Although mass spectrometry is one of the most powerful proteomic tools and has been used successfully for identification and quantification of proteins, Western blotting techniques can be more sensitive, especially for low-abundance proteins (Diamandis 2004). P2X receptor subtype proteins identity was, therefore, based on Western blot experiments.

In the immunohistochemical analysis, palmar digital artery and vein smooth muscle cells showed staining for P2X1, P2X2 and P2X7 receptor subtypes whereas P2X3 receptor subtype was present in smooth muscle cells in vein but not artery. P2X1 receptor subtype is the predominant receptor subtype in vascular smooth muscle cells but smooth muscle cells have been found to express a range of different P2X receptor subtypes, including the P2X2, P2X3 and P2X7 receptor subtypes as found in this study (Cario-Toumaniantz et al. 1998, Nori et al. 1998, Hansen et al. 1999, Lewis & Evans 2001). In addition to the wide range of P2X receptor subtypes expressed in smooth muscle cells, the relative expression of these subtypes varies both in different vascular beds and vessels of different calibre in the same vascular bed accounting, in part, for the magnitude in P2X receptor-mediated responses between different vessels (Lewis & Evans 2001). Functionally, P2X receptors on vascular smooth muscle cells have been linked to a vasoconstrictor role (Harrington

& Mitchell 2004), especially in small arteries (Gitterman & Evans 2001). However, P2X receptor subtypes are also expressed on endothelium where they mediate vasodilation (Harrington & Mitchell 2004). Here, vascular endothelial cells were positive for P2X2 receptor subtype in palmar digital artery and P2X2 and P2X3 receptor subtype in palmar digital vein. P2X2 and P2X3 receptor subtypes have also been described in vascular endothelial cells in other studies (Hansen et al. 1999, Glass et al. 2000, Loesch & Burnstock 2000, Glass & Burnstock 2001) along with other receptor subtypes (P2X4, P2X5) (Schwiebert et al. 2002) and could regulate vasoactive substance release in endothelial cells following activation by extracellular ATP after local hypoxia and haemodynamic changes, such as shear stress (Bodin et al. 1991, Bergfeld & Forrester 1992, Schwiebert et al. 2002).

Hoof epidermal basal cells were positive for P2X1, P2X2, P2X3 and P2X7 receptor subtypes. P2X receptor expression and distribution in the equine hoof has not been previously described. The equine hoof shares a common basic structure with skin but hoof epidermal cells have evolved as a highly modified epidermal layer to enable it to function in its roles within the suspensory apparatus of the distal phalanx in Equids (Bragulla & Hirschberg 2003). Previous studies in human and rat skin keratinocytes have reported the presence of P2X2, P2X3, P2X5 and P2X7 receptor subtypes. P2X receptors found in skin are suggested to have an important physiological role as initial sensors for external stimuli and P2X7 receptors, known to be involved in ATP-induced apoptosis, are likely to participate in the process of the end-stage terminal differentiation of keratinocytes (Inoue et al. 2005). The expression of P2X receptor subtypes in epidermal basal cells suggests a potential role for P2X receptors in relation to cell growth and differentiation in the equine hoof. This finding may have important implications in clinical conditions of the hooves,

such as laminitis, where destruction of the epidermal-dermal interface occurs, resulting in catastrophic mechanical failure of the hoof and extreme pain (Pollitt 1996).

P2X receptor expression and function in peripheral nerve has been extensively studied in other species (for review *see* Dunn et al. 2001) and P2X2 and P2X3 receptor subtype immunoreactivity has been documented in peripheral nerve terminals (Vulchanova et al. 1998, Bo et al. 1999). In this study, the palmar digital nerve fibres were positive for P2X1, P2X2, and P2X3 receptor subtypes. Agonist studies show that C-fibre nociceptors show the greatest response to extracellular nucleotide activation, suggesting a predominately nociceptive role for P2X receptors (Hamilton & McMahon 2000). However, the palmar digital nerve of the horse also includes efferent autonomic neurons involved in local vascular responses (Molyneux et al. 1994), suggesting pain transmission might not be the only role for purinergic receptors in nerve fibres (Bo et al. 1999). Additionally, Schwann cells in sampled palmar digital nerve showed strong staining for P2X7 receptor subtype and faint staining for P2X1 and P2X2 receptor subtypes. Expression of the P2X7 receptor has also been reported in human and mouse Schwann cells where it may be involved in local immunomodulation of axonal function by Schwann cells including regulation of cytokine release (Colomar & Amédée 2001, Chessell et al. 2005); this may be of particular relevance during peripheral nerve injury or neuropathies (Scholz & Woolf 2007).

In DRG, neurons were stained for P2X1, P2X2 and P2X3 receptor subtypes. Although, P2X3 is the predominant subtype reported in DRG neurons, variable levels of immunoreactivity for P2X1-2 and P2X4-6 receptor subtypes have also been detected, with evidence of heteromultimerisation of P2X2 and P2X3 receptor

subtypes (Vulchanova et al. 1997, Xiang et al. 1998, Barden & Bennett 2000). In rats DRG, P2X3 staining is predominantly found in a subset of small and medium diameter neurons, with a nociceptive function, while it is absent from most large neurons (Chen et al. 1995, Bradbury et al. 1998, Barden & Bennett 2000). In contrast, P2X2 receptor subtype immunoreactivity is reported in small and medium as well as in large diameter neurons (Barden & Bennett 2000). Here, P2X1, P2X2 and P2X3 receptor subtype staining was seen in all small, medium, and large neurons. Similarly to the findings in the present study, P2X3 receptor subtype immunoreactivity in rat trigeminal ganglia is also found in large neurons (Cook et al. 1997). The highly selective distribution of P2X3 and P2X2/3 receptors within the nociceptive system suggests a role for these receptors in pain pathways and studies showing alterations in P2X3 receptor expression in pain models have highlighted the importance of these receptors in different pain states (North 2004, Wirkner et al. 2007). Whereas P2X3 receptor subtype immunoreactivity in DRG was seen only in neurons, P2X2, and to a lesser degree P2X1, receptor subtype staining was also present in satellite glial cells. P2X2 receptor subtype immunoreactivity is also documented in rat DRG satellite glial cells (Vulchanova et al. 1997). Indeed, all types of glia are known to express purinergic receptors and a role for ATP in neuron-glial communication (beyond homeostasis of the extracellular environment surrounding neurons, including regulating synaptic strength, gene expression, mitotic rate and differentiation of glia) has been established with a particular interest in a role in the development of neuropathic pain (see Fields & Stevens 2000, Scholz & Woolf 2007). Finally, P2X7 receptor subtype immunoreactivity in the equine DRG was localised to the DRG Schwann cells, similarly to the distribution observed in the equine palmar digital nerve and to findings in rat DRG (Zhang et al. 2005). P2X7

receptor in glia has been shown to participate in inflammatory and neuropathic hypersensitivity with a critical role in glia-neuronal signalling and may have profound effects on neuronal function under injured or diseased states (Chessell et al. 2005, Zhang et al. 2005).

In spinal cord, dorsal horn neurons were found positive for P2X1-3, 7 receptor subtypes. mRNA for all seven P2X receptor subtypes have been found in the spinal cord dorsal horn (Nakatsuka & Gu 2006) and findings consistent with the expression of P2X2-4 and P2X6-7 receptor subtypes in dorsal horn neurons have been documented, especially in lamina II (Bardoni et al. 1997, Llewellyn-Smith & Burnstock 1998, Kanjhan et al. 1999, Deuchars et al. 2001). The lamina II in the spinal cord is a region known to receive strong input from nociceptive primary afferents and release of ATP is known to modulate neurotransmitter release, such as glutamate through P2X receptors in central afferent terminals or second-order neurons of the spinal cord, suggesting a role for P2X receptors in transmitting or modulating nociceptive information in the central nervous system (Bardoni et al. 1997, Chizh & Illes 2001). However, ATP has also been shown to facilitate glycine- (Rhee et al. 2000) and GABAergic (Hugel & Schlichter 2000) spontaneous inhibitory postsynaptic currents at dorsal horn synapses through P2X receptors thus inhibiting nociceptive transmission. This suggests that a fine balance of excitatory and inhibitory components of purinergic transmission in the spinal cord may exist under normal conditions (Chizh & Illes 2001). The spinal cord glial cells in the samples in the present study were positive for P2X1, P2X2 and P2X7 receptor subtypes. In other species, P2X2 and P2X7 receptor subtypes have been reported in spinal cord astrocytes and oligodendrocytes, respectively (Matute 2008, Verkhratsky et al. 2012). P2X4 and P2X7 receptor subtypes are also present in spinal microglia

where P2X7 participates in microglial activation and secretion of proinflammatory factors and P2X4 in the development of allodynia in neuropathic pain (Morioka et al. 2008, Verkhratsky et al. 2012). The development of pathologic pain involves not only neuronal pathways but also glial signalling (see Scholz & Woolf 2007, Cao & Zhang 2008) and P2X receptors may have a key role in it (Chessell et al. 2005, Verkhratsky et al. 2012).

This is the first report of P2X receptor expression and distribution in equine tissue, with particular emphasis on the equine fore limb hoof and associated vasculature and nerve supply (Zamboulis et al. 2013). Equine P2X1-7 receptor transcripts and proteins were identified in these tissues and the distribution of four key members of the P2X receptor family, P2X1-3, 7, was detailed, showing important differences in tissue distribution and suggesting that heterogeneity in receptor expression may be important in normal cellular and tissue function.

Additionally, the equine P2X1-7 receptor mRNA nucleotide sequences were partially annotated and the use of P2X1-3, 7 receptor antibodies in equine tissue was validated. P2X4-6 receptor antibodies specificity in equine tissue could not be validated here. However, more antibodies should be tested in the future, as P2X4-6 receptor subtypes may have a role in the chronic pain state associated with laminitis and the changes occuring in the laminitic equine hoof.

The widespread distribution of P2X receptor subtypes in the equine hoof and associated vasculature and nerve supply along with their implication in cellular processes in health and disease may highlight a potential role for them in the regulation of the normal structure and function of the hoof and in hoof related pain pathways.

Chapter 4

Expression of purinergic P2X1-3 and 7 receptor subtypes in equine laminitis

(work accepted for publication under the title "Expression of purinergic P2X receptor subtypes 1, 2, 3 and 7 in equine laminitis" Zamboulis et al. (2013) *The Veterinary Journal* doi: http://dx.doi.org/10.1016/j.tvjl.2013.08.017) (see Appendix for full text)

4.1 Introduction

Laminitis in horses is manifested by disruption of the lamellar suspensory apparatus of the distal phalanx, with loss of mechanical support and associated pain (Pollitt 2011) with pain being a predominant feature of the condition. Following the development of acute laminitis, up to 75% of horses may develop a protracted form of the disease, resulting in chronic debilitation and eventual mortality (Moore 2009). In the horse, tissue sensitisation and chronic pain states have been documented in joint disease and laminitis (Malone 2002, Jones et al. 2007). Characterisation of pathways involved in tissue sensitisation and chronic pain may reveal new therapeutic targets (Heinzmann & McMahon 2011).

There is a growing body of evidence linking P2X receptors to chronic pain and inflammation in other species (Gu & Heft 2004, Chessell et al. 2005). Changes in P2X3 and P2X7 receptor subtypes expression in the dorsal root ganglia and spinal cord have been implicated in the development of neuropathic pain in rats (Xiang et al. 2008, He et al. 2012). Furthermore, functional studies with the use of P2X3 receptor antisense oligonucleotides, antagonists, and knockout mice confirm the involvement of the P2X3 channel in neuropathic pain (Barclay et al. 2002, Honore et al. 2002, Jarvis et al. 2002, Sharp et al. 2006). Similarly, functional studies involving P2X7 receptor antagonists and knockout mice reveal a role for P2X7 receptor in chronic inflammatory and neuropathic pain (Chessell et al. 2005, Honore et al. 2006). In addition, endogenous ATP release by epithelial and endothelial cells occurs in response to local tissue changes, such as hypoxia and acidosis, altering cell proliferation and survival (Burnstock & Verkratsky, 2010).

In chapter 3, P2X receptor subtype expression in the normal horse was

examined. Here, previous observations were extended to include naturally occurring chronic active laminitis. The aim of this chapter was to investigate altered P2X receptor subtype expression in the hoof, palmar digital vessels and nerve, dorsal root ganglia and spinal cord in horses with chronic active laminitis compared to non-laminitic horses. For this purpose, immunohistochemistry experiments were carried out in tissues collected from horses suffering from chronic active laminitis and P2X1-3, 7 receptor subtypes distribution and expression was compared to that of normal horses. In addition, the histology of H&E stained tissues from chronic laminitic horses was assessed and compared to that of normal horses to investigate the correlation of altered P2X receptor expression with morphological changes in the examined tissues.

4.2 Study design

- **Sample collection** – Tissue samples were collected from euthanased horses (n = 5, mean age 14 years) suffering from naturally occurring chronic active laminitis (in accordance with Pollitt & Collins 2011). Horses had a duration of chronic laminitis ranging from 1-15 months with time of onset of laminitis defined as the first recorded event of laminitis by the owner and/or veterinarian (Table 4.1). The cause of laminitis was not determined here as the main focus was pain in relation to chronicity of the condition and the cases were solely defined by duration of the condition. Sampled tissues included the palmar digital artery, palmar digital vein, palmar digital nerve, hoof, ipsilateral C8 DRG and spinal cord (innervating the hoof) and

ipsilateral C4 DRG and spinal cord (not innervating the hoof) (see 2.1 Samples p.35).

Table 4.1. Ages and duration of laminitis for horses suffering from chronic laminitis.

Case	Age (years)	Duration of chronic laminitis (months)
Case 1	13	1
Case 2	12	1
Case 3	13	8
Case 4	17	10
Case 5	15	15

- **Histologic evaluation of tissues samples from horses with chronic laminitis** – Sampled tissue sections from horses suffering from chronic laminitis were stained with H&E and assessed descriptively. The thickness of the *tunica media* in the palmar digital artery and vein was measured and expressed as ratio of overall vessel thickness. Histopathological changes in the hoof were described as mild, moderate or severe (were graded as 1 (mild), 2 (moderate), 3 (severe)) according to Hampson et al. (2012). Neuronal cell body size in C4 and C8 DRG was measured and defined as small (<30 μm), medium (30-60 μm), and large (>60 μm) according to Holford et al. (1994) and their distribution determined (see 2.4.2 Histology p.55).

- **Characterisation of P2X1-3, 7 receptor subtype proteins distribution in chronic laminitic horses** – P2X1-3, 7 antibodies validated in equine tissue in Chapter 3 were used for immunohistochemical characterisation of their

respective proteins' distribution in sampled tissues from horses suffering from chronic laminitis (see 2.4.3 Immunohistochemistry p.56).

- **Comparison of P2X1-3, 7 receptor subtype distribution and expression between chronic laminitic and normal horses** – P2X1-3, 7 receptor subtype distribution was compared between chronic laminitic and normal horses and semi-quantitative immunohistochemistry was used to compare the expression levels (staining intensity) of two key P2X receptor subtypes in chronic pain, P2X3 and P2X7, between chronic laminitic and normal horses. For semi-quantitative immunohistochemistry, representative fields of view (n = 5) in immunostained sections were randomly selected for semi-quantification and mean grey scale intensity was measured after correction for white balance. Staining intensity for P2X3 receptor subtype in C8 DRG for each laminitic case was normalised against the staining intensity in the C4 DRG of the same horse and expressed as a ratio to the average normalised staining intensity of the C8 DRG in normal horses. Staining intensity for P2X7 receptor subtype in C4 and C8 DRG was normalised to DRG neuron nucleus counterstain (see 2.4.4 Semi-quantitative immunohistochemistry p.60).

- **Statistical analysis** – Data were tested for Normality using the Shapiro-Wilk test and significant differences were determined with Student's *t* test. For correlation analysis of hoof changes vs. time, the Pearson correlation coefficient (*r*) was calculated. The level of significance was set at $P < 0.05$ and data were presented as mean ± SD (see 2.8 Statistical analysis p.79).

4.3 Results

4.3.1 Histological findings

The histological evaluation of chronic laminitic tissues in comparison to normal revealed several findings. The morphometric examination of the palmar digital artery and vein revealed a significant reduction in the thickness of the *tunica media* in the palmar digital vein of horses with laminitis (0.48 ± 0.05, n = 5) compared to unaffected horses (0.57 ± 0.04, n = 5, $P = 0.02$). No difference was observed in the thickness of the *tunica media* in the palmar digital artery of horses with laminitis and normal horses (0.52 ± 0.05, 0.57 ± 0.05, respectively, n = 5, $P = 0.13$) (Figure 4.1).

Histological examination of hoof sections from horses with chronic laminitis displayed characteristic histopathology of laminitis with mild to severe alterations to the lamellar architecture of the hoof, which were related to chronicity ($r = 0.95$, $P = 0.01$) (Figure 4.2a-f). Mild changes were characterised by lengthening of the primary epidermal lamellae (PEL), attenuation and tapering of the tips of secondary epidermal lamellae (SEL) and the presence of abnormal columns of partially keratinised cells on either side of the keratinised axis of the PEL (Figure 4.2b and c and Figure 4.3). Moderate changes included marked straightening and elongation of the SEL (Figure 4.2d). Severe changes comprised complete loss of lamellar architecture, with epidermal cells forming a mass on either side of the PEL keratinised axis instead of being organised into recognisable SEL rows (Figure 4.2e and f). Histological sections from normal horses had no evidence of lamellar pathology (Figure 4.2a).

Examination of DRG sections, revealed a mild, generalised, reduction in organisation of neurons in C8 dorsal root ganglia of horses with laminitis compared with non-laminitic horses (Figure 4.4). In one horse with laminitis of 1 month's duration, there was a decrease in the proportion of large size neurons in the C8 DRG compared to normal horses (5.7% vs. 20.4 ± 3.1%; n = 5) and, to a lesser degree, in the C4 DRG (5.8% vs. 16.6 ± 8.2%; n = 5), but this reduction was not present in other laminitic cases.

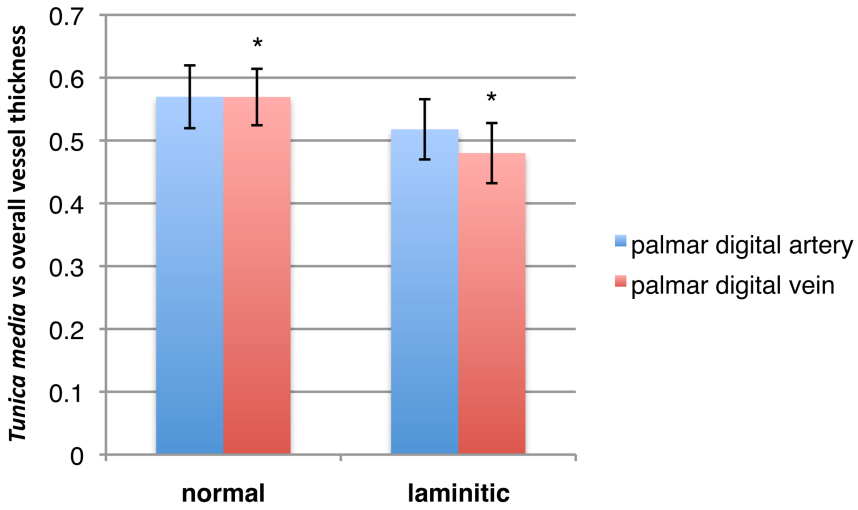

Figure 4.1. Thickness of the *tunica media* expressed as ratio of overall vessel thickness in the palmar digital artery and vein of normal and chronic laminitic horses. A significant reduction in the thickness of the *tunica media* in the palmar digital vein of horses with laminitis compared to unaffected horses was noted. No difference was observed in the palmar digital artery of horses with laminitis and normal horses. Histogram represents means ± SD, n = 5, * $P < 0.05$.

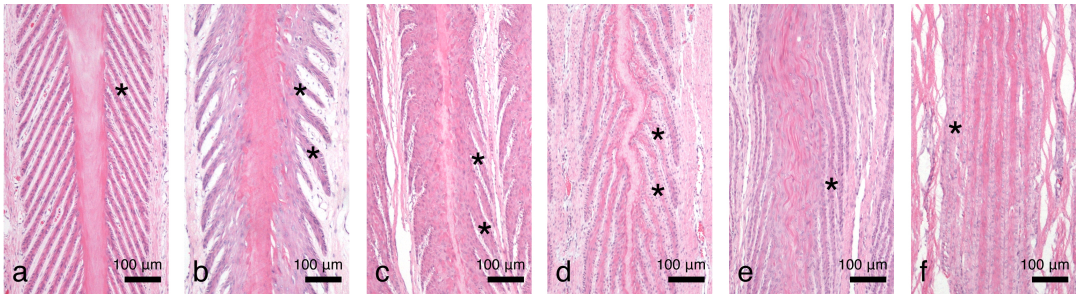

Figure 4.2. Lamellar sections (hoof) of a normal horse (a) and horses with chronic laminitis (b-e) (H&E). Sections show (a) normal lamellar architecture with symmetrical secondary epidermal lamellae (SEL) (asterisk) of equal size with rounded tips, (b and c) presence of SEL (asterisk) of uneven length with tapered tips and abnormal columns of partially keratinised cells on either side of the primary epidermal lamellae (PEL) axis (clinical signs 1 month duration), (d) attenuation of the SEL (asterisk) with marked straightening and elongation (clinical signs 8 months duration), and (e and f) loss of lamellar architecture with epidermal basal cells forming a contiguous mass (asterisk) on either side of the PEL keratinized axis (clinical signs 10 and 15 months duration, respectively).

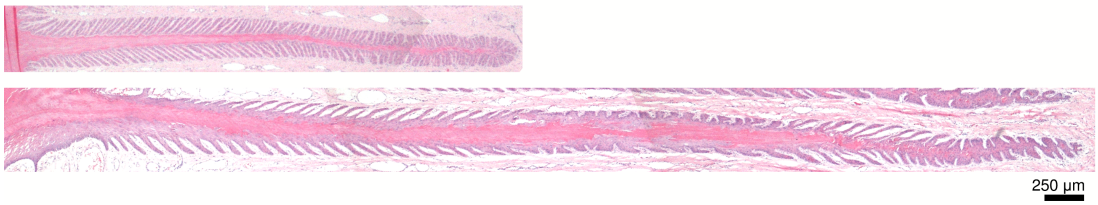

Figure 4.3. Full length PEL from lamellar sections (hoof) of a normal horse (top) and a horse with chronic laminitis (clinical signs 1 month duration) (bottom) (H&E). The PEL from the hoof section of the chronic laminitic horse showed marked lengthening compared to the PEL from the hoof section of the normal horse. (reconstituted)

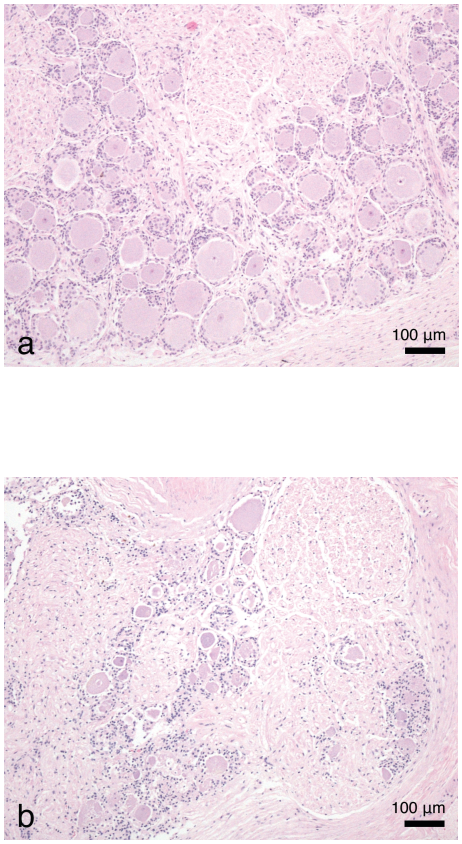

Figure 4.4. C8 DRG sections of a normal horse (a) and a horse with chronic laminitis (b). In the C8 DRG section of the laminitic case (b) there appeared to be a mild, generalised, reduction in organisation of neurons compared to the non-laminitic C8 DRG (a).

4.3.2 P2X1-3, 7 receptor subtype immunohistochemical analysis

Immunohistochemical analysis of the palmar digital vessels in chronic laminitic horses revealed expression of P2X3 receptor subtype in smooth muscle cells of the *tunica media* in the palmar digital artery of horses with laminitis, which was absent from normal horses (Figure 4.5a and c). No differences were observed between the laminitic and normal horses in P2X3 receptor subtype distribution in the palmar digital vein (Figure 4.5b and d) or P2X1, 2 and 7 receptor subtypes in the palmar digital artery or vein.

In the hooves of laminitic horses, expression of P2X1-3 and 7 receptor subtypes was evident in the proliferating, partially keratinised, epidermal cells adjacent to the PEL keratinised axis, which are not present in normal hooves. P2X7 receptor subtype, in particular, appeared to have the strongest immunostaining (Figure 4.6). The basal epidermal cells in laminitic hooves retained the P2X1-3 and 7 receptor subtype expression observed in normal horses and there were no differences in receptor subtype distribution or intensity in this layer between normal and chronic laminitic horses.

In nervous tissue, no alterations were noted in the pattern of distribution of P2X1-3, 7 receptor subtypes in neuronal cell bodies or glial cells in the C4 or C8 DRG, or spinal cord segments, between laminitic and normal horses. However, there were alterations in staining intensity for P2X3 receptor subtype in the C8 DRG, but not the C4 DRG, of two horses with laminitis of 1 month's duration. In one case, a marked increase in the intensity of staining for P2X3 receptor subtype was evident in large neurons, coinciding with a mild reduction in the proportion of large neurons (Figure 4.7). In the other case, there was a small decrease in the intensity of staining

for P2X3 receptor subtype in all neurons, without any alterations in the proportions of the different sizes of neurons. In horses with laminitis of 8, 10 and 15 months' duration, there were no differences in staining intensity for P2X3 receptor subtype in the C8 or C4 DRG compared to normal horses. No alteration in P2X7 staining intensity in Schwann cells was noted in the DRG of laminitic horses compared to normal horses.

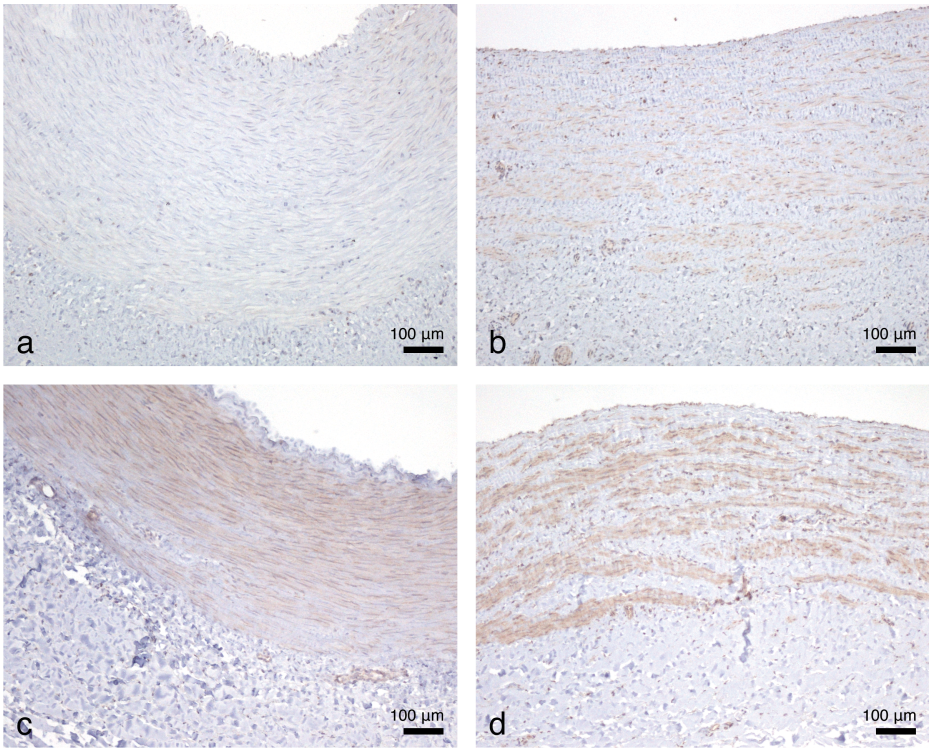

Figure 4.5. P2X3 receptor subtype distribution in the palmar digital artery (a and c) and vein (b and d) of normal (a and b) and laminitic horses (c and d). P2X3 receptor subtype was absent in smooth muscle cells of the palmar digital artery in normal horses (a), whereas it was evident in palmar digital artery smooth muscle cells in laminitic horses (c). No change in P2X3 receptor subtype distribution was noted in the palmar digital vein between normal and laminitic horses (b and d, respectively).

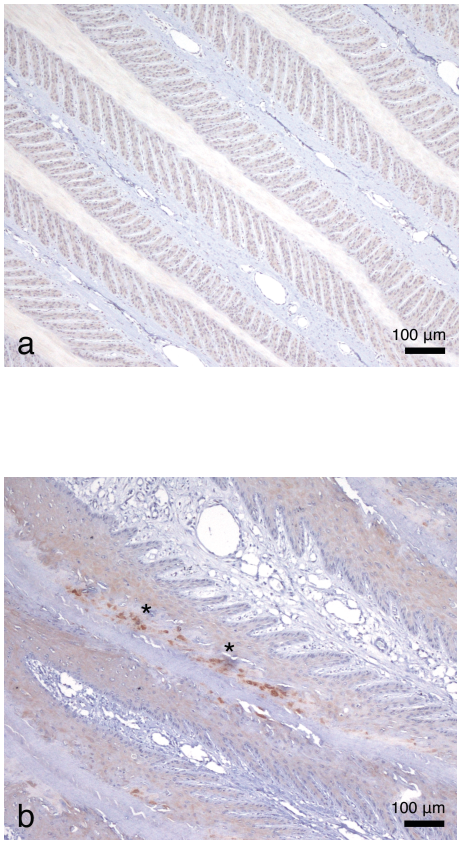

Figure 4.6. P2X7 receptor subtype expression in the hoof of a normal (a) and a laminitic horse (b). Expression of P2X7 receptor subtype was evident in the proliferating, partially keratinised, epidermal cells adjacent to the PEL keratinised axis in the hoof of the laminitic horse (b, asterisks) which are absent in the hooves of normal horses (a). No change in receptor distribution in the basal epidermal cells was noted between the laminitic and normal horses.

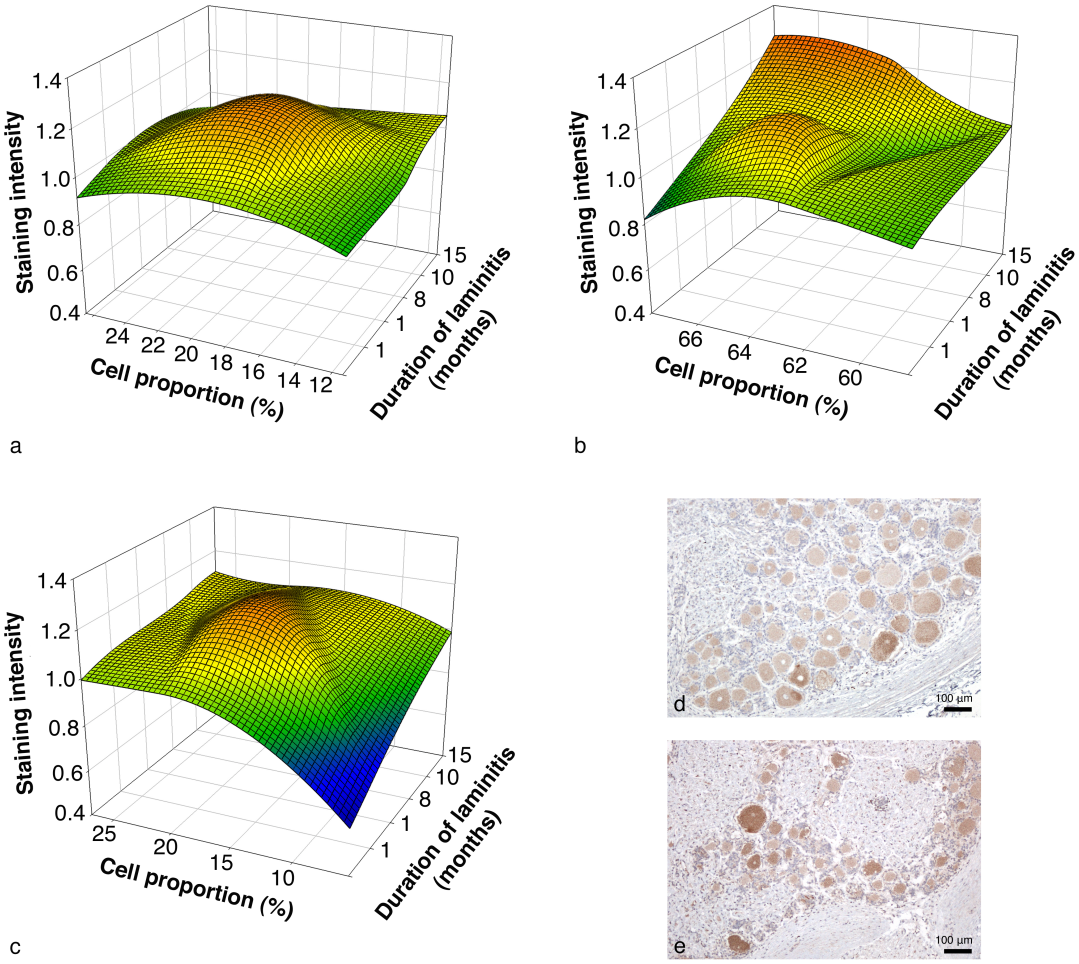

Figure 4.7. (a-c) Surface plots for P2X3 receptor subtype staining intensity and proportion of small (a), medium (b) and large-size neurons (c) in C8 DRG of horses with chronic laminitis (n = 5). Staining intensity in C8 DRG for each laminitic case was normalised against the staining intensity in the C4 DRG of the same horse and expressed as a ratio to the average normalised staining intensity of the C8 DRG in five non-laminitic horses. In grey scale measurements, **high values (orange) indicate low staining intensity**, whereas **low values (blue) indicate high staining intensity**. In one horse with chronic laminitis of 1 month's duration, there was a mild decrease in intensity of staining for P2X3 receptor subtype in small (a) medium-size (b) and large (c) neurons. In another horse with chronic laminitis of 1 month's duration, there was a marked increase in intensity of staining for P2X3 receptor subtype, which coincided with a decrease in the proportion of large neurons in the DRG. (d and e) Representative photos of P2X3 receptor subtype immunostaining in the C8 DRG of a normal (d) and a laminitic (e) horse.

4.4 Discussion

The distribution of purinergic P2X receptor subtypes in the horse has received little attention until recently (Zamboulis et al. 2013, Zerpa et al. 2013). However, since P2X receptors are involved in a diverse range of tissue functions including regulation of vascular tone, tissue sensitisation and chronic pain (Neary et al. 1996, Gu & Heft 2004, Chessell et al. 2005, Burnstock & Verkratsky 2010), they may have relevance in diseases such as equine laminitis. Here, P2X receptor subtype distribution was assessed in tissues likely to be affected by laminitis, such as the palmar digital vessels and nerve, dorsal root ganglia and spinal cord.

Morphometric histological examination of the palmar digital vessels revealed a reduction in the thickness of the *tunica media* of the palmar digital veins in horses with laminitis compared to unaffected horses. Vascular events are considered to be important in the pathogenesis of equine laminitis (Peroni et al. 2006, Menzies-Gow et al. 2008) and in chronic laminitis, venograms show filling-defects, consistent with vascular compression (Baldwin & Pollitt 2010). Vascular remodelling (including thinning of the vessel wall) has been noted in chronic conditions with hyperdynamic circulation, such as cirrhosis (Fernandez-Varo et al. 2003), where chronic shear-stress forces result in increases in endothelium-derived nitric oxide. Short-term vascular tone but also long-term vascular remodelling regulation is associated with purinergic signalling with a widespread expression of P2X receptors in vessels (Burnstock 2009, Ralevic 2012). In addition, ATP released in response to local hypoxia and changes in blood flow (shear stress) regulates digital constriction (Bodin et al. 1991, Bergfeld & Forrester 1992).

In the horse, Zerpa et al. (2013) demonstrated that digital vessels are responsive to purine agonists. Here, P2X3 receptor subtype was expressed in smooth muscle cells in the *tunica media* of the palmar digital artery of horses with laminitis but not in normal horses. In contrast, P2X1, 2 and 7 receptor subtypes were expressed in the palmar digital vessels of horses with and without laminitis. In other species, P2X3 receptors in blood vessels appear to have a role in neurogenic regulation of vascular tone and P2X3 channel is also involved in nociception in vascular disease (Erlinge & Burnstock 2008, Ralevic 2009). In addition, regulation of vascular tone by ET-1 may involve purinergic receptors (Joseph et al. 2013) and ET-1 may play a role in laminitis (Keen et al. 2008, Gauff et al. 2013).

In this study, histological changes in the hooves of horses with chronic laminitis were similar to previous descriptions (Collins et al. 2010b, Hampson et al. 2012) with lengthening of the PEL, attenuation and tapering of the tips of SEL and the presence of abnormal columns of partially keratinised cells on either side of the keratinised axis of the PEL to marked straightening and elongation of the SEL and complete loss of lamellar architecture with fusion of SEL in a contiguous mass. In addition, the severity of the observed histological changes was found to be correlated to the duration of laminitis of each case.

In horses with laminitis, expression of P2X1-3 and 7 receptor subtypes was retained in basal epidermal cells and was also evident in partially keratinised cells; in particular, strong expression of P2X7 receptor subtype was noted in these cells. P2X7 receptor subtype has been co-localised with apoptotic markers and is involved in terminal differentiation in human epidermal keratinocytes (Greig et al. 2003). In addition, an increased rate of apoptosis has been demonstrated in epidermal lamellae

in the hooves of horses with laminitis (Faleiros et al. 2004, Asplin et al. 2010).

Purinergic receptor expression and function in nervous tissue has received considerable attention, particularly in relation to nerve-tissue injury models and neuronal plasticity (Gu & Heft 2004, Chessell et al. 2005). In horses suffering from chronic laminitis, palmar digital nerve injury with abnormal morphology has been shown to occur followed by phenotypic changes in primary sensory neurons in C8 DRG (fore limb) which are associated with neuropathic pain (Jones et al. 2007). In this study, the examined palmar digital nerve sections of normal and chronic laminitic horses were stained with H&E which did not allow for the identification of abnormal morphology and no change in P2X1-3 and 7 receptor subtype distribution and expression was observed. However, variable alterations in P2X3 receptor subtype immunostaining in C8 DRG (involved in innervation of the hoof) were noted in two horses with chronic laminitis of 1 month's duration, but not in the C4 DRG (not involved in hoof innervation). In one case, there was a marked increase in staining of large neurons, which occurred in conjunction with a decrease in the proportion of these neurons. In the other case, there was a mild decrease in staining intensity in all neurons, independent of size; in this case there was no apparent alteration in the proportion of neurons of different sizes. Changes in P2X3 receptor subtype expression were not detected in the DRG of horses with chronic laminitis of longer duration.

Temporal expression of the P2X3 receptor subtype has been described in rodents with P2X3 receptor subtype showing involvement in the induction and early maintenance of long lasting pain rather than in the later phase (Nakagawa et al. 2007). Maintenance of P2X3 receptor subtype expression in large neurons is thought

to mediate mechanical allodynia, i.e. a painful response to a normally innocuous mechanical stimulus, in rats (Kage et al. 2002). Evaluation of DRG in additional cases of equine laminitis in the early stages of chronic disease (1 month's duration) may support this observation.

P2X7 receptor has also an important role in neuropathic pain and has been shown to be upregulated in human DRG and injured nerves from chronic neuropathic pain patients (Chessell et al. 2005). Here, such changes in P2X7 receptor subtype expression were not noted in DRG from chronic laminitic horses.

In this chapter, the examination of DRGs from horses suffering from chronic laminitic pain revealed temporal expression of the P2X3 receptor subtype protein in DRG neurons. Although the findings presented here are descriptive due to the restricted availability of samples, they provide ground for further research in this direction. Examination of more samples could help establish a temporal pattern of purinergic expression in DRG neurons of laminitic horses and reveal potential targets for drug development. Furthermore, immunohistochemical analysis of the palmar digital vessels and the hoof also showed altered purinergic expression. The changes in purinergic expression observed in these tissues could be a result of adaptive mechanisms responding to lamellar changes occuring in laminitis or part of an ongoing pathology due continuous exposure to the inciting cause (e.g. endocrinopathic laminitis). It would therefore be interesting for future work to define, in addition to chronicity, the cause of laminitis in the sampled cases to allow for better understanding of purinergic involvement in the observed lamellar pathology.

Chapter 5

Expression of functional P2X receptors in equine nervous tissue

5.1 Introduction

P2X receptors are involved in many cellular functions and can be altered in pathological conditions. Understanding of their function and properties is therefore important to elucidate their role in pathological conditions and their pharmacological characterisation is required to open the way for development of new drugs.

The patch-clamp technique is the gold standard technolgy for studying ion channel pharmacology and has been widely used in the characterisation of P2X receptors. Additionally, intracellular calcium measurements have also been used for the characterisation of P2X receptors' pharmacological properties with the advantage of allowing a higher throughput for the characterisation (He et al. 2003, Calvert & Evans 2004).

In Chapter 3, P2X1-7 receptor mRNA signal was identified in equine tissue and P2X1-3 and 7 receptor subtype distribution was detailed in the same tissues using immunohistochemical methods. However, evidence for P2X receptor mRNA or the observed P2X receptor immunoreactivity does not necessarily indicate the presence of functional receptors. Furthermore, the co-localisation of P2X1-3 and 7 receptor proteins in equine neurons raised the possibility of multiple subtype expression. The aim of this chapter was to investigate the functionality of the expressed P2X receptors in equine nervous tissue and characterise them pharmacologically. For this purpose, electrophysiolgy and intracellular calcium measuring and imaging methods were used.

5.2 Study design

- **Sample collection** – C4 and C8 DRG and spinal cord segments were dissected from normal horses and cells were extracted with enzymatic digestion of the tissues with collagenase I (2 mg/mL) and dispase II (5 mg/mL). Extracted cells were used for experiments freshly isolated or following culture (see 2.5.1 Tissue digestion and neurons extraction p.62).

- **Whole-cell and perforated whole-cell patch-clamping experiments** – Whole-cell and perforated whole-cell patch-clamping experiments were performed on freshly isolated C4 and C8 DRG neurons. Neurons were plated at high density in poly-lysine coated glass bottom Petri dishes and P2X receptor agonists were applied with a U-tube delivery system. P2X receptor antagonists were perfused in the Petri dish waterbath. For the perforated whole-cell patch-clamp technique, an amphotericin B solution (210 μg/mL) was used as a pore-forming agent for the internal pipette solution. Recordings were made with the cells held at -60 mV (see 2.5 Electrophysiology experiments p.62).

- **Intracellular calcium measurements, fluorescence plate reader** – Intracellular calcium measurements conducted in the fluorescence plate reader were carried out in C8 DRG cells cultured to confluence. After culture, the DRG cell population was mainly consisting of supportive cells, ie. satellite glial cells, Schwann cells, and fibroblasts, and few or no neurons (see 2.6.1 Cells p.69). For the measurements, Fura-2 AM, a UV excitable

ratiometric fluorescent dye with excitation peaks of 340 nm (Ca^{2+}-bound dye) and 380 nm (Ca^{2+}-free dye) and an emission peak of 510 nm, was used. The cells were incubated with 6 μM of Fura-2 AM to load the dye and used at a density of 250,000 cells/mL. The potent P2X7 agonist BzATP and the non-selective P2X antagonist *iso*-PPADS were used to challenge the cells and single F_{340} and F_{380} fluorescence measurements were taken from the wells before and straight after the addition of BzATP (10, 50, 100, 500 μM and 1 mM) (added once) with and without pre-incubation of the cells with *iso*-PPADS. The fluorescence ratios F_{340}/F_{380} were calculated and changes in fluorescence were expressed as percent changes versus baseline fluorescence (fluorescence before application of agonists) (see 2.6.3 Fluorescence plate reader recordings p.73).

- **Intracellular calcium measurements, spectrofluorimeter** – Intracellular calcium measurements were carried out in C8 DRG cells cultured to confluence and freshly isolated C8 spinal cord segment cells. For the measurements, Fura-2 AM was loaded into the cells with a 6 μM Fura-2 AM solution and cells were used at a density of 500,000 cells/mL. P2X agonists and antagonists used to challenge the cells are summarised in Table 5.1. Fluorescence was measured in resting cells to establish the signal baseline and signal recordings were taken after agonist application for periods of 300 seconds, with intervals of 2-3 seconds for the first 30 seconds (0-30 seconds), 10 seconds for the next 150 seconds (30-180 seconds), and 30 seconds for the last 120 seconds (180-300 seconds). Measurements were also carried out as mentioned above in calcium free buffer after stimulation with 5 μM of

BzATP (cultured C8 DRG cells, added once) for 120 seconds (see 2.6.4 Spectrofluorimeter recordings p.74). Fluorescence values were corrected for background fluorescence and the F_{340}/F_{380} fluorescence ratios, reflecting $[Ca^{2+}]_i$ concentrations, were calculated. F_{340}/F_{380} fluorescence ratios following agonist addition were expressed in graphs corrected for baseline signal and maximum fold or percent changes in Fura-2 fluorescence (versus baseline F_{340}/F_{380}) were calculated for all used P2X agonists and antagonists. For P2X antagonists, the percent of inhibition was also calculated (see 2.6.5 Data analysis p.75).

Table 5.1. P2X agonists and antagonists used in intracellular calcium measurements carried out in the spectrofluorimeter, concentrations and tested cells.

P2X agonist/antagonist		**Concentration (μM)**	**Cells**	
ATP	P2X agonist	5, 10, 50, 100, 200, 500	spinal cord cells	n=1
BzATP	potent P2X7 agonist	0.5 , 5, 50	cultured DRG cells	n=1
		10, 50, 100, 200	cultured DRG cells	n=3
iso-PPADS	non-selective P2X antagonist	20	cultured DRG cells	n=3
BBG	P2X7 selective antagonist	1000	cultured DRG cells	n=3

The use of P2X antagonists was combined with stimulation of the cells with 100 μM BzATP.

- I**ntracellular calcium imaging** – Intracellular calcium imaging experiments were carried out in freshly isolated C8 DRG cells with Fluo-4 AM, a single wavelength dye with an excitation peak of 494 nm and an emission peak of 506 nm. Cells were loaded with a 5-10 μM Fluo-4 AM solution and challenged with ATP (1 mM) (added once). A photo of the cells in a resting state was acquired before addition of the agonist and after addition of the agonist, photos of the stimulated cells were taken every 2 seconds for 60

seconds. Neuron cells were identified based on size and fluorescence intensity in stimulated neurons was measured and corrected for background fluorescence. Changes to fluorescence 30 seconds after agonist application were calculated versus baseline fluorescence in resting cells (see 2.7 Intracellular calcium imaging p.76).

- **Statistical analysis** – Where applicable, the mean and standard deviation were calculated and data were presented as mean ± SD. Data were checked for Normality using the Shapiro-Wilk test and significant differences were determined with Student's *t* test. The level of significance was set at $P < 0.05$ (see 2.8 Statistical analysis p.79).

5.3 Results

5.3.1 Electrophysiology experiments

Good quality, stable gigaseals were consistently achieved in the extracted DRG neurons and whole-cell configuration was achieved on a few occasions both with the whole-cell and the perforated whole-cell techniques. However, the quality of the cell or the clamp at each time did not allow for recordings to be made in either whole-cell or perforated whole-cell patch-clamp.

5.3.2 Intracellular calcium measuring experiments

5.3.2.1 Fluorescence plate reader

Monitoring of intracellular calcium ($[Ca^{2+}]_i$) in Fura-2-loaded cultured equine C8 DRG cells with the fluorescence plate reader showed an increase in $[Ca^{2+}]_i$ levels after application of P2X7 potent agonist BzATP to the cells. Specifically, application of 10, 50, 100 and 500 μM of BzATP to the cell suspension was followed by an increase in the recorded F_{340}/F_{380}, reflecting an increase in $[Ca^{2+}]_i$ levels, whereas application of 1 mM of BzATP resulted in a decrease of F_{340}/F_{380}. Incubation of the cell suspensions with the non-selective antagonist *iso*-PPADS (20 μM) before the application of BzATP caused a decrease of the $[Ca^{2+}]_i$ increase observed in BzATP stimulated cells for BzATP concentrations of 50, 100 and 500 μM. Application of 10 μM BzATP to *iso*-PPADS-preincubated cells caused an increase in $[Ca^{2+}]_i$ levels greater than the one recorded in cells without *iso*-PPADS. Finally, application of 1 mM BzATP to *iso*-PPADS-preincubated cells resulted in an increase in $[Ca^{2+}]_i$ levels compared to the decrease observed in cells without *iso*-PPADS (Figure 5.1).

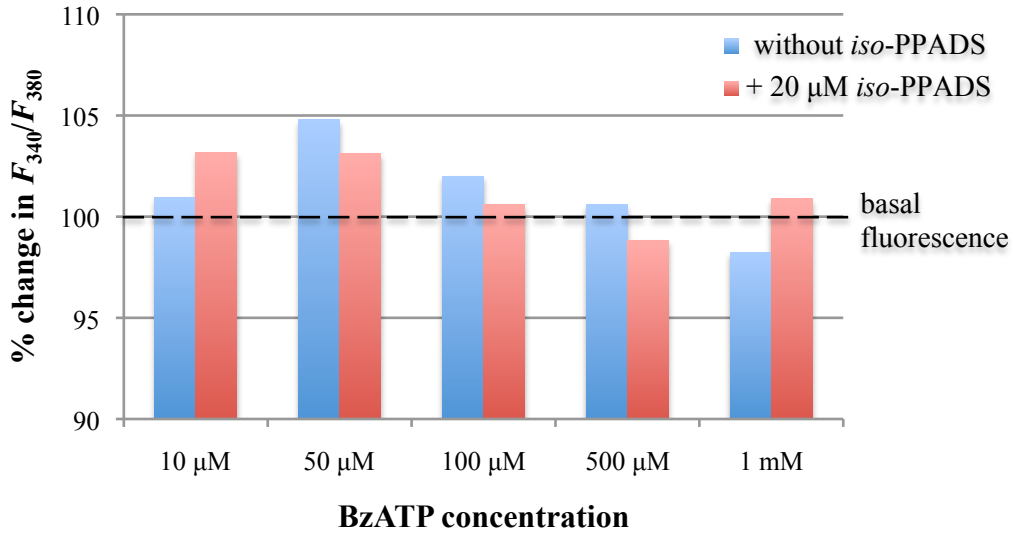

Figure 5.1. Percent changes in F_{340}/F_{380} values for Fura-2-loaded cultured equine C8 DRG cells challenged with P2X7 potent agonist BzATP with (red) and without (blue) pre-incubation with the non-selective P2X antagonist *iso*-PPADS (20 µM). BzATP was used at concentrations of 10, 50, 100, and 500 µM, and 1 mM (n = 1).

5.3.2.2 Spectrofluorimeter

In equine DRG cells, mostly comprised of non-neuronal cells, application of P2X7 receptor potent agonist BzATP resulted in a marked and reproducible increase in $[Ca^{2+}]_i$ levels. The observed increase in $[Ca^{2+}]_i$ levels was concentration-dependent for BzATP concentrations of 10, 50, and 100 μM (n = 3) with 1.27, 1.62, and 2.61-fold changes in F_{340}/F_{380} fluorescence ratio. However, stimulation with 200 μM of BzATP resulted in a 1.30-fold change in F_{340}/F_{380} which was lower than the ones observed with lower BzATP concentrations (Figure 5.2, Table 5.2). Preliminary data with stimulation with 0.5, 5 and 50 μM also displayed a concentration-dependent increase in $[Ca^{2+}]_i$ levels with 1.47, 1.41 and 1.84-fold changes in F_{340}/F_{380}. In Ca^{2+}-free medium, BzATP (5 μM) failed to elicit an $[Ca^{2+}]_i$ increase supporting the expression of functional P2X receptors in DRG non-neuronal cells, since only activated P2X receptors cause calcium influx while activated P2Y receptors cause calcium release from intracellular stores (Idzko et al. 2001). To further confirm the observed rise in $[Ca^{2+}]_i$ levels was mediated by P2X receptors and more specifically P2X7 receptors, the non-selective P2X antagonist *iso*-PPADS and the selective P2X7 receptor antagonist BBG were used. $[Ca^{2+}]_i$ responses evoked by 100 μM BzATP were partially inhibited by 20 μM *iso*-PPADS with 51.0% inhibition and 1 mM BBG with 23.0% inhibition (Table 5.2, Figure 5.3).

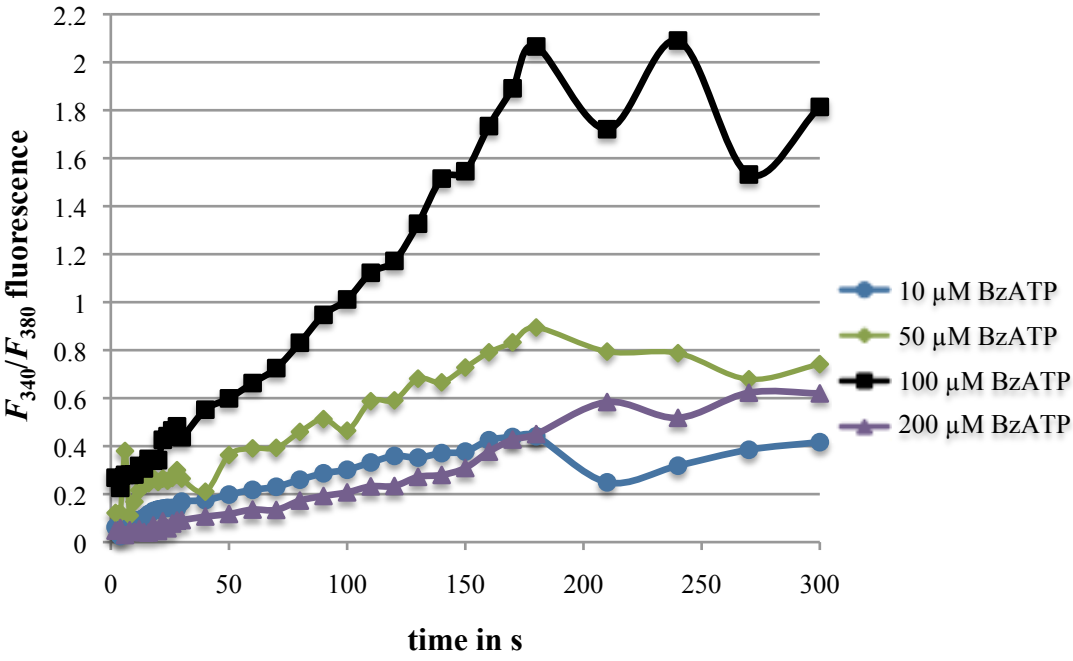

Figure 5.2. F_{340}/F_{380} fluorescence ratios for equine DRG non neuronal cells stimulated with 10, 50, 100, and 200 µM BzATP (normalised for their respective basal fluorescence) (n = 3).

Table 5.2. Maximum fold changes in Fura-2 fluorescence (F_{340}/F_{380} fluorescence ratios) in DRG non-neuronal cells in response to BzATP, *iso*-PPADS and BBG versus basal fluorescence. Where applicable data is presented as mean ± SD, n = 3, * $P < 0.05$.

Agonist and antagonist concentrations	$\boldsymbol{F_{340}/F_{380}}$ **maximum fold change (versus basal fluorescence)**	
10 μM BzATP	1.26 ± 0.08 *	
50 μM BzATP	1.62 ± 0.50	
100 μM BzATP	2.61 ± 0.62	
200 μM BzATP	1.30 ± 0.08 *	
5 μM BzATP in Ca^{2+}-free solution	0.94	
iso-PPADS (20 μM) + 100 μM BzATP	1.28 ± 0.02	51.0 % inhibition
BBG (1mM) + 100 μM BzATP	2.01 ± 0.10	23.0 % inhibition

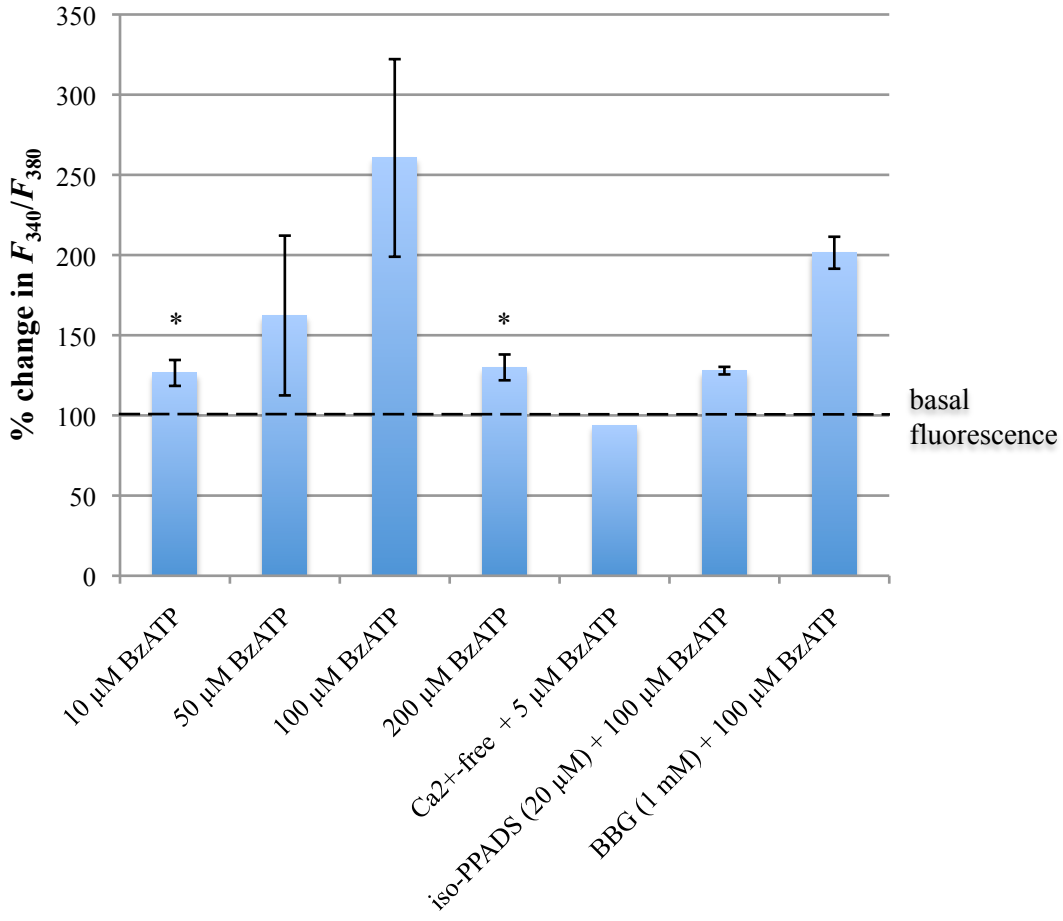

Figure 5.3. Maximum percent changes in Fura-2 fluorescence (F_{340}/F_{380} fluorescence ratios) in DRG non-neuronal cells in response to BzATP, *iso*-PPADS and BBG versus basal fluorescence. Where applicable the histogram represents mean ± SD, (n = 3, Ca^{2+}-free + 5 µM BzATP n = 1), * $P < 0.05$.

In equine spinal cord cells, ATP induced an increase in $[Ca^{2+}]_i$ displaying a biphasic $[Ca^{2+}]_i$ response consisting of an initial transient peak within 30 seconds of agonist stimulation and a sustained component maintained until the end of measurements at 300 seconds. For lower ATP concentrations of 10 and 50 μM the initial transient peak displayed a concentration-depedent response with F_{340}/F_{380} maximum fold-changes of 1.25 and 1.40, respectively, followed by a sustained response which was closer to basal fluorescence (Table 5.3, Figure 5.4 and 5.7). Higher ATP concentrations of 100, 200 and 500 μM elicited the same biphasic $[Ca^{2+}]_i$ response but with a smaller initial peak. The sustained phase showed similar $[Ca^{2+}]_i$ levels to the ones seen with lower ATP concentrations (Figure 5.5). The maximum fold changes in F_{340}/F_{380} observed for these concentrations were 1.25, 1.24 and 1.30, respectively, and were noted in the sustained phase of the $[Ca^{2+}]_i$ repsonse with the exception of the 1.24-fold change for 200 μM ATP which was noted in the initial transient peak (Table 5.3, Figure 5.6).

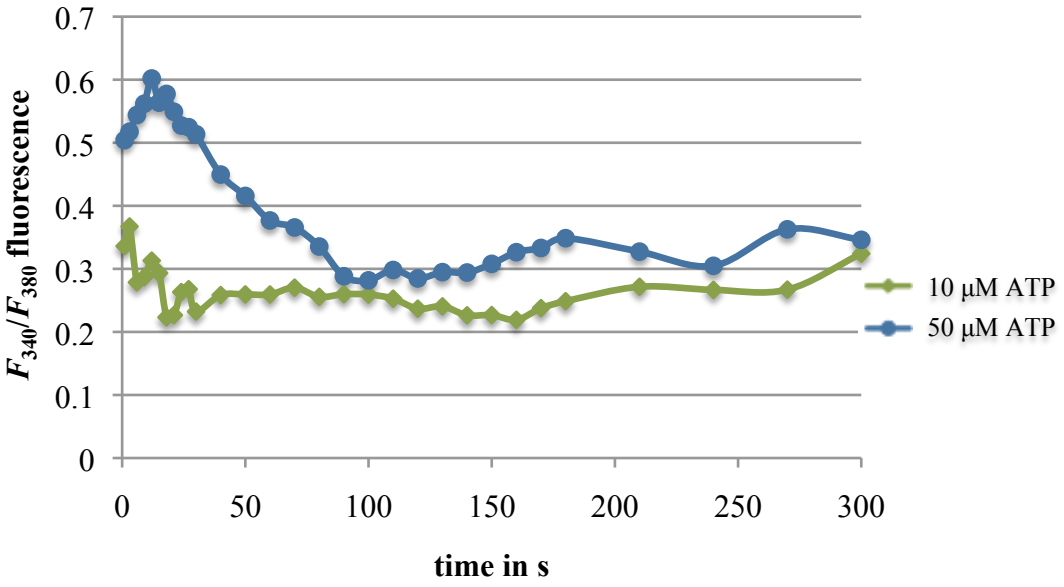

Figure 5.4. F_{340}/F_{380} fluorescence ratios for equine spinal cord cells stimulated with 10 and 50 µM ATP (normalised for their respective basal fluorescence) (n = 1).

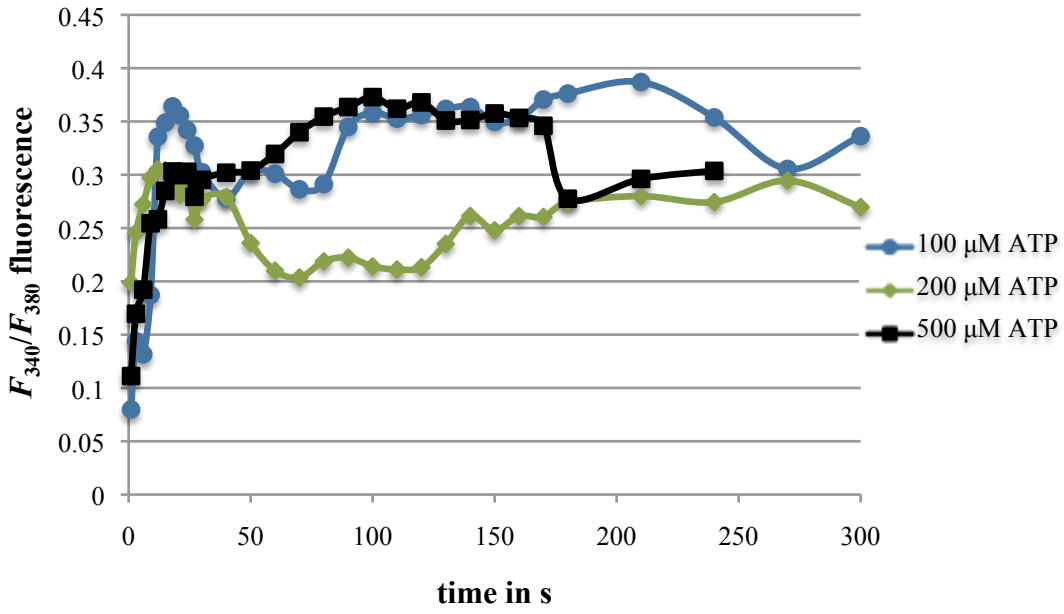

Figure 5.5. F_{340}/F_{380} fluorescence ratios for equine spinal cord cells stimulated with 100, 200 and 500 µM ATP (normalised for their respective basal fluorescence) (n = 1).

Table 5.3. Maximum fold changes in Fura-2 fluorescence (F_{340}/F_{380} fluorescence ratios) in equine spinal cord cells in response to ATP versus basal fluorescence (n = 1).

ATP concentration	**F_{340}/F_{380} maximum fold change (versus basal fluorescence)**
10 µM	1.25
50 µM	1.40
100 µM	1.25
200 µM	1.24
500 µM	1.30

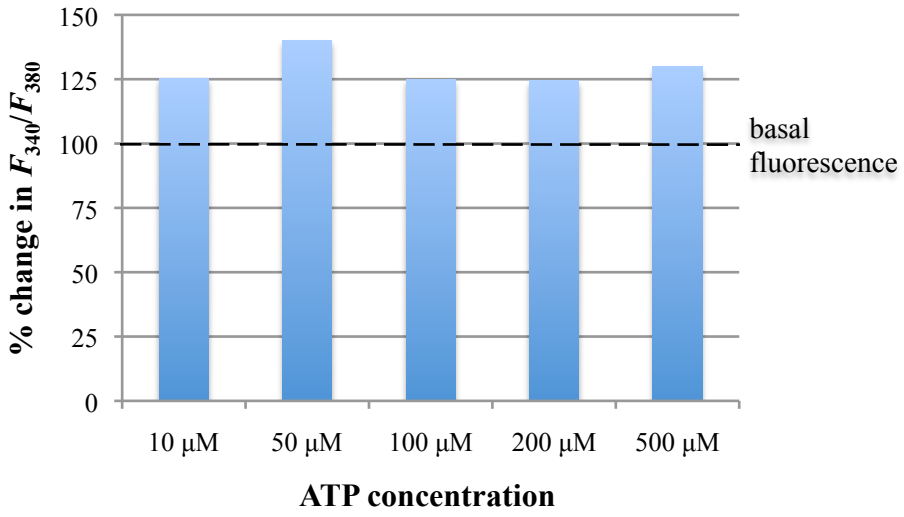

Figure 5.6. Maximum percent changes in Fura-2 fluorescence (F_{340}/F_{380} fluorescence ratios) in spinal cord cells stimulated with 10, 50, 100, 200 and 500 µM ATP versus basal fluorescence (n = 1).

5.3.3 Intracellular calcium imaging experiments

Loading of equine DRG cells with Fluo4-AM was not consistently successful and only one series of measurements was achieved after agonist stimulation. More specifically, application of 1 mM of ATP elicited an increase in fluorescence ratio (F_{490}/F_0, where F_0 is the background fluorescence) in all tested DRG neurons (n = 19) with a mean $\Delta F_{490}/F_0$, of 0.045 (SD=0.03, range 0.005 – 0.102) after 30 seconds of exposure (Figure 5.7).

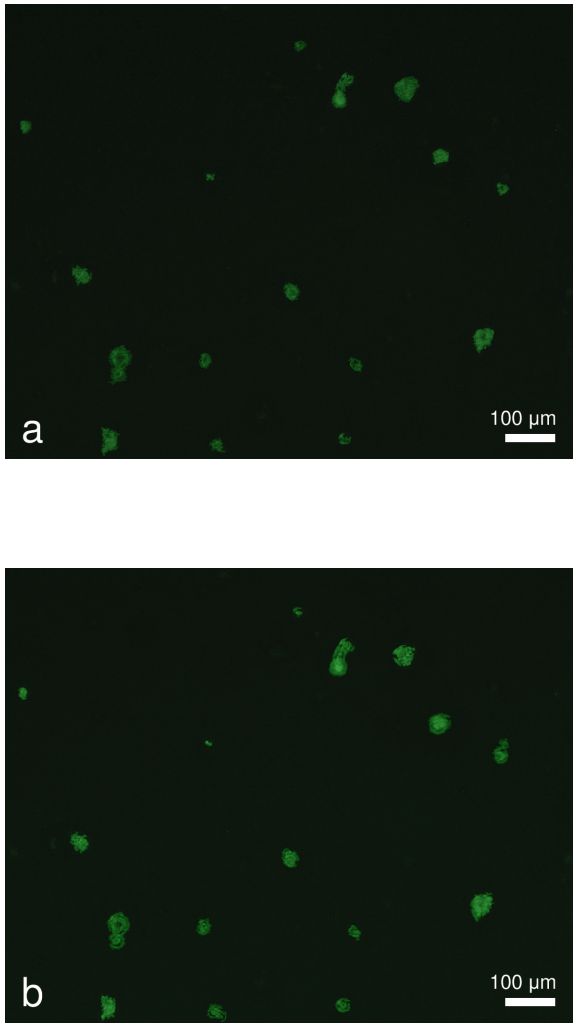

Figure 5.7. Fluo4-AM calcium imaging in DRG neurons in (a) a resting state and (b) 30 seconds after application of 1 mM of ATP (fluorescence artificially enhanced for display purpose).

5.4 Discussion

In Chapter 3, the presence of P2X receptor proteins in equine tissues was demonstrated. In this chapter, intracellular calcium measurements and electrophysiology were used to investigate the functionality of the expressed P2X receptors in equine nervous tissue. The use of P2X agonists in intracellular calcium measurements elicited an $[Ca^{2+}]_i$ response which was partially inhibited by P2X antagonists providing evidence for the presence of functional purinergic receptors in equine DRG and spinal cord cells.

Application of P2X7 receptor potent agonist BzATP and ATP in equine DRG non-neuronal cells and spinal cord cells, respectively, caused a marked and reproducible increase of free $[Ca^{2+}]_i$ supporting the presence of functional P2X and purinergic receptors, respectively, in these cells. Stimulation of the cells with different agonist concentrations showed a concentration-dependent pattern in $[Ca^{2+}]_i$ responses both for ATP and BzATP. Interestingly, agonist concentrations of 200 μM BzATP and 100 μM ATP or greater produced an $[Ca^{2+}]_i$ rise of smaller magnitude than lower concentrations. Similar findings are reported in eosinophils and astroglial cells with 1 mM of ATP and BzATP, showing similar or smaller $[Ca^{2+}]_i$ changes compared to 100 μM, whereas a clear increase in the magnitude of $[Ca^{2+}]_i$ responses is noted between concentrations of 10 μM and 100 μM of the same agonists (Idzko et al. 2001, Hamilton et al. 2008). The decreased response observed with higher concentrations of ATP may be due to cell death following P2X7 receptor activation (Luo et al. 2013). Also, in DRG non-neuronal cells, prolonged BzATP stimulation evoked a gradually increasing long lasting response, whereas upon prolonged ATP

stimulation spinal cord cells displayed a biphasic $[Ca^{2+}]_i$ response consisting of a rapid peak followed by a sustained elevation. In the ATP-stimulated biphasic response, the two phases displayed distinct characteristics with the transient phase showing changes in magnitude according to the agonist concentration and the sustained phase showing similar magnitude for all concentrations. The biphasic pattern in ATP-stimulated $[Ca^{2+}]_i$ responses has been previously reported and has been attributed to presence of heterogenous populations of purinergic receptors, where P2Y receptors would appear to mediate the transient phase and P2X, including P2X7, receptors the sustained phase (White et al. 2001, Nobile et al. 2003, Gifford et al. 2004, Weng et al. 2008).

In DRG non-neuronal cells, mediation of $[Ca^{2+}]_i$ responses by P2X receptors was coroborrated by the abolition of the observed $[Ca^{2+}]_i$ responses in Ca^{2+}-free media, as P2X receptors depend on extracellular Ca^{2+} influx whereas P2Y receptors regulate Ca^{2+} mobilisation from intracellular stores (Idzko et al. 2001). Additional measurements with preincubation of DRG non-neuronal cells with the non-selective P2X receptor antagonist *iso*-PPADS (20 μM) and the selective P2X7 receptor antagonist BBG (1 mM) resulted in partial inhibition of $[Ca^{2+}]_i$ responses to BzATP (100 μM) (51.0% and 23.0% respectively), further confirming the expression of functional P2X receptors, including P2X7 receptors, in equine DRG non-neuronal cells. Partial inhibition of $[Ca^{2+}]_i$ responses by the antagonists could be due to insufficient preincubation (10 minutes), or insufficient antagonist concentration, as antagonist potency is greatly affected by preincubation time and antagonist concentration, especially across species (North 2002). In rat cortical astrocytes, 50 μM *iso*-PPADS with 15 minutes of preincubation was used to achieve 65% inhibition of the effect of 100 μM BzATP (Jacques-Silva et al. 2004). Also, although

iso-PPADS is referred to as a P2X antagonist, data about its potency against P2X7 receptors is equivocal and species-dependent (North 2002, Jacques-Silva et al. 2004). BBG is a P2X7 receptor selective antagonist effective in the nanomollar range but concentrations of 10 mM have also been used (Jiang et al. 2000, Noguchi et al. 2008). Here, BBG results confirmed that BzATP acted on functional P2X7 receptors in equine DRG cells. However, persistence of part of the BzATP-stimulated response after BBG preincubation could be attributed to, except for insufficient preincubation and antagonist concentration, the presence of functional P2X receptors other than P2X7 receptors. Although BzATP has been widely used as a selective P2X7 receptor agonist (Idzko et al. 2001), it is not as it has been documented to have agonistic effects on other P2X receptors as well as P2Y receptors (Fischer et al. 2001, North et al. 2002, Zhang et al. 2005).

Spectrofluorimeters have been widely used for intracellular calcium measurements, their main disadvantage however being the requirements in cell numbers. When using freshly isolated DRG cells the number of available cells is limited and do not allow for many sets of measurements. An alternative to the use of the spectrofluorimeter is the use of a plate reader for intracellular calcium measurements which has lower requirements in cell numbers. In this study, intracellular calcium measurements carried out in a plate reader with application of P2X7 potent agonist BzATP produced an increase in DRG non-neuronal cells $[Ca^{2+}]_i$ levels. This gave an indication for the presence of functional P2X7 receptors in equine DRG non-neuronal cells. However, the time required for the plate reader to go through all the wells resulted in measurements being taken at slightly different

timepoints for each well and did not allow for a close and accurate monitoring of $[Ca^{2+}]_i$ levels through time.

Calcium imaging experiments with Fluo4-AM were chosen for their smaller requirement in cell numbers compared to spectrophotometric calcium measurements and because they allowed for differentiation of DRG neurons and non-neuronal cells when measuring the elicited $[Ca^{2+}]_i$-responses. Fluo-4 AM has been used for calcium imaging in neurons (Hegg et al. 2003, Hung et al. 2010), although unsuccessful loading of neurons has also been reported (Newman 2001, Weick et al. 2003). Here, loading of C8 DRG neurons with the dye was not consistently successful and only one series of measurements was possible. In these measurements, stimulation with 1 mM ATP evoked an $[Ca^{2+}]_i$-rise of ranging amplitude in DRG neurons providing evidence for the presence of functional purinergic receptors in equine DRG neurons.

Electrophysiological methods have been most commonly used for the identification of functional P2X receptors and their pharmacological characterisation (Khakh et al. 1995, Bianchi et al 1999). Moreover, electrophysiology has proven a useful tool in the linking of P2X receptor phenotypic changes to functional changes and in the determination of the role of P2X receptors under injurious conditions (Xu & Huang 2002, Pan et al. 2009). Here, whole-cell and perforated whole-cell patch-clamp were used to study the functional properties of P2X receptors in equine DRG. Good quality whole-cell configurations, however, could not be achieved due to a combination of inexperience in electrophysiology techniques and equine DRG tissue limitations for cell extraction. To overcome tissue limitation issues future work could include the establishment of an equine neuron cell line. An equine neuron cell line

would provide a continuous source of cells and allow optimisation of the whole-cell patch-clamp technique to achieve whole-cell configurations.

A number of limitations were present in this set of experiments starting with limited availability of tissue for cell extraction. Also, equipment and time restrictions contributed to the difficulties faced in this chapter. However, intracellular calcium measurements with the spectrofluorimeter gave consistent and reliable results providing evidence for the presence of functional purinergic and P2X receptors in equine spinal cord and DRG cells, respectively. Future work with measurements on additional cells with different P2X agonists and antagonists could provide more details about the receptors expressed in these cells. Furthermore, the establishment of an equine neuron cell line would provide the required cell numbers to test additional P2X agonists and antagonists.

Chapter 6

General discussion

Chronic pain in equine laminitis often leads to debilitation and euthanasia of the horse. It is a significant welfare issue for horses worldwide. Therefore, it is important to try to understand the molecular mechanisms in chronic laminitis pain pathways with the eventual aim to develop novel, targeted therapeutics to reduce morbidity and mortality. Furthermore, the mechanisms behind the development of laminitis have not been fully elucidated and research in this area would advance our understanding of laminitis. Purinergic P2X receptors have a pivotal role in pain pathways as well as regulation of vascular tone, cell differentiation and apoptosis, and other tissue functions relevant to laminitis but have, as yet, not been studied in detail in naturally occurring laminitis, where pain and tissue damage is such a central feature.

In this study, the presence and distribution of P2X receptors in tissues of the equine digit and its associated vasculature and innervation was investigated in normal horses and horses suffering from naturally occurring chronic active lamintis. In addition the functionality of P2X receptors expressed in equine nervous tissue was investigated.

6.1 Expression of purinergic P2X receptors in horses

Purinergic P2X receptors are ubiquitous receptors and although they are involved in numerous physiological and pathological processes they have received little attention in the horse. Here, purinergic P2X receptors were identified in the equine hoof and its associated vasculature and innervation. Gene expression (mRNA) for all seven receptors and protein expression for P2X1-3 and 7 receptor subtype

proteins was found in the studied tissues. The expression of P2X receptor subtypes in a variety of equine tissues confirms the widespread expression of P2X receptors noted in other vertebrates and highlights the importance of understanding their role in cellular processes in the horse.

Validation of antibodies for use in equine tissue, in this study, was only possible for P2X1-3 and 7 receptor subtype proteins, and future work should include testing of more P2X4-6 receptor subtype protein antibodies manufactured against different epitopes to enable the study of these receptor subtypes, too. Custom made antibodies against the equine P2X4-6 receptor protein amino acid sequences could also be used in case commercial antibodies were not successful.

6.2 Expression and distribution of purinergic P2X receptors in normal and chronic laminitic horses

Immunohistochemical analysis of P2X1-3 and 7 receptor subtypes distribution showed differential cellular distribution in equine tissue suggesting a subtype-specific regulation of functions in these tissues (Glass et al. 2000). Extension of these results in tissues from chronic laminitic horses demonstrated that distribution and expression of P2X1-3 and 7 receptor subtypes differed between normal and diseased tissues. Differential expression of P2X receptor subtypes in naturally occurring disease states in other species has been previously reported and supports a role for P2X receptors in pathological processes offering insights for disease regulation (review Burnstock & Kennedy 2011).

In this study, immunohistochemical analysis of equine nervous tissue revealed P2X3 receptor subtype was expressed solely in neuronal cells whereas P2X7 receptor subtype demonstrated strong expression in glial cells. This tissue-specific distribution is also reported in other species and supports a special role for these receptors in nervous tissue physiology. More specifically, P2X3 receptor has a major role in nociception, both physiological and pathological whereas P2X7 receptors in glial cells are involved in the induction and maintenance of inflammatory and neuropathic pain (Hughes et al. 2007, Wirkner et al. 2007).

Expression of these two key receptors was therefore compared in C8 DRGs (innervating the forelimb) of normal horses and horses suffering from chronic laminitis revealing P2X3 receptor subtype expression was altered in horses with a shorter duration of chronic laminitis (1 month). In particular, one case presented a marked increase in immunostaining in large neurons which coincided with a decrease in the proportion of these neurons in the DRG. A temporal pattern in P2X expression in chronic pain has also been described in rodents with the participation of P2X3-containing receptors in the induction and early maintenance of long-lasting pain but not the late phase (Nakagawa et al. 2007).

Further investigation of changes occurring in the early maintenance of chronic pain in laminitis but also investigation of P2X receptors involvement in the later phase of chronic pain could therefore reveal new targets amongst P2X receptors for pain management. Future work with more DRG samples from horses suffering from chronic laminitis would help identify changes in P2X receptors expression which may be significant in neuropathic pain pathways.

P2X receptor subtypes' widespread distribution in horses suggests a role in regulation of other functions in addition to pain pathways. In this study, horses suffering from chronic laminitis displayed expression of P2X3 receptor subtype in smooth muscle cells of the palmar digital artery which was absent in normal horses. In normal horses, P2X1-3 and 7 receptor subtype expression was identified in palmar digital vein smooth cells but P2X3 receptor subtype was absent from the palmar digital artery smooth muscle cells. Vascular events have a central role in the pathogenesis of laminitis but are also shown to persist in the chronic phase (Baldwin & Pollitt 2010). Additionally, in endocrinopathic laminitis, laminitis-inducing factors are ongoing and so may be vasoconstriction and vascular events.

Here, morphometric analysis of equine digital vessels revealed a decrease in the thickness of the smooth muscle layer (*tunica media*) of palmar digital veins from chronic lamintic horses compared to normal horses, confirming the presence of vascular pathology in chronic laminitis. Further morphometric analysis of palmar digital vessel samples at different phases of lamintis may help understand if the observed changes here are part of the ongoing vascular pathology in laminitis or an adaptive change as a result of altered digital blood flow. Furthermore, P2X1-3 and 7 have been found to participate in the regulation of vascular tone in the equine digital vessels (Zerpa et al. 2013). There is therefore evidence for the participation of P2X receptors in vascular regulation in horses and P2X3 receptor subtype expression in the palmar digital artery of horses with laminitis may develop in response to the occurring vascular events.

Finally, in chronic laminitic hooves, P2X1-3 and 7 receptor subtypes were present in the basal epidermal cells, similarly to distribution in normal hooves, but

also in partially keratinised cells present in the lamellae of laminitic hooves, with particularly strong staining for P2X7 receptor subtype. P2X7 receptor is linked to apoptosis and is also known to participate in terminal differentiation in epidermal cells (Greig et al. 2003). Furthermore, in chronic laminitic hooves, epidermal cells demonstrate an increased apoptosis rate (Faleiros et al. 2004). P2X7 receptor subtype could therefore be involved in the regulation of apoptosis in basal epidermal cells and the dyskeratosis observed in chronic laminitic hooves. Further investigation of this hypothesis with co-localisation studies of apoptosis markers and P2X7 receptor subtype could provide insight in the mechanisms responsible for lamellar histopathology in chronic laminitis.

Table 6.1. Summary of P2X1-3 and 7 distribution in key equine tissues associated with laminitis in normal and chronic laminitic horses.

Tissue	**Cells**	**P2X receptor subtype expression**	
		Normal	**Chronic laminitic**
Palmar digital artery	Endothelial cells	P2X2	
	Smooth muscle cells	P2X1, 2, 7	+ P2X3
Palmar digital vein	Endothelial cells	P2X2, 3	
	Smooth muscle cells	P2X1-3, 7	
Palmar digital nerve	Nerve fibres	P2X1-3	
	Schwann cells	P2X1, 2, 7	
Hoof	Basal epidermal cells	P2X1-3, 7	+ partially keratinised basal epidermal cells
DRG (C4, C8)	Neurons	P2X1-3	altered P2X3 expression in C8 DRG
	Satellite glial cells	P2X1, 2	
	Schwann cells	P2X7	
Spinal cord (C4, C8)	Neurons	P2X1-3, 7	
	Glial cells	P2X1, 2, 7	
	Ependymal cells	P2X1-3, 7	

6.3 Expression of functional purinergic P2X receptors in equine nervous tissue

Despite the use of a number of techniques to investigate functional aspects of P2X receptors, limitations were present in this set of experiments. Due to the reliance of naturally occurring disease from a hospital population, there was often a limited availability of tissue for cell extraction. In addition, equipment and time restrictions contributed to the difficulties faced in this part of the project. However, it was possible to measure intracellular calcium using spectrofluorimetric methods and through the use of purinergic agonists and antagonists, this provided evidence for the presence of functional purinergic and P2X receptors in equine spinal cord and DRG cells.

Further measurements using additional samples and refinement of techniques, particularly electrophysiological methods, could provide more details about the receptors expressed in these cells. For this purpose the establishment of an equine neuronal cell line might be beneficial, especially to address the limited availability of equine samples.

6.4 General remarks

The study of naturally occurring chronic active laminitis is necessary to be able to understand the mechanisms of disease and provide novel routes for therapeutic intervention, but provides significant challenges to the researcher. The use of naturally occurring models rather than induced disease models has to take into account the temporal nature of the condition, wide biological variation and limited

tissue availability. There are a number of models available for the induction of laminitis however they are undesirable for welfare reasons and are not available in the United Kingdom based on this fact.

The expression of P2X receptor subtypes in key equine tissues associated with laminitis and its chronic pain state, the presence of alterations in their expression and distribution in laminitic tissues and their wide-range of physiological roles highlight an important avenue of hitherto underdeveloped research in this area. Further work to elucidate the involvement of P2X receptors in laminitis and associated chronic pain may help understand the mechanisms involved in its pathology and offer insights for disease modulation and pain management in chronic laminitis and other conditions of the horse associated with chronic pain.

References

1. Abbracchio MP, Burnstock G, Verkhratsky A, Zimmermann H (2009) Purinergic signalling in the nervous system: an overview. *Trends in Neurosciences* 32:19-29.
2. Adair III HS, Goble DO, Schmidhammer JL, Shires MH (2000) Laminar microvascular flow, measured by means of laser Doppler flowmetry, during the prodromal stages of black walnut-induced laminitis in horses. *American Journal of Veterinary Research* 61:862-868.
3. Arandjelovic S, McKenney KR, Leming SS, Mowen KA (2012) ATP induces protein arginine deiminase 2-dependent citrullination in mast cells through the $P2X_7$ purinergic receptor. *The Journal of Immunology* 189:4112-4122.
4. Asplin KE, Curlewis JD, McGowan CM, Pollitt CC, Sillence MN (2011) Glucose transport in the equine hoof. *Equine Veterinary Journal* 43:196-201.
5. Asplin KE, Patterson-Kane JC, Sillence MN, Pollitt CC, McGowan CM (2010) Histopathology of insulin-induced laminitis in ponies. *Equine Veterinary Journal* 42:700-706.
6. Asplin KE, Sillence MN, Pollitt CC, McGowan CM (2007) Induction of laminitis by prolonged hyperinsulinaemia in clinically normal ponies. *The Veterinary Journal* 174:530-535.
7. Bailey SR, Adair HS, Reinemeyer CR, Morgan SJ, Brooks AC, Longhofer SL, Elliot J (2009) Plasma concentrations of endotoxin and platelet activation in the developmental stage of oligofructose-induced laminitis. *Veterinary Immunology and Immunopathology* 129:167-173.
8. Bailey SR, Menzies-Gow NJ, Marr CM, Elliott J (2004) The effects of vasoactive amines found in the equine hindgut on digital blood flow in the normal horse. *Equine Veterinary Journal* 36:267-272.
9. Baldwin GI, Pollitt CC (2010) Progression of venographic changes after experimentally induced laminitis. *Veterinary Clinics of North America: Equine Practice* 26:135-140.
10. Baraldi PG, Di Virgilio F, Romagnoli R (2004) Agonists and antagonists acting at $P2X_7$ receptor. *Current Topics in Medicinal Chemistry* 4:1707-1717.
11. Barclay J, Patel S, Dorn G, Wotherspoon G, Moffatt S, Eunson L, Abdel'al S, Natt F, Hall J, Winter J, Bevan S, Wishart W, Fox A, Ganju P (2002) Functional downregulation of $P2X_3$ receptor subunit in rat sensory neurons reveals a significant role in chronic neuropathic and inflammatory pain. *The Journal of Neuroscience* 22:8139-8147.
12. Barden JA, Bennett MR (2000) Distribution of P2X purinoceptor clusters on individual rat dorsal root ganglion cells. *Neuroscience Letters* 287:183-186.
13. Bardoni R, Goldstein PA, Lee J, Gu JG, MacDermott AB (1997) ATP P2X receptors mediate fast synaptic transmission in the dorsal horn of the rat spinal cord. *Journal of Neuroscience* 17:5297-5304.
14. Belknap JK, Giguère S, Pettigrew A, Cochran AM, van Eps AW, Pollitt CC (2007) Lamellar pro-inflammatory cytokine expression patterns in laminitis at the

developmental stage and at the onset of lameness: innate vs. adaptive immune response. *Equine Veterinary Journal* 39:42-47.
15. Bergfeld GR, Forrester T (1992) Release of ATP from human erythrocytes in response to a brief period of hypoxia and hypercapnia. *Cardiovascular Research* 26:40-47.
16. Bianchi BR, Lynch KJ, Touma E, Niforatos W, Burgard EC, Alexander KM, Park HS, Yu H, Metzger R, Kowaluk E, Jarvis MF, van Biesen T (1999) Pharmacological characterization of recombinant human and rat P2X receptor subtypes. *European Journal of Pharmacology* 376:127-138.
17. Bo X, Alavi A, Xiang Z, Oglesby I, Ford A, Burnstock G (1999) Localization of ATP-gated $P2X_2$ and $P2X_3$ receptor immunoreactive nerves in rat taste buds. *NeuroReport* 10:1107-1111.
18. Bo X, Kim M, Nori SL, Schoepfer R, Burnstock G, North RA (2003) Tissue distribution of $P2X_4$ receptors studied with an ectodomain antibody. *Cell and Tissue Research* 313:159-165.
19. Bodin P, Bailey D, Burnstock G (1991) Increased flow-induced ATP release from isolated vascular endothelial cells but not smooth muscle cells. *British Journal of Pharmacology* 103:1203-1205.
20. Bodin P, Burnstock G (2001a) Evidence that release of adenosine triphosphate from endothelial cells during increased shear stress is vesicular. *Journal of Cardiovascular Pharmacology* 38:900-908.
21. Bodin P, Burnstock G (2001b) Purinergic signalling: ATP release. *Neurochemical Research* 26:959-969.
22. Bours MJL, Swennen ELR, Di Virgilio F, Cronstein BN, Dagnelie PC (2006) Adenosine 5'-triphosphate and adenosine as endogenous signaling molecules in immunity and inflammation. *Pharmacology & Therapeutics* 112:358-404.
23. Bovell DL, Riggs CM, Sidlow G, Troester S, MacLaren W, Yip W, Ko WH (2013) Evidence of purinergic neurotransmission in isolated, inctact horse sweat glands. *Veterinary Dermatology* 24:398-e86.
24. Bradbury EJ, Burnstock G, McMahon SB (1998) The expression of $P2X_3$ purinoreceptors in sensory neurons: effects of axotomy and glial-derived neurotrophic factor. *Molecular and Cellular Neurosciences* 12:256-268.
25. Bragulla H, Hirschberg RM (2003) Horse hooves and bird feathers: Two model systems for studying the structure and development of highly adapted integumentary accessory organs – the role of the dermo-epidermal interface for the micro-architecture of complex epidermal structures. *Journal of Experimental Zoology Part B: Molecular and Developmental Evolution* 298:140-151.
26. Buckley P, Morton J, Coleman GT (2007) Repeated observations of naturally occurring laminitis in pony club horses in regional Australia. *In*: Australia College of Veterinary Scientists Science week Scientific Meeting Equine Chapter Prooceedings, pp10-11.
27. Budak MT, Orsini JA, Pollitt CC, Rubinstein NA (2009) Gene expression in the lamellar dermis-epidermis during the developmental phase of carbohydrate overload-induced laminitis in the horse. *Veterinary Immunology and Immunopathology* 131:86-96.
28. Burnstock G (1972) Purinergic nerves. *Pharmacological Reviews* 24:509-581.

29. Burnstock G (2009) Purinergic regulation of vascular tone and remodelling. *Autonomic & Autacoid Pharmacology* 29:63-72.
30. Burnstock G (2006) Purinergic signalling. *Birtish Journal of Pharmacology* 147:S172-S181.
31. Burnstock G, Kennedy C (1985) Is there a basis for distinguishing two types of P_2-purinoceptor? *General Pharmacology* 16:433-440.
32. Burnstock G, Kennedy C (2011) P2X receptors in health and disease. *Advances in Pharmacology* 61:333-372.
33. Burnstock G, Knight GE (2004) Cellular distribution and functions of P2 receptor subtypes in different systems. *International Review of Cytology* 240:31-304.
34. Burnstock G, Verkhratsky A (2009) Evolutionary origins of the purinergic signalling system. *Acta Physiologica* 195:415-447.
35. Burnstock G, Verkhratsky A (2010) Long-term (trophic) purinergic signalling: purinoceptors control cell proliferation, differentiation and death. *Cell Death and Disease* 1:e9.
36. Calvert JA, Evans RJ (2004) Heterogeneity of P2X receptors in sympathetic neurons: contribution of neuronal $P2X_1$ receptors revealed using knockout mice. *Molecular Pharmacology* 65:139-148.
37. Cao H, Zhang YQ (2008) Spinal glial activation contributes to pathological pain states. *Neuroscience Biobehavioural Reviews* 32:972-983.
38. Cario-Toumaniantz C, Loirand G, Ladoux A, Pacaud P (1998) $P2X_7$ receptor activation-induced contraction and lysis in human saphenous vein smooth muscle. *Circulation Research* 83:196-203.
39. Carpenter D, Meadows HJ, Brough S, Chapman G, Clarke C, Coldwell M, Davis R, Harrison D, Meakin J, McHale M, Rice SQJ, Tomlinson WJ, Wood M, Sanger GJ (1999) Site-specific splice variation of the human $P2X_4$ receptor. *Neuroscience Letters* 273:183-186.
40. Cavaliere F, D'Ambrosi N, Ciotti MT, Mancino G, Sancesario G, Bernardi G, Volonté C (2001) Glucose deprivation and chemical hypoxia: neuroprotection by P2 receptor antagonists. *Neurochemistry International* 38:189-197.
41. Chen CC, Akopian AN, Sivilotti L, Colquhoun D, Burnstock G, Wood JN (1995) A P2X purinoceptor expressed by a subset of sensory neurons. *Nature* 377:428-431.
42. Chessell IP, Hatcher JP, Bountra C, Michel AD, Hughes JP, Green P, Egerton J, Murfin M, Richardson J, Peck WL, Grahames CBA, Casula MA, Yiangou Y, Birch R, Anand P, Buell GN (2005) Disruption of the $P2X_7$ purinoceptor gene abolishes chronic inflammatory and neuropathic pain, *Pain* 114:386-396.
43. Chizh BA, Illes P (2001) P2X receptors and nociception. *Pharmacological Reviews* 53:553-568.
44. Clifford EE, Parker K, Humphreys BD, Kertesy SB, Dubyak GR (1998) The $P2X_1$ receptor, an adenosine triphosphate-gated cation channel, is expressed in human platelets but not in human blood leukocytes. *Blood* 91:3172-3181.
45. Cockayne DA, Dunn PM, Zhong Y, Rong W, Hamilton SG, Knight GE, Ruan HZ, Ma B, Yip P, Nunn P, McMahon SB, Bunrstock G, Ford APDW (2005) $P2X_2$ knockout mice and $P2X_2/P2X_3$ double knockout mice reveal a role for the

$P2X_2$ receptor subunit in mediating multiple sensory effects of ATP. *Journal of Physiology* 567:621-639.
46. Cockayne DA, Hamilton SG, Zhu QM, Dunn PM, Zhong Y, Novakovic S, Malmberg AB, Cain G, Berson A, Kassotakis L, Hedley L, Lachnit WG, Burnstock G, McMahon SB, Ford APDW (2000) Urinary bladder hyporeflexia and reduced pain-related behaviour in $P2X_3$-deficient mice. *Nature* 407:1011-1015.
47. Coddou C, Yan Z, Obsil T, Huidobro-Toro JP, Stojilkovic SS (2011) Activation and regulation of purinergic P2X receptor channels. *Pharmacological Reviews* 63:641-683.
48. Collins SN, Pollitt CC, Wylie CE, Matiasek K (2010a) Laminitic pain: parallels with pain states in humans and other species. *Veterinary Clinics of North America: Equine Practice* 26:643-671.
49. Collins SN, van Eps AW, Pollitt CC, Kuwano A (2010b) The lamellar wedge. *Veterinary Clinics of North America: Equine Practice* 26:179-195.
50. Collo G, Neidhart S, Kawashima E, Kosco-Vilbois M, North RA, Buell G (1997) Tissue distribution of the $P2X_7$ receptor. *Neuropharmacology* 36:1277-1283.
51. Collo G, North RA, Kawashima E, Merlo-Pich E, Neidhart S, Surprenant A, Buell G (1996) Cloning of $P2X_5$ and $P2X_6$ receptors and the distribution and properties of an extended family of ATP-gated ion channels. *The Journal of Neuroscience* 16:2495-2507.
52. Colomar A, Amédéé T (2001) ATP stimulation of $P2X_7$ receptors activates three different ionic conductances on cultured mouse Schwann cells. *European Journal of Neuroscience* 14:927-936.
53. Connolly GP (1995) Differentiation by pyridoxal 5-phosphate, PPADS and IsoPPADS between responses mediated by UTP and those evoked by α,β-methylene-ATP on rat sympathetic ganglia. *British Journal of Pharmacology* 114:727-731.
54. Constigan M, Scholz J, Woolf CJ (2009) Neuropathic paain: a maladaptive response of the nervous system to damage. *Annual Review of Neuroscience* 32:1-32.
55. Cook SP, McCleskey EW (2002) Cell damage excites nociceptors through release of cytosolic ATP. *Pain* 95:41-47.
56. Cook SP, Vulchanova L, Hargreaves KM, Elde R, McCleskey EW (1997) Distinct ATP receptors on pain-sensing and stretch-sensing neurons. *Nature* 387:505-508.
57. Cotrina ML, Lin JHC, Alves-Rodrigues A, Liu S, Li J, Azmi-Ghadimi H, Kang J, Naus CCG, Nedergaard M (1998) Connexins regulate calcium signaling by controlling ATP release. *Proceedings of the National Academy of Sciences of the United States of America* 95:15735-15740.
58. Coyne MJ, Cousin H, Loftus JP, Johnson PJ, Belknap JK, Gradil CM, Black SJ, Alfandari D (2009) Cloning and expression of ADAM-related metalloproteases in equine laminitis. *Veterinary Immunology and Immunopathology* 129:231-241.
59. Dandona P, Aljada A, Bandyopadhyay A (2004) Inflammation: the link between insulin resistance, obesity and diabetes. *Trends in Immunology* 25:4-7.

60. de Laat MA, Kyaw-Tanner MT, Nourian AR, Sillence MN, Pollitt CC (2011) The developmental and acute phases of insulin-induced laminitis involve minimal metalloproteinase activity. *Veterinary Immunology and Immunopathology* 140:275-281.
61. de Laat MA, McGowan CM, Sillence MN, Pollitt CC (2010) Equine laminitis: Induced by 48 h hyperinsulinaemia in Standardbred horses. *Equine Veterinary Journal* 42:129-135.
62. de Laat MA, Patterson-Kane JC, Pollitt CC, Sillence MN, McGowan CM (2013) Histological and morphometric lesions in the pre-clinical, developmental phase of insulin-induced laminitis in Standardbred horses. *The Veterinary Journal* 195:305-312.
63. Deuchars SA, Atkinson L, Brooke RE, Musa H, Milligan CJ, Batten TFC, Buckley NJ, Parson SH, Deuchars J (2001) Neuronal $P2X_7$ receptors are targeted to presynaptic terminals in the central and peripheral nervous systems. *Journal of Neuroscience* 21:7143-7152.
64. Diamandis EP (2004) Mass spectrometry as a diagnostic and a cancer biomarker discovery tool. *Molecular & Cellular Proteomics* 3:367-378.
65. Donnelly-Roberts DL, Jarvis MF (2007) Discovery of $P2X_7$ receptor-selective antagonists offers new insights into $P2X_7$ receptor function and indicates a role in chronic pain states. *British Journal of Pharmacology* 151:571-579.
66. Donelly-Roberts DL, Namovic MT, Faltynek CR, Jarvis MF (2004) Mitogen-activated protein kinase and caspase signaling pathways are required for $P2X_7$ receptor ($P2X_7R$)-induced pore formation in human THP-1 cells. *The Journal of Pharmacology and Experimental Therapeutics* 308:1053-1061.
67. Dray A (1995) Inflammatory mediators of pain. *British Journal of Anaesthesia* 75:125-131.
68. Driessen B, Bauquier SH, Zarucco L (2010) Neuropathic pain management in chronic laminitis. *Veterinary Clinics of North America: Equine Practice* 26:315-337.
69. Drury AN, Szent-Györgyi A (1929) The physiological activity of adenine compounds with especial reference to their action upon the mammalian heart. *The Journal of Physiology* 68:213-237.
70. Dunn PM, Blakeley AGH (1988) Suramin: a reversible P_2-purinoceptor antagonist in the mouse vas deferens. *British Journal of Pharmacology* 93:243-245.
71. Dunn PM, Zhong Y, Burnstock G (2001) P2X receptors in peripheral neurons. *Progress in Neurobiology* 65:107-134.
72. Dutton DW, Lashnits KJ, Wegner K (2009) Managing severe hoof pain in a horse using multimodal analgesia and a modified composite pain score. *Equine Veterinary Education* 21:37-43.
73. Eades SC, Stokes AM, Johnson PJ, LeBlanc CJ, Ganjam VK, Buff PR, Moore RM (2007) Serial alterations in digital hemodynamics and endothelin-1 immunoreactivity, platelet-neutrophil aggregation, and concentrations of nitric oxide, insulin, and glucose in blood obtained from horses following carbohydrate overload. *American Journal of Veterinary Research* 68:87-94.

74. Eaton SA, Allen D, Eades SC, Schneider DA (1995) Digital Starling forces and hemodynamics during early laminitis induced by an aqueous extract of black walnut (Juglans nigra) in horses. *American Journal of Veterinary Research* 56:1338-1344.
75. Egan TM, Samways DSK, Li Z (2006) Biophysics of P2X receptors. *European Journal of Physiology* 452:501-512.
76. Elliot J, Bailey SR (2006) Gastrointestinal derived factors are potential triggers for the development of acute equine laminitis. *The Journal of Nutrition* 136:2103S-2107S.
77. Elliot J, Berhane Y, Bailey SR (2003) Effects of monoamines formed in the cecum of horses on equine digital blood vessels and platelets. *American Journal of Veterinary Research* 64:1124-1131.
78. Elliott RA, Tonnu A, Ghaffar N, Taylor AH, Tincello DG, Norman RI (2013) Enhanced purinergic contractile responses and $P2X_1$ receptor expression in detrusor muscle during cycles of hypoxia–glucopenia and reoxygenation. *Experimental Physiology* 98:1683-1695.
79. Erlinge D, Burnstock G (2008) P2 receptors in cardiovascular regulation and disease. *Purinergic Signalling* 4:1-20.
80. Faleiros RR, Stokes AM, Eades SC, Kim DY, Paulsen DB, Moore RM (2004) Assessment of apoptosis in epidermal lamellar cells in clinically normal horses and those with laminitis. *American Journal of Veterinary Research* 65:578-585.
81. Feldberg W, Hebb C (1948) The stimulating action of phosphate compounds on the perfused superior cervical ganglion of the cat. *The Journal of Physiology* 107:210-221.
82. Fernandez-Varo G, Ros J, Morales-Ruiz M, Cejudo-Martin P, Arroyo V, Sole M, Rivera F, Rodes J, Jimenez W (2003) Nitrix oxide synthetase 3-dependent vascular remodeling and circulatory dysfunction in cirrhosis. *American Journal of Pathology* 162:1985-1993.
83. Fields RD, Stevens B (2000) ATP: an extracellular signaling molecule between neurons and glia. *Trends in Neurosciences* 23:625-633.
84. Fischoeder A, Meyborg H, Stibenz D, Fleck E, Graf K, Stawowy P (2007) Insulin augments matrix metalloproteinase-9 expression in monocytes. *Cardiovascular Research* 73:841-848.
85. Fisher KG, Saueressig U, Jacobshagen C, Wichelmann A, Pavenstadt H (2001) Extracellular nucleotides regulate cellular functions of podocytes in culture. *American Journal of Physiology Renal Physiology* 281:F1075-F1081.
86. French KR, Pollitt CC (2004a) Equine laminitis: cleavage of laminin 5 associated with basement membrane dysadhesion. *Equine Veterinary Journal* 36:242-247.
87. French KR, Pollitt CC (2004b) Equine laminitis: glucose deprivation and MMP activation induce dermo-epidermal separation *in vitro*. *Equine Veterinary Journal* 36:261-266.
88. Fukui M, Nakagawa T, Minami M, Satoh M, Kaneko S (2006) Inhibitory role of supraspinal $P2X_3$/$P2X_{2/3}$ subtypes on nociception in rats. *Molecular Pain* 2:19.
89. Galey FD, Twardock AR, Goetz TE, Schaeffer DJ, Hall JO, Beasley VR (1990) Gamma scintigraphic analysis of the distribution of perfusion of blood in the

equine hoof during black walnut (Juglans nigra)-induced laminitis. *American Journal of Veterinary research* 51:688-695.
90. Gargett CE, Wiley JS (1997) The isoquinoline derivative KN-62 a potent antagonist of the P2Z-receptor of human lymphocyes. *Britixh Journal of Pharmacology* 120:1483-1490.
91. Gartland A, Hipskind RA, Gallagher JA, Bowler WB (2001) Expression of $P2X_7$ receptor by a subpopulation of human osteoblasts. *Journal of Bone and Mineral Research* 16:846-856.
92. Gauff F, Patan-Zugaj B, Licka TF (2013) Hyperinsulinaemia increases vascular resistance and endothelin-1 expression in the equine digit. *Equine Veterinary Journal* doi: 10.1111/evj.12040.
93. Geyti CS, Odgaard E, Overgaard MT, Juul Jensen ME, Leipziger J, Praetorius HA (2008) Slow spontaneous $[Ca^{2+}]_I$ oscillations reflect nucleotide release from renal epithelia. *European Journal of Physiology* 455:1105-1117.
94. Gifford SM, Grummer MA, Pierre SA, Austin JL, Zheng J, Bird IM (2004) Functional characterization of HUVEC-CS: Ca^{2+} signaling, ERK 1/2 activation, mitogenesis and vasodilator production. *Journal of Endocrinology* 182:485-499.
95. Gitterman DP, Evans RJ (2001) Nerve evoked P2X receptor contractions of rat mesenteric arteries; dependence on vessel size and lack of role of L-type calcium channels and calcium induced calcium release. *British Journal of Pharmacology* 132:1201-1208.
96. Glass R, Burnstock G (2001) Immunohistochemical identification of cells expressing ATP-gated cation channels (P2X receptors) in the adult rat thyroid. *Journal of Anatomy* 198:569-579.
97. Glass R, Townsend-Nicholson A, Burnstock G (2000) P2 receptors in the thymus: expression of P2X and P2Y receptors in adult rats, an immunohistochemical and in situ hybridisation study. *Cell and Tissue Research* 300:295-306.
98. Gourine AV, Llaudet E, Dale N, Spyer KM (2005) Release of ATP in the ventral medulla during hypoxia in rats: role in hypoxic ventilatory response. *The Journal of Neuroscience* 25:1211-1218.
99. Greig AVH, Linge C, Terenghi G, McGrouther DA, Burnstock G (2003) Purinergic receptors are part of a functional signaling system for proliferation and differentiation of human epidermal keratinocytes. *Journal of Investigative Dermatology* 120:1007-1015.
100. Gröschel-Stewart U, Bardini M, Robson T, Burnstock G (1999a) Localisation of $P2X_5$ and $P2X_7$ receptors by immunohistochemistry in rat stratified squamous epithelia. *Cell and Tissue Research* 296:599-605.
101. Gröschel-Stewart U, Bardini M, Robson T, Burnstock G (1999b) P2X receptors in the rat duodenum villus. *Cell and Tissue Research* 297:111-117.
102. Grosenbaugh DA, Morgan SJ, Hood DM (1999) The digital pathologies of chronic laminitis. *Veterinary Clinics of North America: Equine Practice* 15:419-436.
103. Gu JG, Heft MW (2004) P2X receptor-mediated purinergic sensory pathways to the spinal cord dorsal horn. *Purinergic Signalling* 1:11-16.

104. Gu BJ, Wiley JS (2006) Rapid ATP-induced release of matrix metalloproteinase 9 is mediated by the $P2X_7$ receptor. *Blood* 107:4946-4953.
105. Guedes AG, Matthews NS, Hood DM (2012) Effect of ketamine hydrochloride on the analgesic effects of tramadol hydrochloride in horses with signs of chronic laminitis-associated pain. *American Journal of Veterinary Research* 73:610-619.
106. Guo C, Masin M, Qureshi OS, Murrell-Lagnado RD (2007) Evidence for functional $P2X_4/P2X_7$ heteromeric receptors. *Molecular Pharmacology* 72:1447-1456.
107. Hamilton N, Vayro S, Kirchhoff F, Verkhratsky A, Robbins J, Gorecki DC, Butt AM (2008) Mechanisms of ATP- and glutamate-mediated calcium signaling in white matter astrocytes. *GLIA* 56:734-749.
108. Hamilton SG, McMahon SB (2000) ATP as a peripheral mediator of pain. *Journal of the Autonomic Nervous System* 81:187-194.
109. Hampson BA, de Laat MA, Beausac C, Rovel T, Pollitt CC (2012) Histopathological examination of chronic laminitis in Kaimanawa feral horses of New Zealand. *New Zealand Veterinary Journal* 60:285-289.
110. Hansen MA, Dutton JL, Balcar VJ, Barden JA, Bennett MR (1999) P2X (Purinergic) receptor distributions in rat blood vessels. *Journal of the Autonomic Nervous System* 75:147-155.
111. Harrington LS, Mitchell JA (2004) Novel role for P2X receptor activation in endothelium-dependent vasodilation. *British Journal of Pharmacology* 143:611-617.
112. Harris PA (2012) Laminitis after 2000 years: Adding bricks to our wall of knowledge. *The Veterinary Journal* 191:273-274.
113. He WJ, Cui J, Du L, Zhao YD, Burnstock G, Zhou HD, Ruan HZ (2012) Spinal $P2X_7$ receptor mediates microglia activation-induced neuropathic pain in the sciatic nerve injury rat model. *Behavioural Brain Research* 226:163-170.
114. He ML, Zemkova H, Koshimizu T, Tomic M, Stojilkovic SS (2003) Intracellular calcium measurements as a method in studies on activity of purinergic P2X receptor channels. *American Journal of Physiology Cell Physiology* 285:C467-479.
115. Hegg CC, Greenwood D, Huang W, Han P, Lucero MT (2003) Activation of purinergic receptor subtypes modulates odor sensitivity.*The Journal of Neuroscience* 23:8291-8301.
116. Heinzmann S, McMahon SB (2011) New molecules for the treatment of pain. *Current Opinion in Supportive and Palliative Care* 5:111-115.
117. Hoebertz A, Arnett TR, Burnstock G (2003) Regulation of bone resorption and formation by purines and pyrimidines. *TRENDS in Pharmacological Sciences* 24:290-297.
118. Holford LC, Case P, Lawson SN (1994) Substance-P, neurofilament, peripherin and SSEA4 immunocytochemistry of human dorsal-root ganglion neurons obtained from post-mortem tissue: a quantitative morphometric analysis. *Journal of Neurocytology* 23:577-589.
119. Holton P (1959) The liberation of adenosine triphosphate on antidromic stimulation of sensory nerves. *The Journal of Physiology* 145:494-504.

120. Honore P, Donnelly-Roberts D, Namovic MT, Hsieh G, Zhu CZ, Mikusa JP, Hernandez G, Zhong C, Gauvin DM, Chandran P, Harris R, Perez Medrano A, Carroll W, Marsh K, Sullivan JP, Faltynek CR, Jarvis MF (2006) A-740003 [*N*-(1-{[(cyanoimino)(5-quinolinylamino)methyl]amino}-2,2-dimethylpropyl)-2-(3,4-dimethoxyphenyl)acetamide], a novel and selective $P2X_7$ receptor antagonist, dose-dependently reduces neuropathic pain in the rat. *The Journal of Pharmacology and Experimental Therapeutics* 319:1376-1385.
121. Honore P, Kage K, Mikusa J, Watt AT, Johnston JF, Wyatt JR, Faltynek CR, Jarvis MF, Lynch K (2002) Analgesic profile of intrathecal $P2X_3$ antisense oligonucleotide treatment in chronic inflammatory and neuropathic pain states in rats. *Pain* 99:11-19.
122. Hood DM (1999a) Laminitis as a systemic disease. *Veterinary Clinics of North America: Equine Practice* 15:481-494.
123. Hood DM (1999b) Laminitis in the horse. *Veterinry Clinics of North America: Equine Practice* 15:287-294.
124. Hood DM (1999c) The mechanisms and consequences of structural failure of the foot. *Veterinary Clinics of North America: Equine Practice* 15:437-461.
125. Hood DM (1999d) The pathophysiology of developmental and acute laminitis. *Veterinry Clinics of North America: Equine Practice* 15:321-343.
126. Hood DM, Amoss MS, Grosenbaugh DA (1990) Equine laminitis: a potential model of Raynaud's phenomenon. *Angiology* 41:270-277.
127. Hood DM, Grosenbaugh DA, Mostafa MB, Morgan SJ, Thomas BC (1993) The role of vascular mechanisms in the development of acute laminitis. *Journal of Veterinary Internal Medicine* 7:228-234.
128. Hood DM, Grosenbaugh DA, Slater MR (1994) Vascular perfusion in horses with chronic laminitis. *Equine Veterinary Journal* 26:191-196.
129. Hood DM, Wagner IP, Brumbaugh GW (2001) Evaluation of hoof wall surface temperature as an index of digital vascular perfusion during the prodromal and acute phases of carbohydrate-induced laminitis in horses. *American Journal of Veterinary Research* 62:1167-1172.
130. Hugel S, Schlichter R (2000) Presynaptic P2X receptors facilitate inhibitory GABAergic transmission between cultured rat spinal cord dorsal horn neurons. *Journal of Neuroscience* 20:2121-2130.
131. Hughes JP, Hatcher JP, Chessell IP (2007) The role of $P2X_7$ in pain and inflammation. *Purinergic Signalling* 3:163-169.
132. Hung J, Chansard M, Ousman SS, Nguyen MD, Colicos MA (2010) Activation of microglia by neuronal activity: Results from a new *in vitro* paradigm based on neuronal-silicon interfacing technology. *Brain, Behavior, and Immunity* 24:31-40.
133. Idzko M, Dichmann S, Panther E, Ferrari D, Herouy Y, Virchow C Jr, Luttmann W, Di Virgilio F, Norgauer J (2001) Functional characterization of P2Y and P2X receptors in human eosinophils. *Journal of Cell Physiology* 188:329-336.
134. Inoue K, Denda M, Tozaki H, Fujishita K, Koizumi S, Inoue K (2005) Characterization of multiple P2X receptors in cultured normal human epidermal keratinocytes. *Journal of Investigative Dermatology* 124:756-763.

135. Jacques-Silva MC, Rodnight R, Lenz G, Liao Z, Kong Q, Tran M, Kang Y, Gonzalez FA, Weisman GA, Neary JT (2004) $P2X_7$ receptors stimulate AKT phosphorylation in astrocytes. *British Journal of Pharmacology* 141:1106-1117.
136. Jarvis MF (2003) Contributions of $P2X_3$ homomeric and heteromeric channels to acute and chronic pain. *Expert Opinion on Therapeutic Targets* 7:513-522.
137. Jarvis MF, Burgard EC, McGaraughty S, Honore P, Lynch K, Brennan TJ, Subieta A, van Biesen T, Cartmell J, Bianchi B, Niforatos W, Kage K, Yu H, Mikusa J, Wismer CT, Zhu CZ, Chu K, Lee CH, Stewart AO, Polakowski J, Cox BF, Kowaluk E, Williams M, Sullivan J, Faltynek C (2002) A-317491, a novel potent and selective non-nucleotide antagonist of $P2X_3$, and $P2X_{2/3}$ receptors, reduces chronic inflammatory and neuropathic pain in the rat. *PNAS* 99:17179-17184.
138. Jiang L, Bardini M, Keogh A, dos Remedios CG, Burnstock G (2005) $P2X_1$ receptors are closely associated with connexin 43 in human ventricular myocardium. *International Journal of Cardiology* 98:291-297.
139. Jiang LH, Mackenzie AB, North RA, Surprenant A (2000) Brilliant Blue G selectively blocks ATP-gated rat $P2X_7$ receptors. *Molecular Pharmacology* 58:82-88.
140. Johnson PJ, Messer NT, Slight SH, Wiedmeyer C, Buff P, Ganjam VK (2004) Endocrinopathic laminitis in the horse. *Clinical Techniques in Equine Practice* 3:45-56.
141. Johnson PJ, Tyagi SC, Katwa LC, Ganjam VK, Moore LA, Kreeger JM, Messer NT (1998) Activation of extracellular matrix metalloproteinases in equine laminitis. *Veterinary Record* 142:392-396.
142. Jones E, Viñuela-Fernandez I, Eager RA, Delaney A, Anderson H, Patel A, Robertson DC, Allchorne A, Sirinathsinghji EC, Milne EM, MacIntyre N, Shaw DJ, Waran NK, Mayhew J, Fleetwood-Walker SM (2007) Neuropathic changes in equine laminitis pain. *Pain* 132:321-331.
143. Joseph EK, Green PG, Bogen O, Alvarez P, Levine JD (2013) Vascular endothelial cells mediate mechanical stimulation-induced enhancement of endothelin hyperalgesia via activation of $P2X_{2/3}$ receptors on nociceptors. *Journal of Neuroscience* 33:2849-2859.
144. Kaczmarek-Hájek K, Lörinczi E, Hausmann R, Nicke A (2012) Molecular and functional properties of P2X receptors-recent progress and persisting challenges. *Purinergic Signalling* 8:375-417.
145. Kage K, Niforatos W, Zhu CZ, Lynch KJ, Honore P, Jarvis MF (2002) Alteration of dorsal root ganglion $P2X_3$ receptor expression and function following spinal nerve ligation in the rat. *Experimental Brain Research* 147:511-519.
146. Kanjhan R, Housley GD, Burton LD, Christie DL, Kippenberger A, Thorne PR, Luo L, Ryan AF (1999) Distribution of the $P2X_2$ receptor subunit of the ATP-gated ion channels in the rat central nervous system. *Journal of Comparative Neurology* 407:11-32.
147. Katwa LC, Johnson PJ, Ganjam VK, Kreeger JM, Messer NT (1999) Expression of endothelin in equine laminitis. *Equine Veterinary Journal* 31:243-247.
148. Katz LM, Bailey SR, (2012) A review of recent advances and current hypotheses on the pathogenesis of acute laminitis. *Equine Veterinary Journal* 44:752-761.

149. Keen JA, Hillier C, McGorum BC, Nally JE (2008) Endothelin mediated contraction of equine laminar veins. *Equine Veterinary Journal* 40:488-492.
150. Khakh BS, Humphrey PPA, Surprenant A (1995) Electrophysiological properties of P_{2X}-purinoceptors in rat superior cervical, nodose and guinea-pig coeliac neurones. *Journal of Physiology* 484.2:385-395.
151. Kidd BL, Urban LA (2001) Mechanisms of inflammatory pain. *British Journal of Anaesthesia* 87:3-11.
152. Knight GE, Bodin P, De Groat WC, Burnstock G (2002) ATP is released from guinea pig ureter epithelium on distension. *American Journal of Physiology Renal Physiology* 282:F281-F288.
153. Ko WH, O'Dowd JJM, Pediani JD, Bovell DL, Elder HY, McEwan Jenkinson D, Wilson SM (1994) Extracellular ATP can activate autonomic signal transduction pathways in cultured equine sweat gland epithelial cells. *Journal of experimental Biology* 190:239-252.
154. Kong Q, Wang M, Liao Z, Camden JM, Yu S, Simonyi A, Sun GY, Gonzalez FA, Erb L, Seye CI, Weisman GA (2005) $P2X_7$ nucleotide receptors mediate caspase-8/9/3-dependent apoptosis in rat primary cortical neurons. *Purinergic Signalling* 1:337-347.
155. Kyaw-Tanner MT, Wattle O, van Eps AW, Pollitt CC (2008) Equine laminitis: Membrane type matrix metalloproteinase-1 (MMP-14) is involved in acute phase onset. *Equine Veterinary Journal* 40:482-487.
156. Labasi JM, Petrushova N, Donovan C, McCurdy S, Lira P, Payette MM, Brissette W, Wicks JR, Audoly L, Gabel CA (2002) Absence of the $P2X_7$ receptor alters leukocyte function and attenuates an inflammatory response. *The Journal of Immunology* 168:6436-6445.
157. Lê KT, Paquet M, Nouel D, Babinski K, Séguéla P (1997) Primary structure and expression of a naturally truncated human P2X ATP receptor subunit from brain and immune system. *FEBS Letters* 418:195-199.
158. Lemperg RK, Arnoldi CC (1978) The significance of intraosseous pressure in normal and diseased states with special reference to the intraosseous engorgement-pain syndrome. *Clinical Orthopaedics and Related Research* 136:143-156.
159. Lewis CJ, Evans RJ (2001) P2X receptor immunoreactivity in different arteries from the femoral, pulmonary, cerebral, coronary and renal circulations. *Journal of Vascular Research* 38:332-340.
160. Leung L, Cahill CM (2010) TNF-α and neuropathic pain – a review. *Journal of Neuroinflammation* 7:27.
161. Li J, Liu D, Ke HZ, Duncan RL, Turner CH (2005) The $P2X_7$ nucleotide receptor mediates skeletal mechanotransduction. *Journal of Biological Chemistry* 280:42952-42959.
162. Li Z, Liang D, Chen L (2008) Potential therapeutic targets for ATP-gated P2X receptor ion channels. *Assay and Drug Development Technologies* 6:277-284.
163. Llewellyn-Smith IJ, Burnstock G (1998) Ultrastructural localization of $P2X_3$ receptors in rat sensory neurons. *NeuroReport* 9:2545-2550.

164. Loesch A, Burnstock G (2000) Ultrastructural localisation of ATP-gated $P2X_2$ receptor immunoreactivity in vascular endothelial cells in rat brain. *Endothelium* 7:93-98.
165. Loftus JP, Black SJ, Pettigrew A, Abrahamsen EJ, Belknap JK (2007) Early laminar events involving endothelial activation in horses with black walnut-induced laminitis. *American Journal of Veterinary Research* 68:1205-1211.
166. Loftus JP, Johnson PJ, Belknap JK, Pettigrew A, Black SJ (2009) Leukocyte-derived and endogenous matrix metalloproteinases in the lamellae of horses with naturally acquired and experimentally induced laminitis. *Veterinary Immunology and Immunopathology* 129:221-230.
167. Luo J, Lee S, Wu D, Yeh J, Ellamushi H, Wheeler AP, Warnes G, Zhang Y, Bo X (2013) P2X7 purinoceptors contribute to the death of Schwann cells transplanted into the spinal cord. *Cell Death and Disease* 4:e829.
168. Lynch KJ, Touma E, Niforatos W, Kage KL, Burgard EC, Biesen TV, Kowaluk EA, Jarvis MF (1999) Molecular and functional characterization of Human $P2X_2$ receptors. *Molecular Pharmacology* 56:1171-1181.
169. Malone ED (2002) Managing chronic arthritis. *Veterinary Clinics of North America: Equine Practice* 18:411-437.
170. Mankus C, Rich C, Minns M, Trinkaus-Randall V (2011) Corneal epithelium expresses a variant of $P2X_7$ receptor in health and disease. *PLoS ONE* 6:e28541.
171. Marchand F, Perretti M, McMahon SB (2005) Role of the immune system in chronic pain. *Nature Reviews Neuroscience* 6:521-532.
172. Matute C (2008) $P2X_7$ receptors in oligodendrocytes: a novel target for neuroprotection. *Molecular Neurobiology* 38:123-128.
173. McGowan C (2008) The role of insulin in endocrinopathic laminitis. *Journal of Equine Veterinary Science* 28:603-607.
174. Menzies-Gow NJ, Bailey SR, Berhane Y, Brooks AC, Elliott J (2008) Evaluation of the induction of vasoactive mediators from equine digital vein endothelial cells by endotoxin. *American Journal of Veterinary Research* 69:349-355.
175. Molyneux GS, Haller CJ, Mogg K, Pollitt CC (1994) The structure, innervation and location of arteriovenous anastomoses in the equine foot. *Equine Veterinary Journal* 26:305-312.
176. Moore R (2009) Laminitis vision: 20/20 by 2020. *In*: Fifth International Equine Conference on Laminitis and diseases of the foot Proceedings, pp15-20.
177. Moore RM, Eades SC, Stokes AM (2004) Evidence for vascular and enzymatic events in the pathophysiology of acute laminitis: which pathway is responsible for initiation of this process in horses? *Equine Veterinary Journal* 36:204-209.
178. Morgan SJ, Grosenbaugh DA, Hood DM (1999) The pathophysiology of chronic laminitis. Pain and anatomic pathology. *Veterinry Clinics of North America: Equine Practice* 15:395-417.
179. Morioka N, Abdin MJ, Kitayama T, Morita K, Nakata Y, Dohi T (2008) $P2X_7$ receptor stimulation in primary cultures of rat spinal microglia induces downregulation of the activity for glutamate transport. *Glia* 56:528-538.
180. Morrisset S, Hawkins JF, Kooreman K (1999) High intraosseous pressure as a cause of lameness in a horse with degloving injury of the metatarsus. *Journal of American Veterinary Medical Association* 215:1478-1480.

181. Mounkaïla B, Marthan R, Roux E (2005) Biphasic effect of extracellular ATP on human and rat airways is due to multiple P2 purinoceptor activation. *Respiratory Research* 6:143.
182. Mungall BA, Kyaw-Tanner M, Pollitt CC (2001) In vitro evidence for a bacterial pathogenesis of equine laminitis. *Veterinary Microbiology* 79:209-223.
183. Nakagawa T, Wakamatsu K, Zhang N, Maeda S, Minami M, Satoh M, Kaneko S (2007) Intrathecal administration of ATP produces long-lasting allodynia in rats: Differential mechanisms in the phase of the induction and maintenance. *Neuroscience* 147:445-455.
184. Nakatsuka T, Gu JG (2006) P2X purinoreceptors and sensory transmission. *European Journal of Physiology* 452:598-607.
185. Nawa G, Urano T, Tokino T, Ochi T, Miyoshi Y (1998) Cloning and characterization of the murine *P2XM* receptor gene. *Journal of Human Genetics* 43:262-267.
186. Neary JT, Burnstock G (1996) Purinoceptors in the regulation of cell growth and differentiation. *Drug Development Research* 39:407–412.
187. Neary JT, Rathbone MP, Cattabeni F, Abbracchio MP, Burnstock G (1996) Trophic actions of extracellular nucleotides and nucleosides on glial and neuronal cells. *Trends in Neuroscience* 19:13-18.
188. Newman EA (2001) Propagation of intercellular calcium waves in retinal astrocytes and Müller cells. *The Journal of Neuroscience* 21:2215-2223.
189. Nicholson B (2006) Differential diagnosis: nociceptive and neuropathic pain. *American Journal of Managed Care* 12:S256-S262.
190. Nobile M, Monaldi I, Alloisio S, Cugnoli C, Ferroni S (2003) ATP-induced, sustained calcium signalling in cultured rat cortical astrocytes: evidence for a non-capacitative, P2X7-like-mediated calcium entry. *FEBS Letters* 538:71-76.
191. Noguchi T, Ishii K, Fukutomi H, Naguro I, Matsuzawa A, Takeda K, Ichijo H (2008) Requirement of reactive oxygen species-dependent activation of ASK1-p38 MAPK pathway for extracellular ATP-induced apoptosis in macrophage. *The Journal of Biological Chemistry* 283:7657-7665.
192. Nori S, Fumagalli L, Bo X, Bogdanov Y, Burnstock G (1998) Coexpression of mRNAs for $P2X_1$, $P2X_2$ and $P2X_4$ receptors in rat vascular smooth muscle: an is situ hybridization and RT-PCR study. *Journal of Vascular Research* 35:179-185.
193. North RA (2002) Molecular Physiology of P2X receptors. *Physiological Reviews* 82:1013-1067.
194. North RA (2004) $P2X_3$ receptors and peripheral pain mechanisms. *Journal of Physiology* 554:301-308.
195. Noschka E, Moore JN, Peroni JF, Lewis SJ, Morrow JD, Robertson TP (2009) Thromboxane and isoprostanes as inflammatory and vasoactive mediators in black walnut heartwood extract induced equine laminitis. *Veterinary Immunology and Immunopathology* 129:200-210.
196. Orriss IR, Knight GE, Utting JC, Taylor SEB, Burnstock G, Arnett TR (2009) Hypoxia stimulates vesicular release from rat osteoblasts. *Journal of Cellular Physiology* 220:155-162.

197. Ossipov MH, Lai J, Malan JR TP, Porreca F (2000) Spinal and supraspinal mechanisms of neuropathic pain. *Annals of the New York Academy of Sciences* 909:12-24.
198. Pan AH, Lu DH, Luo XG, Chen L, Li ZY (2009) Formalin-induced increase in $P2X_3$ receptor expression in dorsal root ganglia: implications for nociception. *Clinical and Experimental Pharmacology and Physiology* 36:e6-e11.
199. Panupithu N, Rogers JT, Zhao L, Solano-Flores LP, Possmayer F, Sims SM, Dixon SJ (2008) P2X7 receptors on osteoblasts couple to production of lysophosphatidic acid: a signaling axis promoting osteogenesis. *The Journal of Cell Biology* 181:859-871.
200. Paredes RM, Etzler JC, Watts LT, Zheng W, Lechleiter JD (2008) Chemical calcium indicators. *Methods* 46:143-151.
201. Parks AH, Mair TS (2009) Laminitis: A call for unified terminology. *Equine Veterinary Education* 21:102-106.
202. Pass MA, Pollitt S, Pollitt CC (1998) Decreased glucose metabolism causes separation of hoof lamellae *in vitro*: a trigger for laminitis? *Equine Veterinary Journal Supplement* 26:133-138.
203. Peroni JF, Harrison WE, Moore JN, Graves JE, Lewis SJ, Krunkosky TM, Robertson TP (2005) Black walnut extract-induced laminitis in horses associated with heterogenous dysfunction of the laminar microvasculature. *Equine Veterinary Journal* 37:546-551.
204. Peroni JF, Moore JN, Noschka E, Grafton ME, Aceves-Avila M, Lewis SJ, Robertson TP (2006) Predisposition for venoconstriction in the equine laminar dermis: implications in equine laminitis. *Journal of Applied Physiology* 100:759-763.
205. Petruska JC, Cooper BY, Gu JG, Rau KK, Johnson RD (2000) Distribution of $P2X_1$, $P2X_2$, and $P2X_3$ receptor subunits in rat primary afferents: relation to population markers and specific cell types. *Journal of Chemical Neuroanatomy* 20:141-162.
206. Pollitt CC (1996) Basement membrane pathology: a feature of acute equine laminitis. *Equine Veterinary Journal* 28:38-46.
207. Pollitt CC (1992) Clinical anatomy and physiology of the normal equine foot. *Equine Veterinary Education* 4:219-224.
208. Pollitt CC (2004b) Equine laminitis. *Clinical Techniques in Equine Practice* 3:34-44.
209. Pollitt CC (2011) Pathophysiology of laminitis. *In*: Diagnosis and Management of Lameness in the Horse 2nd Edition, Eds. Ross MW, Dyson SJ, Saunders, Missouri ISBN 978-1-4160-6069-7, pp. 366-370.
210. Pollitt CC (1998) The anatomy and physiology of the hoof wall. *Equine Veterinary Education* 10:318-325.
211. Pollitt CC (1994) The basement membrane at the equine hoof dermal epidermal junction. *Equine Veterinary Journal* 26:399-407.
212. Pollitt CC, Collins SN (2011) Chronic laminitis. *In*: Diagnosis and Management of Lameness in the Horse 2nd Edition, Eds. Ross MW, Dyson SJ, Saunders, Missouri ISBN 978-1-4160-6069-7, pp. 374-376.

213. Pollitt CC, Davies CT (1998) Equine laminitis: its development coincides with increased sublamellar blood flow. *Equine Veterinary Journal Supplement* 26:125-132.
214. Pollitt CC, Kyaw-Tanner M, French KR, van Eps AW, Hendrikz JK, Daradka M (2003) Equine laminitis. *In*: 49th Annual Convention of the American Association of Equine Practitioners Proceedings.
215. Pollitt CC, Pass MA, Pollitt S (1998) Batimastat (BB-94) inhibits matrix metalloproteinases of equine laminitis. *Equine Veterinary Journal Supplement* 26:119-124.
216. Potenza MA, Addabbo F, Montagnani M (2009) Vascular actions of insulin with implications for endothelial dysfunction. *Am J Physiol Endocrinol Metab* 297:E568-E577.
217. Praetorius HA, Leipziger J (2009) ATP release from non-excitable cells. *Purinergic Signalling* 5:433-446.
218. Prasad M, Fearon IM, Zhang M, Laing M, Vollmer C, Nurse CA (2001) Expression of P2X2 and P2X3 receptor subunits in rat carotid body afferent neurones: role in chemosensory signalling. *Journal of Physiology* 537:667-677.
219. Ralevic V (2012) P2X receptors in the cardiovascular system. *WIREs Membrane Transport Signaling* 1:663-674.
220. Ralevic V (2009) Purines as neurotransmitters and neuromodulators in blood vessels. *Current Vascular Pharmacology* 7:3-14.
221. Ralevic V, Burnstock G (1998) Receptors for purines and pyrimidines. *Pharmacological Reviews* 50:413-492.
222. Ray FR, Huang W, Slater M, Barden JA (2002) Purinergic receptor distribution in endothelial cells in blood vessels: a basis for selection of coronary artery grafts. *Atherosclerosis* 162:55–61.
223. Redden RF (2004) Preventing laminitis in the contralateral limb of horses with nonweight-bearing lameness. *Clinical Techniques in Equine Practice* 3:57-63.
224. Rhee JS, Wang ZM, Nabekura J, Inoue K, Akaike N (2000) ATP facilitates spontaneous glycinergic IPSC frequency at dissociated rat dorsal horn interneuron synapses. *Journal of Physiology* 524.2:471-483.
225. Rietmann TR, Stauffacher M, Bernasconi P, Auer JA, Weishaupt MA (2004) The association between heart rate, heart rate variability, endocrine and behavioural pain measures in horses suffering from laminitis. *Journal of Veterinary Medicine A* 51:218-225.
226. Robertson TP, Bailey SR, Peroni JF (2009) Equine laminitis: A journey to the dark side of venous. *Veterinary Immunology and Immunopathology* 129:164-166.
227. Scholz J, Woolf CJ (2007) The neuropathic pain triad: neurons, immune cells and glia. *Nature Neuroscience* 10:1361-1368.
228. Schulze-Lohoff E, Hugo C, Rost S, Arnold S, Gruber A, Brüne B, Sterzel RB (1998) Extracellular ATP causes apoptosis and necrosis of cultured mesangial cells via P2Z/$P2X_7$ receptors. *American Journal of Renal Physiology* 275:F962-F971.
229. Schwiebert EM, Zsembery A (2003) Extracellular ATP as a signalling molecule for epithelial cells. *Biochimica et Biophysica Acta* 1615:7-32.

230. Schwiebert LM, Rice WC, Kudlow BA, Taylor AL, Schwiebert EM (2002) Extracellular ATP signaling and P2X nucleotide receptors in monolayers of primary human vascular endothelial cells. *American Journal of Physiology Cell Physiology* 282:C289–C301.
231. Seino D, Tokunaga A, Tachibana T, Yoshiya S, Dai Y, Obata K, Yamanaka H, Kobayashi K, Noguchi K (2006) The role of ERK signaling and the P2X receptor on mechanical pain evoked by movement of inflamed knee joint. *Pain* 123:193-203.
232. Sharp CJ, Reeve AJ, Collins SD, Martindale JC, Summerfield SG, Sargent BS, Bate ST, Chessell IP (2006) Investigation into the role of $P2X_3$/$P2X_{2/3}$ receptors in neuropathic pain following chronic constriction injury in the rat: an electrophysiological study. *British Journal of Pharmacology* 148:845-852.
233. Slater MR, Hood DM, Carter GK (1995) Descriptive epidemiological study of equine laminitis. *Equine Veterinary Journal* 27:364-367.
234. Solle M, Labasi J, Perregaux DG, Stam E, Petrushova N, Koller BH, Griffiths RJ, Gabel CA (2001) Altered cytokine production in mice lacking $P2X_7$ receptors. *The Journal of Biological Chemistry* 276:125-132.
235. Souslova V, Cesare P, Ding Y, Akopian AN, Stanfa L, Suzuki R, Carpenter K, Dickenson A, Boyce S, Hill R, Nebenius-Oosthuizen D, Smith AJH, Kidd EJ, Wood JN (2000) Warm-coding deficits and aberrant inflammatory pain in mice lacking $P2X_3$ receptors. *Nature* 407:1015-1017.
236. Stashak TS (2002) The foot. *In*: Adams' lameness in horses 5th Edition, Eds Stashack TS, Lippincott Williams & Wilkins, Philadelphia, pp645-664.
237. Steelman SM, Johnson D, Wagner B, Stokes AM, Chowdhary BP (2013) Cellular and humoral immunity in chronic equine laminitis. *Veterinary Immunology and Immunopathology* 153:217-226.
238. Swanson TD (1999) Clinical presentation, diagnosis, and prognosis of acute laminitis. *Veterinry Clinics of North America: Equine Practice* 15:311-319.
239. Taylor AL, Schwiebert LM, Smith JJ, King C, Jones JR, Sorscher EJ, Schwiebert EM (1999) Epithelial P2X purinergic receptor channel expression and function. *The Journal of Clinical Investigation* 104:875-884.
240. Thomas S, Virginio C, North RA, Surprenant A (1998) The antagonist trinitrophenyl-ATP reveals co-existence of distinct P2X receptor channels in rat nodose neurones. *Journal of Physiology* 509:411-417.
241. Torres GE, Egan TM, Voigt MM (1999) Hetero-oligomeric assembly of P2X receptor subunits. *The Journal of Biological Chemistry* 274:6653-6659.
242. Trang T, Salter MW (2012) $P2X_4$ purinoceptor signaling in chronic pain. *Purinergic Signalling* 8:621-628.
243. Treiber K, Carter R, Gay L, Williams C, Geor R (2009) Inflammatory and redox status of ponies with a history of pasture-associated laminitis. *Veterinary Immunology and Immunopathology* 129:216-220.
244. Treiber KH, Kronfeld DS, Geor RJ (2006a) Insulin resistance in equids:possible role in laminitis. *The Journal of Nutrition* 136:2094S-2098S.
245. Treiber KH, Kronfeld DS, Hess TM, Byrd BM, Splan RK, Staniar WB (2006b) Evaluation of genetic and metabolic predispositions and nutritional risk factors

for pasture-associated laminitis in ponies. *Journal of American Veterinary Medical Association* 228:1538-1545.
246. Tsuda M, Shigemoto-Mogami Y, Koizumi S, Mizokoshi A, Kohsaka S, Salter MW, Inoue K (2003) $P2X_4$ receptors induced in spinal microglia gate tactile allodynia after nerve injury. *Nature* 424:778-783.
247. Tu J, Le G, Ballard HJ (2010) Involvement of the cystic fibrosis transmembrane conductance regulator in the acidosis-induced efflux of ATP from rat skeletal muscle. *The Journal of Physiology* 588:4563-4578.
248. Turner CM, Vonend O, Chan C, Burnstock G, Unwin RJ (2003) The pattern of distribution of selected ATP-sensitive P2 receptor subtypes in normal rat kidney: an immunohistological study. *Cells Tissues Organs* 175:105-117.
249. Ueno S, Moriyama T, Honda K, Kamiya H, Sakurada T, Katsuragi T (2003) Involvement of $P2X_2$ and $P2X_3$ receptors in neuropathic pain in a mouse model of chronic constriction injury. *Drug Development Research* 59:104-111.
250. Valera S, Hussy N, Evans RJ, Adami N, North RA, Surprenant A, Buell G (1994) A new class of ligand-gated ion channel defined by P_{2X} receptor for extracellular ATP. *Nature* 371:516-519.
251. van der Wijk T, Tomassen SFB, Houtsmuller AB, de Jonge HR, Tilly BC (2003) Increased vesicle recycling in response to osmotic cell swelling. *The Journal of Biological Chemistry* 278:40020-40025.
252. van Eps A, Collins SN, Pollitt CC (2010) Supporting limb laminitis. *Veterinary Clinics of North America: Equine Practice* 26:287-302.
253. Venugopal CS, Eades S, Holmes EP, Beadle RE (2011) Insulin resistance in equine digital vessel rings: An *in vitro* model to study vascular dysfunction in equine laminitis. *Equine Veterinary Journal* 43:744-749.
254. Verkhratsky A, Pankratov Y, Lalo U, Nedergaard M (2012) P2X receptors in neuroglia. *WIREs Membrane Transport and Signaling* 1:151-161.
255. Vial C, Evans RJ (2000) P2X receptor expression in mouse urinary bladder and the requirement of $P2X_1$ receptors for functional P2X receptor responses in the mouse urinary bladder smooth muscle. *British Journal of Pharmacology* 131:1489-1495.
256. Vial C, Roberts JA, Evans RJ (2004) Molecular properties of ATP-gated P2X receptor ion channels. *Trends in Pharmacological Sciences* 25:487-493.
257. Virgin JE, Goodrich LR, Baxter GM, Rao S (2011) Incidence of support limb laminitis in horses treated with half limb, full limb or transfixation pin casts: A retrospective study of 113 horses (2000-2009). *Equine Veterinary Journal* 43:7-11.
258. Virginio C, MacKenzie A, Rassendren FA, North RA, Surprenant A (1999) Pore dilation of neuronal P2X receptors channels. *Nature Neuroscience* 2:315-321.
259. Virginio C, Robertson G, Surprenant A, North RA (1998) Trinitrophenyl-substituted nucleotides are potent antagonists selective for $P2X_1$, $P2X_3$ and heteromeric $P2X_{2/3}$ receptors. *Molecular Pharmacology* 53:969-973.
260. Visser MB, Pollitt CC (2011) The timeline of lamellar basement membrane changes during equine laminitis development. *Equine Veterinary Journal* 43:471-477.

261. Visser MB, Pollitt CC (2012) The timeline of metalloprotease events during oligofructose induced equine laminitis development. *Equine Veterinary Journal* 44:88-93.
262. Volonté C, Amadio S, D'Ambrosi N, Colpi M, Burnstock G (2006) P2 receptor web: complexity and fine-tuning. *Pharmacology & Therapeutics* 112:264-280.
263. Vonend O, Oberhauser V, von Kügelgen I, Apel TW, Amann K, Ritz E, Rump LC (2002) ATP release in human kidney cortex and its mitogenic effects in visceral glomerular cells. *Kidney International* 61:1617-1626.
264. Vulchanova L, Riedl MS, Shuster SJ, Buell G, Surprenant A, North RA, Elde R (1997) Immunohistochemical study of the $P2X_2$ and $P2X_3$ receptor subunits in rat and monkey sensory neurons and their central terminals. *Neuropharmacology* 36:1229-1242.
265. Vulchanova L, Riedl MS, Shuster SJ, Stone LS, Hargreaves KM, Buell G, Surprenant A, North RA, Elde R (1998) $P2X_3$ is expressed by DRG neurons that terminate in inner lamina II. *European Journal of Neuroscience* 10:3470-3478.
266. Wang ZJ, Neuhuber WL (2003) Intraganglionic laminar endings in the rat esophagus contain purinergic $P2X_2$ and $P2X_3$ receptor immunoreactivity. *Anatomy and Embryology* 207:363-371.
267. Watano T, Calvert JA, Vial C, Forsythe ID, Evans RJ (2004) P2X receptor subtype-specific modulation of excitatory and inhibitory synaptic inputs in the rat brainstem. *The Journal of Physiology* 558:745-757.
268. Wattle O, Pollitt CC (2004) Lamellar metabolism. *Clinical Techniques in Equine Practice* 3:22-33.
269. Weick M, Cherkas PS, Härtig W, Pannicke T, Uckermann O, Bringmann A, Tal M, Reichenbach A, Hanani M (2003) P2 receptors in satellite glial cells in trigeminal ganglia of mice. *Neuroscience* 120:969-977.
270. Weiss DJ, Geor RJ, Johnston G, Trent AM (1994) Microvascular thrombosis associated with onset of acute laminitis in ponies. *American Journal of Veterinary Research* 55:606-612.
271. Weiss DJ, Trent AM, Johnston G (1995) Prothrombotic events in the prodromal stages of acute laminitis in horses. *American Journal of Veterinary Research* 56:986-991.
272. Weng JY, Hsu TT, Sun SH (2008) Functional characterization of $P2Y_1$ versus P2X receptors in RBA-2 astrocytes: elucidate the roles of ATP release and protein kinase C. *Journal of Cellular Biochemistry* 104:554-567.
273. White SM, Imig JD, Kim TT, Hauschild BC, Inscho EW (2001) Calcium signaling pathways utilized by P2X receptors in freshly isolated preglomerular MVSMC. *American Journal of Physiology Renal Physiology* 280:F1054-F1061.
274. Wiley JS, Chen JR, Snook MB, Jamieson GP (1994) The P_{2Z}-purinoceptor of human lymphocytes: actions of nucleotide agonists and irreversible inhibition by oxidized ATP. *British Journal of Pharmacology* 112:946-950.
275. Wilson SM, Law VWY, Pediani JD, Allen EA, Wilson G, Khan ZE, Ko WH (1998) Nucleotide-evoked calcium signals and anion seretion in equine cultured epithelia that express apical $P2Y_2$ receptors and pyrimidine nucleotide receptors. *British Journal of Pharmacology* 124:832-838.

276. Wirkner K, Sperlagh B, Illes P (2007) $P2X_3$ involvement in pain states. *Molecular Neurobiology* 36:165-183.
277. Wylie CE, Collins SN, Verheyen KL, Newton JR (2013) A cohort study of equine laminitis in Great Britain 2009-2011: estimation of disease frequency and description of clinical signs in 577 cases. *Equine Veterinary Journal* doi:10.1111/evj.12047.
278. Xiang Z, Bo X, Burnstock G (1998) Localization of ATP-gated P2X immunoreactivity in rat sensory and sympathetic ganglia. *Neuroscience Letters* 256:105-108.
279. Xiang Z, Xiong Y, Yan N, Li X, Mao Y, Ni X, He C, LaMotte RH, Burnstock G, Sun J (2008) Functional up-regulation of $P2X_3$ receptors in the chronically compressed dorsal root ganglion. *Pain* 140:23-34.
280. Xu GY, Huang LYM (2002) Peripheral inflammation sensitizes P2X receptor-mediated responses in rat dorsal root ganglion neurons. *The Journal of Neuroscience* 22:93-102.
281. Yaksh TL (2010) The pain state arising from the laminitic horse: insights into future analgesic therapies. *Journal of Equine Veterinary Science* 30:79-82.
282. Yan Z, Li S, Liang Z, Tomic M, Stojilkovic S (2008) The $P2X_7$ receptor channel pore dilates under physiological ion conditions. *The Journal of General Physiology* 132:563-573.
283. Zamboulis DE, Senior JM, Clegg PD, Gallagher JA, Carter SD, Milner PI (2013) Distribution of purinergic P2X receptors in the equine digit, cervical spinal cord and dorsal root ganglia. *Purinergic Signalling* in press doi:10.1007/s11302-013-9356-5.
284. Zerpa H, Crawford C, Knight GE, Fordham AF, Janska SE, Peppiatt-Wildman CM, Elliott J, Burnstock G, Wildman SS (2013) Extracellular ATP signaling in equine digital blood vessels. *European Journal of Pharmacology* 702:242-249.
285. Zhang XF, Han P, Faltynek CR, Jarvis MF, Shieh CC (2005) Functional expression of $P2X_7$ receptors in non-neuronal cells of rat dorsal root ganglia. *Brain Research* 1052:63-70.
286. Zhong Y, Dunn PM, Bardini M, Ford APDW, Cockayne DA, Burnstock G (2001) Changes in P2X receptor responses of sensory neurons from $P2X_3$-deficient mice. *European Journal of Neuroscience* 14:1784-1792.

Appendix

This text box is where the unabridged thesis included the following third party copyrighted material:

Zamboulis DE, Senior JM, Clegg PD, Gallagher JA, Carter SD, Milner PI (2013) Distribution of purinergic P2X receptors in the equine digit, cervical spinal cord and dorsal root ganglia. *Purinergic Signalling* in press doi:10.1007/s11302-013-9356-5.